(15)

AV FR 439

INVESTIGATION OF THE MOTION AND DECAY OF THE VORTEX WAKE OF A LIGHT TWIN-ENGINE AIRCRAFT

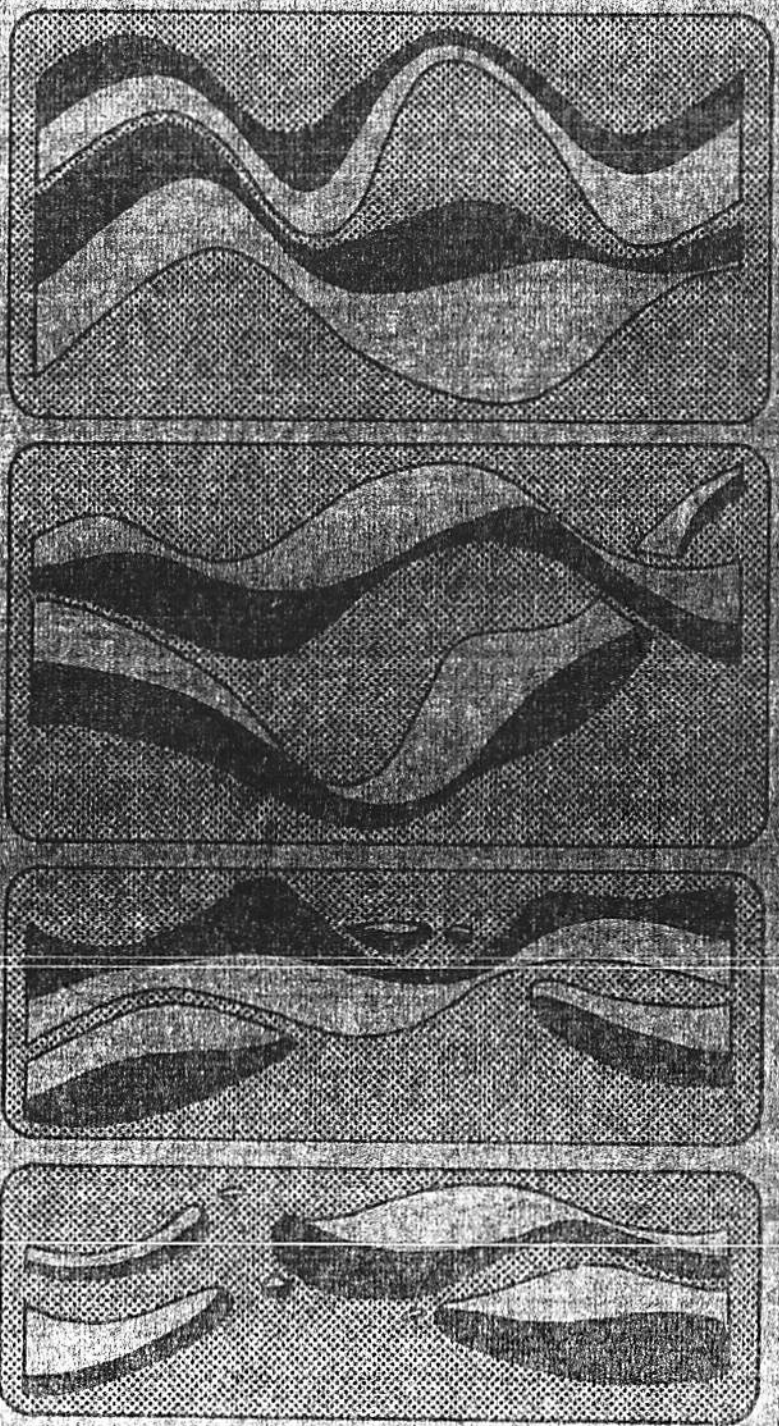

I. H. TOMBACH
E. R. BATE, JR.
AND
P. B. MacCREADY JR.
AEROVIRONMENT INC.

1974

FOR
THE DEPARTMENT
OF TRANSPORTATION,
TRANSPORTATION
SYSTEMS CENTER

TECHNICAL REPORT STANDARD TITLE PAGE

1. Report No.	2. Government Accession No.	3. Recipient's Catalog No.

4. Title and Subtitle	5. Report Date
Investigation of the Motion and Decay of the Vortex Wake of a Light Twin-Engine Aircraft	31 October 1974
	6. Performing Organization Code
7. Author(s) Ivar Tombach, Edward R. Bate, Jr., and Paul B. MacCready, Jr.	8. Performing Organization Report No. AV FR 439
9. Performing Organization Name and Address AeroVironment Inc. 145 Vista Avenue Pasadena, California 91107	10. Work Unit No.
	11. Contract or Grant No. DOT-TSC-523
12. Sponsoring Agency Name and Address U. S. Department of Transportation Transportation Systems Center Kendall Square Cambridge, Massachusetts 02142	13. Type of Report and Period Covered Final 13 Apr 1973 - 15 Oct 1974
	14. Sponsoring Agency Code

15. Supplementary Notes

16. Abstract

The properties of the smoke-marked trailing vortex wake generated by a light, twin-engine aricraft (Aero Commander 560F) were investigated experimentally. Velocity and temperature fields in the wake were measured by another instrumented probe aircraft. Ground-based and airborne cameras recorded the motion and decay of the smoke-marked vortices.

Meteorological measurements were made by a number of ground-based and airborne instruments. Analysis of these measurements shows that, for the particular conditions encountered, prediction of atmospheric turbulence aloft (up to 70 m, say) from surface measurements of wind is feasible within bounds of error acceptable for some operational purposes.

As has been noted previously, the local meteorologcial conditions significantly affect the development and ultimate disposition of the wake. In these experiments, a clear correlation between wake tilting and wind shear transverse to the wake was observed. Single persistent vortices were regularly observed in shear conditions. The measured descent speed of wakes decreased with time in a stable atmosphere, and the spacing between the vortex pair and the size of the buoyant wake oval both increased slightly as the wake descended. Termination of the organized motion in the wakes was always brought about by vortex

(over)

17. Key Words	18. Distribution Statement
Wake turbulence Vortex wakes	The distribution of this document is unlimited.

19. Security Classif. (of this report)	20. Security Classif. (of this page)	21. No. of Pages	22. Price
Unclassified	Unclassified	124	

Form DOT F 1700.7 (8-69)

instabilities, with vortex breakdown (bursting) predominating for the aircraft scale and flight conditions investigated. Increasing levels of ambient atmospheric turbulence had the expected result of decreasing wake lifetimes, and the behavior correlated quantitatively with similar measurements for other aircraft. The experiments also showed that wakes descending in a stably stratified atmosphere acquire buoyancy and then subsequently begin to lose it through mixing before they break up.

These results provide further confirmation of a previously presented categorization of vortex wake behavior into three evolutionary stages -- an initial period of motion similar to that of a classical inviscid wake, which subsequently evolves into a stage in which turbulent mixing between the wake and its surroundings begins to significantly affect its characteristics, and then terminates as the origanized motion decays through turbulence or instabilities. Also, further validation of the Crow-Bate theory for wake decay by the sinuous instability of the vortex filaments was provided by the experiments. Needed areas of theoretical exploration, building on the observations reported here, include the behavior of wakes in wind shear and the impact of ambient turbulence on vortex core breakdown.

Final Report

INVESTIGATION OF THE MOTION AND DECAY OF THE VORTEX WAKE OF A LIGHT TWIN-ENGINE AIRCRAFT

by

Ivar Tombach,
Edward R. Bate, Jr,
and
Paul B. MacCready, Jr.

31 October 1974

Prepared for

U. S. Department of Transportation
Transportation Systems Center
Kendall Square
Cambridge, Massachusetts 02142

Contract DOT-TSC-523

AeroVironment Inc.
145 Vista Avenue
Pasadena, California 91107

ABSTRACT

The properties of the smoke-marked trailing vortex wake generated by a light, twin-engine aircraft (Aero Commander 560F) were investigated experimentally. Velocity and temperature fields in the wake were measured by another instrumented probe aircraft. Ground-based and airborne cameras recorded the motion and decay of the smoke-marked vortices.

Meteorological measurements were made by a number of ground-based and airborne instruments. Analysis of these measurements shows that, for the particular conditions encountered, prediction of atmospheric turbulence aloft (up to 70 m, say) from surface measurements of wind is feasible within bounds of error acceptable for some operational purposes.

As has been noted previously, the local meteorological conditions significantly affect the development and ultimate disposition of the wake. In these experiments, a clear correlation between wake tilting and wind shear transverse to the wake was observed. Single persistent vortices were regularly observed in shear conditions. The measured descent speed of wakes decreased with time in a stable atmosphere, and the spacing between the vortex pair and the size of the buoyant wake oval both increased slightly as the wake descended. Termination of the organized motion in the wakes was always brought about by vortex instabilities, with vortex breakdown (bursting) predominating for the aircraft scale and flight conditions investigated. Increasing levels of ambient atmospheric turbulence had the expected result of decreasing wake lifetimes, and the behavior correlated quantitatively with similar measurements for other aircraft. The experiments also showed that wakes descending in a stably stratified atmosphere acquire buoyancy and then subsequently begin to lose it through mixing before they break up.

These results provide further confirmation of a previously presented categorization of vortex wake behavior into three evolutionary stages -- an initial period of motion similar to that of a classical inviscid wake, which subsequently evolves into a stage in which turbulent mixing between the wake and its surroundings begins to significantly affect its characteristics, and then terminates as the organized motion decays through turbulence or instabilities. Also, further validation of the Crow-Bate theory for wake decay by the sinuous instability of the vortex filaments was provided by the experiments. Needed areas of theoretical exploration, building on the observations reported here, include the behavior of wakes in wind shear and the impact of ambient turbulence on vortex core breakdown.

PREFACE

The tests which are described in this report are a continuation of a program concerned with the study, both experimental and analytical, of meteorological effects on aircraft wakes. This work was begun with the support of the Air Force Office of Scientific Research in 1970 and has continued uninterrupted to this date. Support by the U.S. Department of Transportation, Transportation Systems Center, for theoretical analysis of some of the phenomena observed in these tests began in 1972, and was augmented to include flight test work complementary to that of the AFOSR program early in 1973. Because of the related nature of the flight test activities under the AFOSR and DOT-TSC contracts, the experimental portions of the two programs were largely integrated (with the concurrence of the technical monitors of both sponsoring agencies). Thus, although this report concentrates on the information obtained under DOT-TSC support, it also includes related information which was obtained under the scope of the AFOSR contract.

The aircraft operations required for this study were carried out under subcontract by Flight Systems, Inc., of Newport Beach, California. The cooperation of FSI personnel, especially FSI President Dr. Robert Laidlaw, Director of Aircraft Programs James Pearce, and Chief Mechanic Kenneth Anderson, was indispensable to the program. Dr. Laidlaw and Mr. Pearce flew the two aircraft used.

Meteorological forecasts for the rather restrictive wind and stability conditions required for these tests were provided by Mr. John Aldrich. Dr. Steven Crow of Poseidon Research provided further insight into analysis of the wake instability phenomenon which bears his name.

Significant contributions to the experiments and analysis of their results were provided by Mr. Bruce Wright in field operations, Mr. Robert Moran in instrumentation for the probe aircraft, Mr. John Blair in all aspects of photography and photogrammetric analysis, and Messrs. Mel Smith, Chris Lansdown, and Bill Akwari in data analysis.

TABLE OF CONTENTS

1. INTRODUCTION

The flow characteristics of a vortex pair, such as that generated by an aircraft in flight, have been understood from days predating the airplane itself. However, aircraft vortex wakes are real flows generated in a real atmosphere and undergo interactions with that atmosphere. Because of the complicated nature of these interactions, the classical analytical models are limited in their usefulness for predicting actual aircraft wake behavior, and therefore experimental programs need to provide many of the answers required for proper understanding of wake motion and decay.

This report describes one such experimental study investigating the effects of wind shear, ambient turbulence, and atmospheric stability on wake lifetime, descent, banking of the plane of the vortices, and wake buoyancy. This experimental program extends and complements the experimental data presented in previous reports and papers by Tombach (1972, 1973, 1974) and by Bate (1974), as well as analytical work by Tombach (1971) and Lissaman, et al (1973). In the previous experimental works generation of vortices in experiments was performed by light single-engine and twin-engine aircraft, and the vortices were marked with smoke.

The overall picture of the nature of aircraft wake behavior in the atmosphere which evolves from this previous work can be summarized as follows:

1. The vortices probably never decay due to viscous or turbulent dissipation, but are instead destroyed by some form of instability.

2. Two main modes of instability exist. One is observed as a localized breakdown or "bursting" of the smoke-marked core of

an individual vortex. The other instability is the well-known sinuous instability of the vortex pair, which results in their linking into vortex rings. Bursting is the dominant mode of decay in most tests with smaller aircraft, and generally also in similar tests with transport aircraft.

3. There is a clear correlation between wake lifetime and atmospheric turbulence, with the life of the wake dramatically shortened by even small amounts of turbulence. A model has been developed to satisfactorily explain this correlation for the sinuous instability.

4. Sometimes, it is observed that one vortex is destroyed prematurely by bursting while the marking smoke in the core of the other vortex is still clearly visible much longer than would have normally been the case if both vortices decayed together.

5. There is an apparent correlation of wake lifetime with the lapse rate (at fixed turbulence level), but the effect is very weak.

6. The majority of wakes bank to some degree. A few bank so much that the plane of the vortices is vertical or has passed the vertical.

7. The vortex spacing remains essentially unchanged during the descent of the wake, increasing only slightly. Steeply banked wakes often have larger vortex separations than relatively level wakes.

8. A wake descending in a stably stratified atmosphere acquires buoyancy initially and subsequently loses it through turbulent mixing with its surroundings. The buoyancy may be totally eliminated while organized vortical motion remains.

9. The overall circulation of the vortex system decays slowly initially, then more rapidly as the wake decays.

10. Atmospheric stability has a strong effect on total distance the wake descends, both because of its effect on wake lifetime and because of an observed relationship between descent speed and stability. The greatest descent distances are observed in stable conditions, while the most rapid descents occur in neutral conditions.

11. Most models of wake descent in a stable atmosphere predict an increasing descent speed and a decreasing vortex spacing as the wake becomes buoyant, contrary to the observed behavior. These models do not consider turbulent mixing, which apparently dominates this motion. Analytical treatments including mixing (which must, of necessity, be more conjectural in their formulation) correlate qualitatively with the experimental observations.

The work described in this report explores some of these observations further, and augments the data base upon which some of them are constructed. Particular emphasis is paid to the effects of wind shear, especially near the ground, and to the correlation of wake instabilities with turbulence.

A few remarks about the organization of this report may be helpful. Chapter 2 describes the experimental procedures and instrumentation used to acquire the data. Chapter 3 contains some observations about the peculiarities of the meteorology of the test site, and discusses the feasibility of predicting turbulence aloft from surface measurements of wind. The flight test experimental data are presented in detail in Chapter 4, and the reasoning used to arrive at the conclusions of this study is discussed thoroughly there. Each

section of that chapter contains at its end a brief summarization of the key observations related to the particular phenomenon discussed in that section.

Chapter 5 contains a comprehensive discussion of the conclusions derived in the various sections of Chapters 3 and 4. This chapter completely reviews all of the key points of this study, thus the reader who wishes to skip the details of Chapters 3 and 4 can do so freely.

Some of the data presented in this report has appeared in an earlier progress report to DOT-TSC (Tombach and Bate, 1973). That report, which has seen a very limited distribution, contains a considerably smaller data base than that contained herein, and therefore some of the observations and conclusions in that document were speculative. In a few cases, additional information has significantly modified the conclusions of that report, therefore this report supersedes that previous report.

For reference, the report which describes the parallel work performed under AFOSR sponsorship, often on the same test, is AFOSR-TR-74-1507, listed in the references as Tombach (1974).

2. DESCRIPTION OF EXPERIMENT

In order to experimentally determine the effects of meteorology on vortex behavior, the laboratory was, of necessity, the "great outdoors". Although no direct control could be exercised over the experimental conditions (that is, the meteorology itself), it was possible to select those days for testing that exhibited the desired range in meteorological conditions. Thus, a variation in winds, turbulence, stability, etc., could be obtained by choosing the proper days for testing -- and having the good fortune of the services of a forecaster who could predict when those days would most likely occur.

The experimental program had as its objectives the study of wake descent speed, decay, banking, and buoyancy as functions of atmospheric stability, turbulence, and wind shear. In addition, supporting data on vortex properties such as tangential velocity profiles and vortex spacing were to be routinely acquired.

2.1 Experimental Equipment and Approach

A twin-engine Aero Commander 560F aircraft was used for the generation of the vortices and a specially instrumented Cessna Cardinal RG made detailed measurements of wake structure by penetrating the wake. The vortices were made visible by smoke from colored smoke grenades mounted on each wingtip. Land-based photography provided records from which quantitative measurements of overall wake behavior, e.g., descent speed, the growth of instabilities, vortex spacing, etc., were made. In addition, the Cessna carried instrumentation to measure the ambient atmospheric conditions, in particular stability and turbulence. The experiments described here were performed on 8 test days between 1 March 1973 and 26 February 1974.

Test Site and Ground-Based Equipment

All tests were conducted at the Mojave Airport in the Mojave Desert of California.

A typical flight pattern is shown in Figure 2-1. The orientation of the pattern varied with the objectives of the test; the pattern shown, with the generator aircraft flying perpendicular to the prevailing wind, was used to study wake behavior in wind shear. An eastbound heading, into the generally prevailing westerly wind, was used for those tests in which no crosswind was desired, while extremely low level tests ($h \leq 30$ m above ground) were performed along the long diagonal runway to insure satisfactory obstruction clearance for the probe aircraft.

Most tests had three ground-based camera sites, as shown in the figure. Site 1 was the test command post and the site for vertically oriented 16 mm cine and 35 mm still cameras which were used to photograph the wake some 50 to 250 m directly overhead. The Cessna Cardinal probe aircraft first crossed the wake over Site 1 in early tests; in later tests the first probes were made 300-600 m after the Aero Commander passed over Site 1 (as in the figure), allowing observation of the undisturbed vortices by the Site 1 cameras.

Site 2 was generally some 1500 m from Site 1 along a line perpendicular to the flight pattern. There, 16 mm cine and 35 mm still cameras with telephoto lenses provided side views of the wake and of its penetration by the probe aircraft. In later tests Site 3 was added to document the details of each wake crossing on 35 mm still photographs. Various extra ground and airborne camera sites were used on occasion for special purposes, and a different camera arrangement was used on low-level tests. Table 2-1 tabulates the camera specifications for a typical test of the form shown in Figure 2-1.

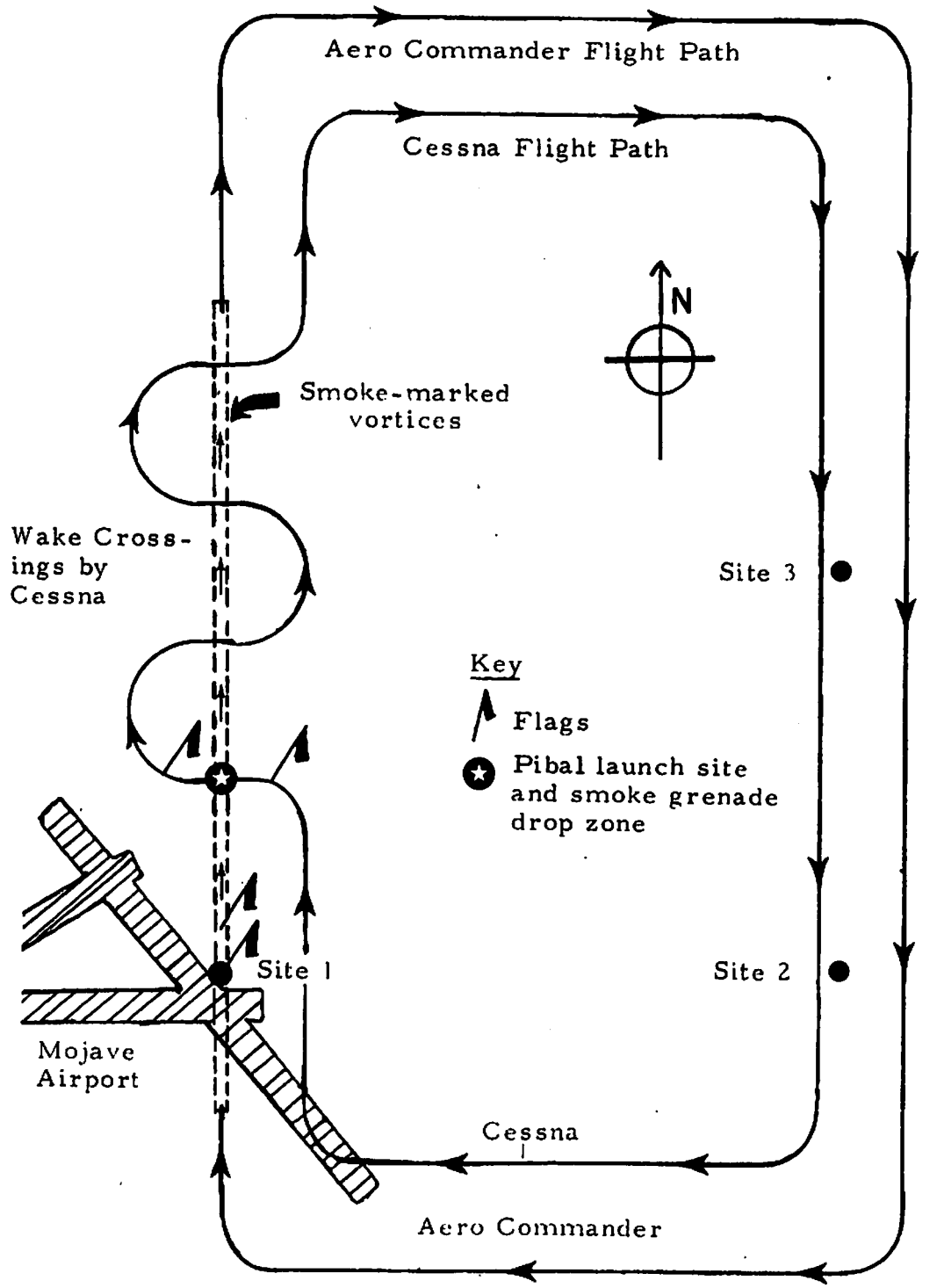

Figure 2-1. Schematic Representation of Test Area Layout and Aircraft Flight Patterns.

Table 2-1. Cameras Used During Typical Wake Test Shown in Figure 2-1.

Camera	Type	Lens	Framing Rate	Mounting
Site 1				
Arriflex 16S	16 mm Cine	5.7 mm	16 fr/sec	Vertical
Nikon F	35 mm Still	21 mm	1 fr/5 sec	Vertical
Nikon F	35 mm Still	28 mm	1 fr/2 sec	Horizontal (north facing)
Kodak Retina III Reflex	35 mm Still	50 & 135 mm	--	Hand-held
Site 2				
Arriflex 16S	16 mm Cine	100 mm	16 fr/sec	Horizontal (west facing)
Nikon F	35 mm Still	135 mm	1 fr/5 sec	Horizontal (west facing)
Site 3				
Nikon F	35 mm Still	28 mm	1 frame per wake crossing	Horizontal (west facing)
Cessna Cardinal				
Olympus 35SP	35 mm Still	50 mm	- -	Hand-held

The motion picture cameras at Sites 1 and 2 provided detailed temporal data on wake motion and breakup and on probe aircraft operations, while the still cameras provided higher resolution photographs of the wake at 5-second intervals. Clocks mounted in the fields of view of all cameras provided a time reference, and flags at known spacings within the fields of view of many of the cameras gave a scale reference for later photogrammetry.

Site 1 also had an additional 35 mm camera which was pointed horizontally along the track of the wake generator aircraft. This camera served two functions. It documented the probe wake penetration times and it photographed the motion of ascending pilot balloons (pibals) and of smoke filaments made by smoke grenades dropped from an aircraft, both of the latter being used to define the wind profile throughout the test altitude range.

Generator Aircraft

The Aero Commander 560F vortex generator aircraft has a wing span of 14.9 meters and had an average weight of 3000 kg during the tests. All tests were flown at 100 kts indicated airspeed (about 54 m/s true airspeed), which gives a calculated circulation, assuming elliptic wing loading, of $\Gamma_e = 42$ m^2/sec, at the test altitude of approximately 1000 meters above sea level.

Each wingtip of the Aero Commander was outfitted with nine U.S. Army M-18 colored smoke grenades, as shown in Figure 2-2. To mark the vortices, these grenades were fired in groups of three for each experimental run, allowing a sortie of three runs before the Aero Commander had to land for replacement of grenades. Red grenades were mounted on the left wingtip and green grenades were mounted on the right wingtip, and both sets of grenades were fired simultaneously from within the cockpit to give the visual effect shown in Figure 2-3.

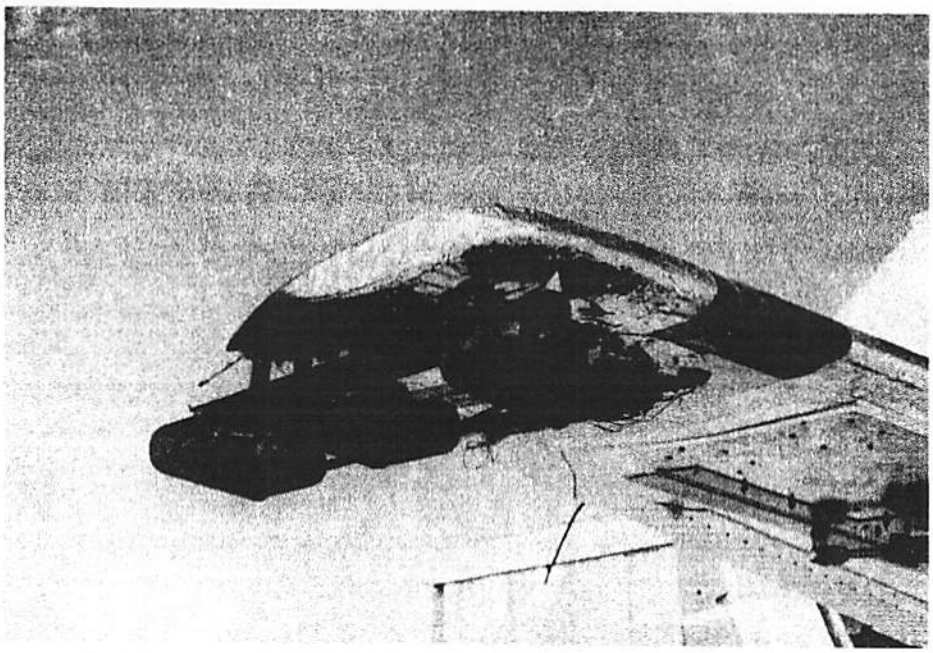

Figure 2-2. Smoke Grenade Installation on Wingtip of Aero Commander Vortex Generating Aircraft.

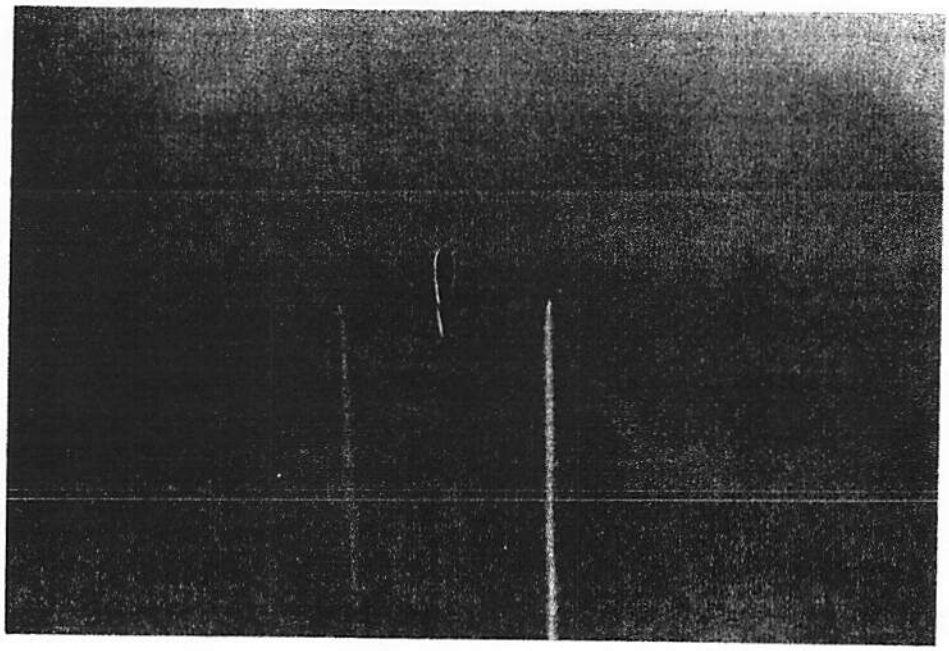

Figure 2-3. Aero Commander Aircraft with Trailing Smoke-Marked Vortices. The red smoke (the vortex to the right of the photo) is denser than the green smoke -- a characteristic of the smoke grenades used.

Probe Aircraft

The Cessna Cardinal RG probe aircraft shown in Figure 2-4 had mounted on it two .15 mm diameter quartz fiber hot film probes for velocity measurement and two aspirated choked-flow probes, with hot film sensors inside, for temperature measurement, both of which were designed and built especially for this study. These probes were mounted in pairs on a vertical boom attached to the right wing-tip of the aircraft, as shown in Figure 2-5, and were positioned so that the two velocity probes were spaced .76 meters apart on the vertical boom and the two temperature probes were likewise spaced .76 meters apart, with each set of temperature and velocity probes offset by 7.6 cm from each other. Also installed on the boom during the program was a static tube for the pressure altitude measurement system. A pitot-static tube, connected to a turbulence measurement system, was also used on a few test days. All instrumentation cabling and vacuum lines from the probes were installed inside the wing structure of the Cessna. The aircraft vacuum system supplied the vacuum for the aspirating temperature probes and for the purpose of retracting a shield surrounding each velocity probe during take-off and landing.

Inside the rear of the cabin of the Cessna was the instrument package shown in Figure 2-6. At the top of the package was a Thermo Systems Inc. constant temperature hot-wire anemometer system with two linearized velocity channels and two non-linearized channels for the aspirated temperature probes. The outputs from these four channels were processed by the signal conditioning circuitry in the middle of the package and then recorded on the oscillographic recorder below it. The instrumentation in the Cessna also included a pressure altitude sensor and associated electronics, as well as inverters which converted the 12 volt DC aircraft power to 115 volts AC.

Eight channels of processed data were recorded on the oscillograph with one additional channel used as an event marker. The

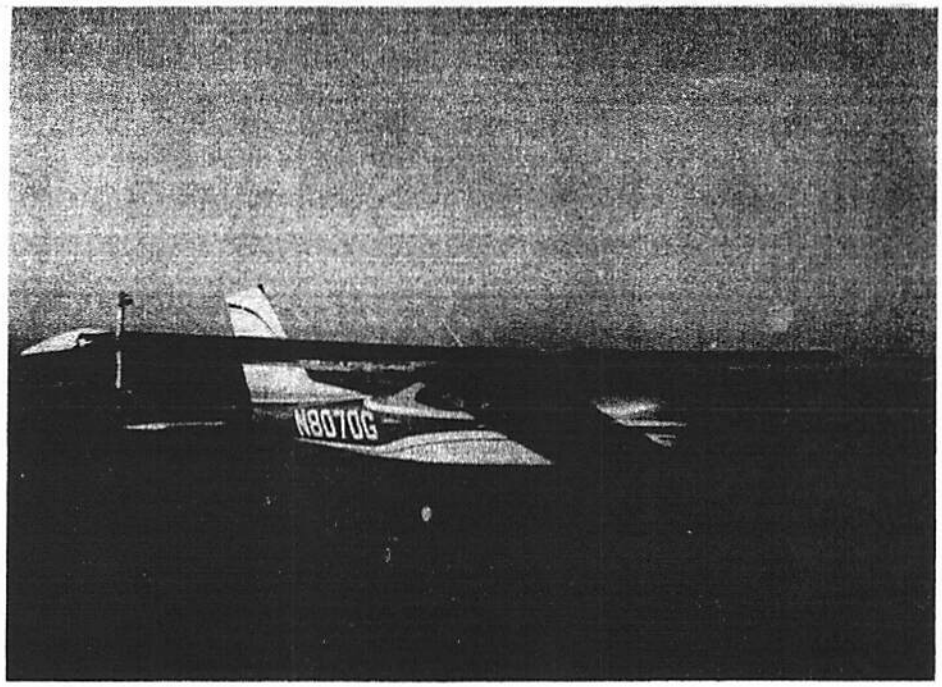

Figure 2-4. Cessna Cardinal RG Wake Probing Aircraft with Probe Boom on Wingtip at Left of Photo.

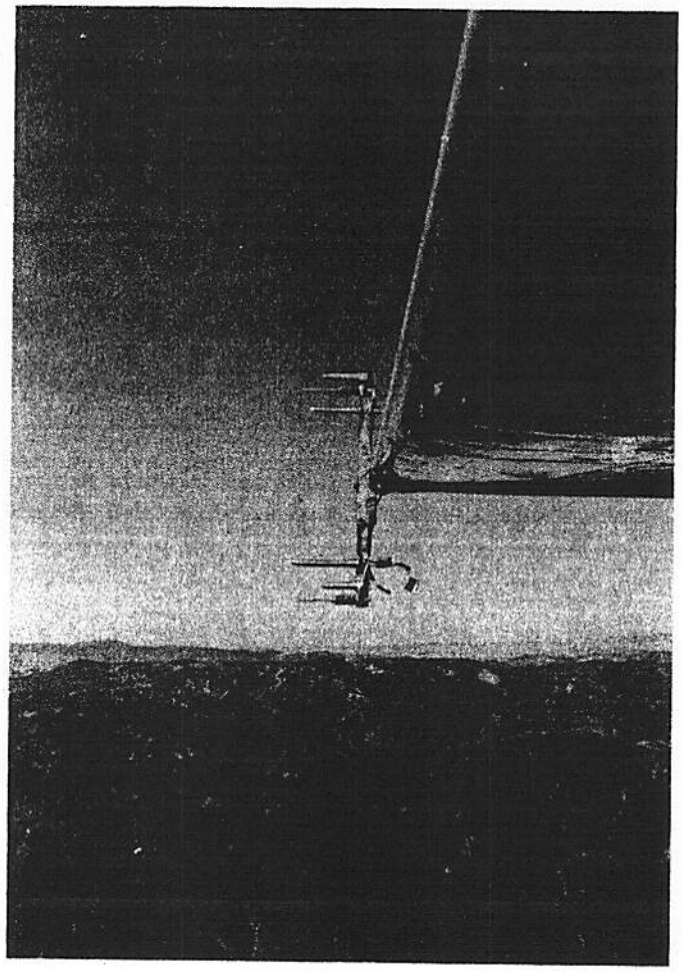

Figure 2-5. Probes on Cessna Cardinal Wingtip. From top: (1) aspirated temperature, (2) velocity, (3) static pressure (altitude), (4) pitot-static pressure (for special turbulence and velocity calibrations), (5) aspirated temperature, (6) velocity.

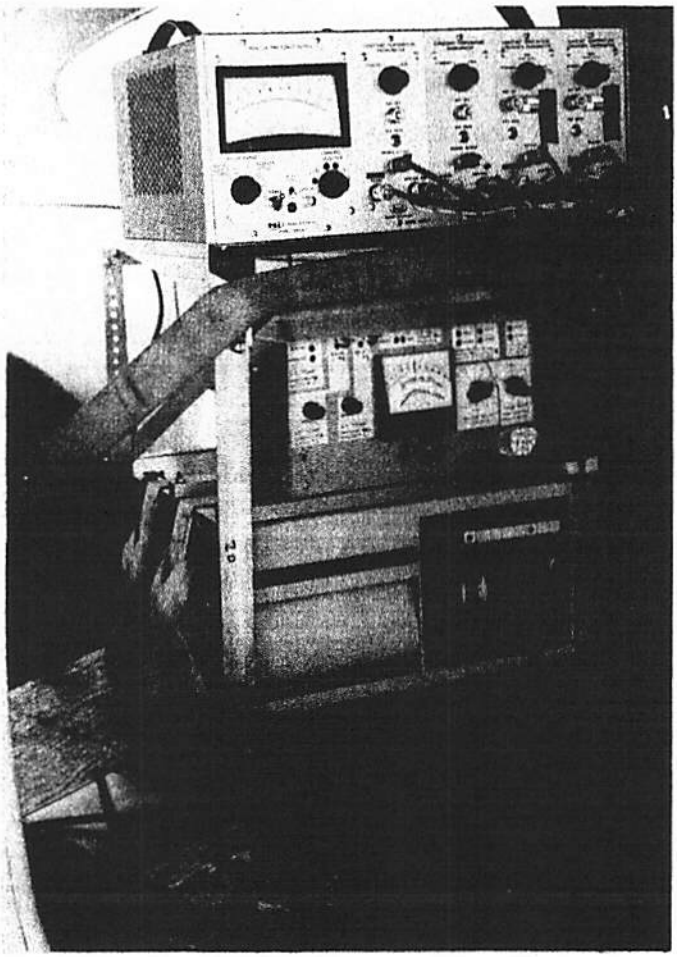

Figure 2-6. Instrument Package in Rear of Cessna Cardinal Cockpit. From top: (1) 4-channel hot wire anemometer; (2) signal conditioning package; (3) oscillographic chart recorder. In foreground is the cassette tape recorder used for documentation. Not shown are the pressure altitude sensor and electronics and the 12 VDC to 115 VAC inverter.

recorded data consisted of two high frequency, high gain temperature traces from each temperature probe, two high frequency velocity traces from each velocity probe, smoothed velocity and temperature traces from the upper velocity and temperature probes, the pressure altitude of the aircraft, and the ambient turbulence level. This latter signal was generated by an electronic network which filtered the velocity fluctuations measured by one velocity probe through a 3 to 20 Hz filter and averaged the result with a 3-second time constant in order to compute the turbulence dissipation rate, $\epsilon^{1/3}$. On some tests, a Meteorology Research Universal Indicated Turbulence System, which operates in much the same manner, but uses a pitot-static probe for turbulence measurement, was added. The response frequency of the hot wire probes and electronics system was about 1 kHz for velocity and 100 Hz for temperature.

2.2 Experiment Procedure

A typical test began at twilight, in the pre-dawn calm, with an atmospheric sounding by the Cessna Cardinal and, if wind shear was of interest, by the dropping of a smoke grenade from the Aero Commander to mark a filament of air for photographic observation of wind drift. The first test sortie followed as soon as there was sufficient light for photography. The sortie of three runs was followed by a pilot balloon launch for wind profile determination, another sounding, and often by another smoke grenade drop. The Aero Commander then returned to base for reloading of smoke grenades, after which the entire sequence was repeated. This pattern continued typically for four or five sorties and a total duration of 2-3 hours, until the ambient turbulence and winds had become great enough to break up the wake too rapidly for meaningful testing to continue.

During a test, all stations (the camera sites, the aircraft, and the ground crew) were in constant radio communication. This

gave the required flexibility for changes in the test plan due to such things as wind shift, increased turbulence, etc. Overall control of test operations was from camera Site #1, directly below the flight pattern.

During each run, the smoke grenades on the Aero Commander were actuated before crossing over Site 1 and then the aircraft heading was held constant until the grenades stopped smoking. The Cessna Cardinal probed the wake by crossing it perpendicular to the generator's flight path and then making a series of consecutive S-turns following behind the Aero Commander (as was shown in Figure 2-1), intersecting the wake as many times as possible until it was no longer visible. The airspeeds and relative flight paths of both aircraft were such that each wake crossing resulted in observation of an older wake than the one before. Figure 2-7 shows one such wake crossing from below, and shows the influence of the probing aircraft on the wake, while Figure 2-8 shows in detail the probes on the right wingtip of the Cardinal penetrating a smoke-marked vortex. For well-marked vortices in calm conditions, positioning of the probes within the order of 1 meter of the desired position was possible; more turbulent conditions and more poorly defined vortices resulted in poorer positioning accuracy.

During each wake crossing an oscillographic record of probe data was made and the crossing time was verbally recorded on a cassette tape recorder, which continued to operate during the entire run. From the latter, the time between penetrations was recorded, and thus the wake age at each crossing could be calculated, given the flight speeds of both the Aero Commander and the Cessna and the geometry of the flight paths of both aircraft. For those tests in which Site 3 was operational, direct photographic records of wake age were available and the recordings of elapsed time served only as a backup.

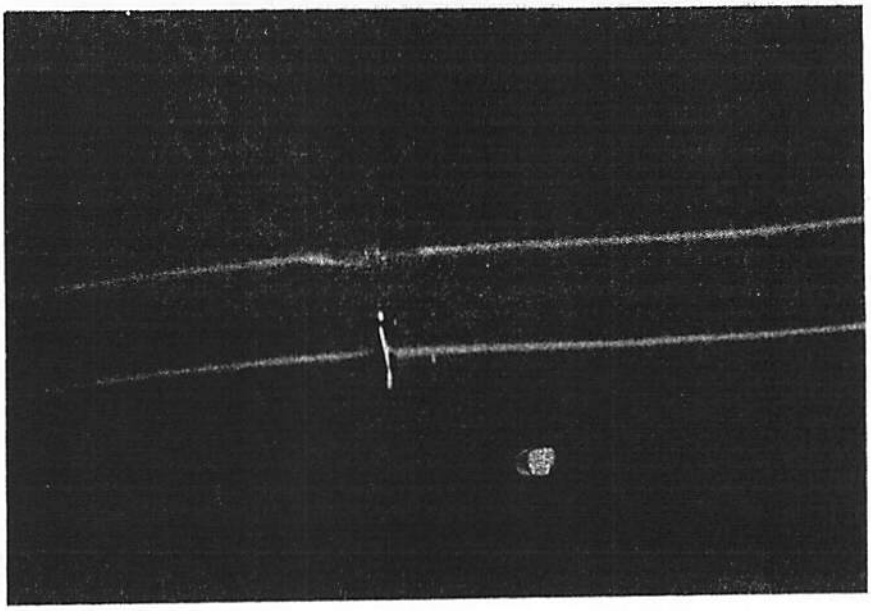

Figure 2-7. Cessna Cardinal penetrating vortices. Note how the first vortex penetrated has been deformed by the downwash field of the probe aircraft.

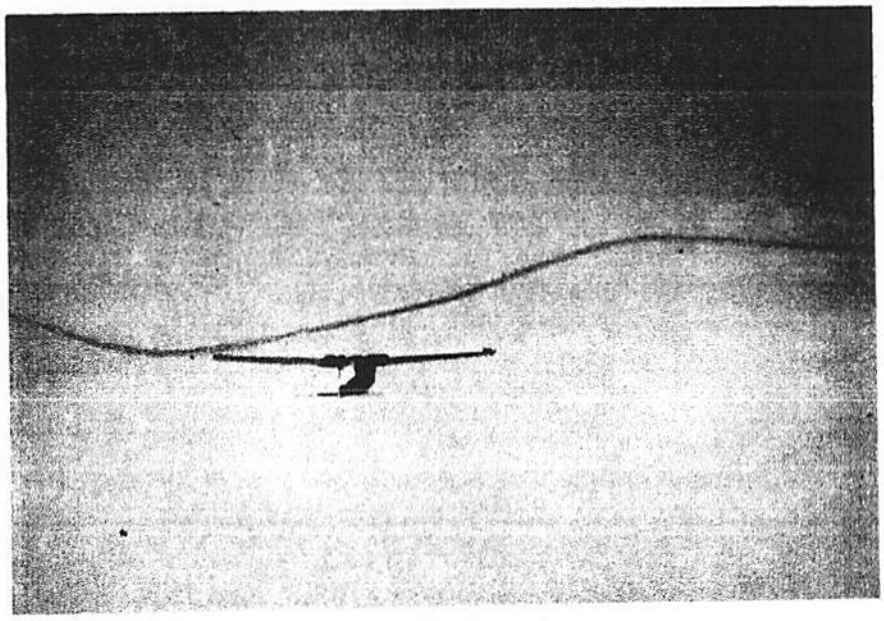

Figure 2-8. Head-on view of Cessna probing vortex. Probes on wingtip to left of picture are passing through smoke-marked core.

During the course of the test day, several series of atmospheric soundings were made with the instrumented Cessna. Relevant data were temperature and turbulence profiles as a function of altitude in the vicinity of Site 1. For these soundings, the Cessna was flown in descending or ascending spirals at a constant air speed between approximately 60 meters above the altitude of the testing pattern and 6 meters above ground level. Sounding data for one typical test day is shown in Figure 2-9. The increase in the turbulence as the early morning stability is eroded by solar heating is clearly shown there.

Figure 2-10 is an oscillographic record of a wake crossing, with all traces identified. Traces 2 and 3 (high frequency temperature) and traces 6 and 7 (high frequency velocity) are AC coupled with a 3-second time constant, so that their zero levels are at the ambient temperature and at the aircraft speed. All other traces are directly coupled to the sensors, and their zero level values are shown in the figure. Direct interpretation of traces 6 and 7 is not possible, because the thin film probes only indicate the magnitude change of the velocity vector, which in turn is the vector sum of the aircraft velocity and the vortex flow. Interpretation of all traces is discussed in greater detail in later chapters.

Qualitative information obtained by studied viewing of the films and photographs included the effects of the probe aircraft on the wake, the locations of burst-type vortex instabilities relative to the sinuous deformation of the wake, the extent of banking exhibited by the vortex pair, and the detailed appearance of the vortex just before probing by the Cessna Cardinal.

Quantitative observation of the photographs enabled measurement of the time required for instabilities to affect the wake, and photogrammetry gave spacing, descent, and vertical separation of the

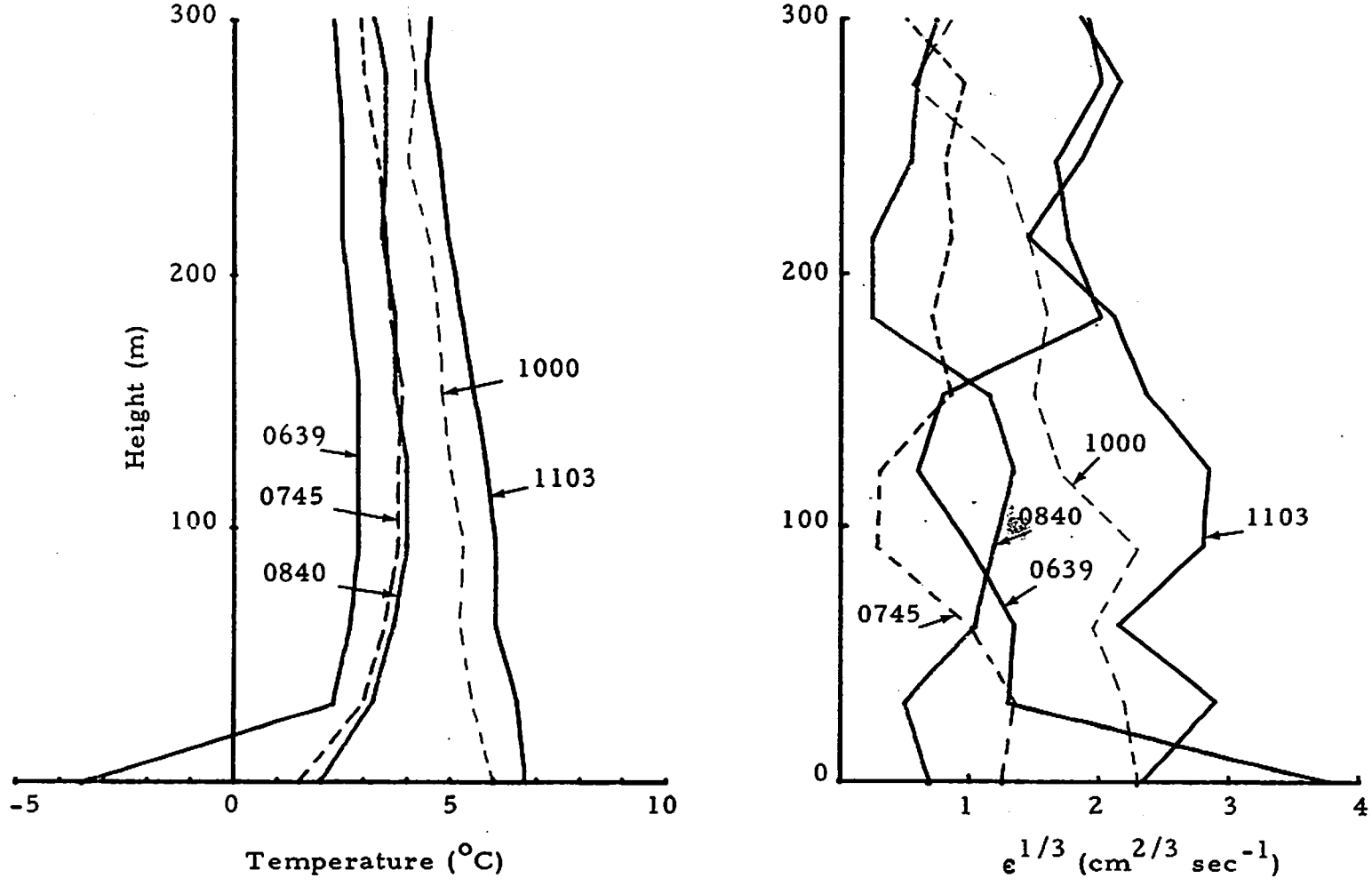

Figure 2-9. Temperature and turbulence soundings for a typical test day (19 December 1973). At 0639 there is a strong surface based inversion and low-level shear turbulence. By 1103 the lapse rate is nearly neutral and thermal turbulence extends uniformly over the whole altitude range.

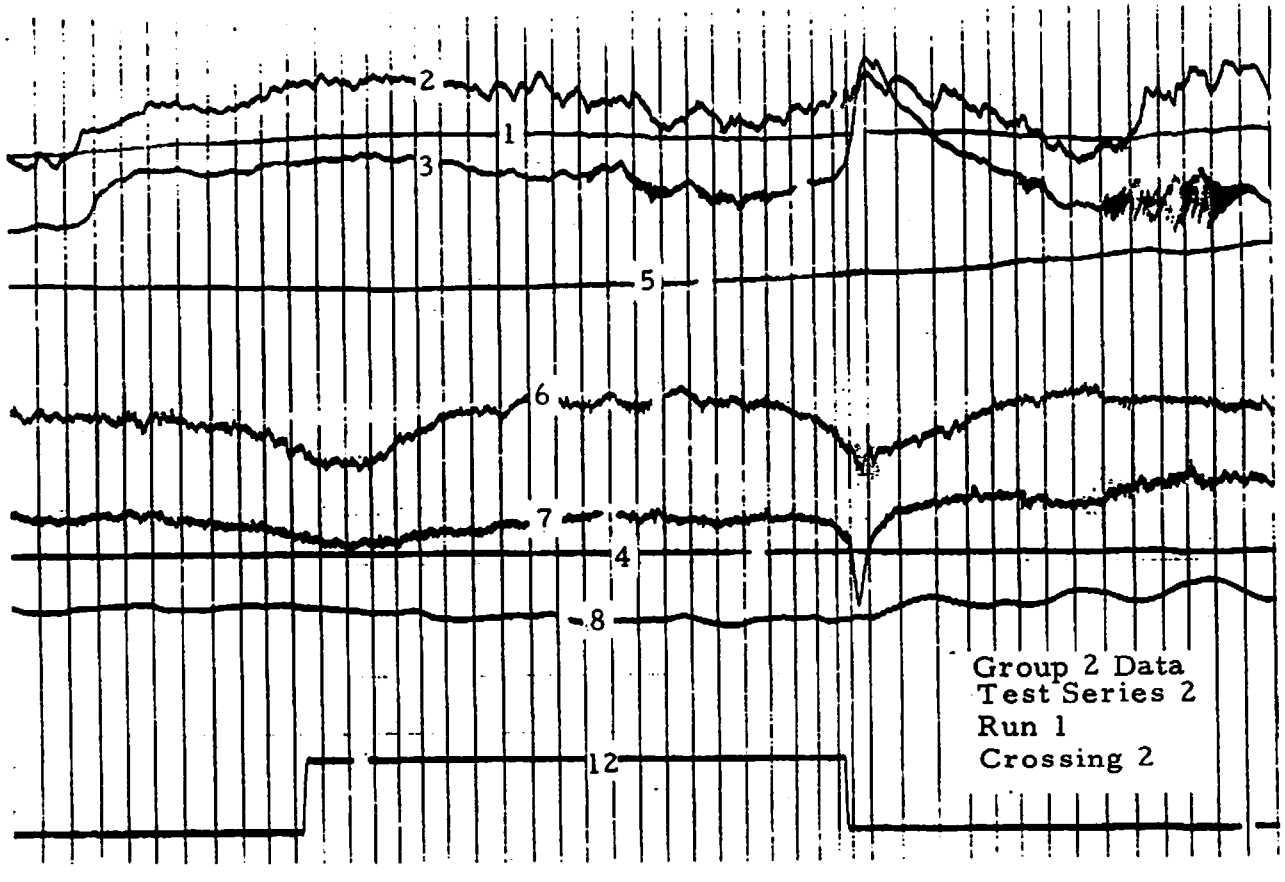

Figure 2-10. Sample oscillographic record of wake crossing. Trace identification: 1 - ambient temperature; 2 & 3 - high frequency temperature; 4 - Cessna airspeed; 5 - turbulence; 6 & 7 - high frequency velocity; 8 - altitude; 12 - event mark. All values increase upward, except that the velocity traces are inverted. The spacing of the vertical lines is 0.01 seconds.

vortices. For the quantitative analyses, the clock in the field of view, and the presence of Site 1 in the Site 2 photographs (with the exception of a few special tests), allowed accurate (within 1 second) correlation of phenomena as seen by all cameras, as well as with that measured by the probe aircraft during wake crossings. The image size of the aircraft or the spacing between specially installed flags provided a size reference for photogrammetry. In a few cases direct computation of image size from knowledge of camera and subject locations and of lens focal length provided a secondary reference.

2.3 Summary of Experimental Conditions

Many of the variables of the test program were under the control of the test team; others were dictated by Nature. Those which were under human control and were essentially constant throughout the entire test program are tabulated in Table 2-2 for reference.

A detailed summarization of the conditions prevailing during each test run is presented subsequently in Table 2-3. The tabulations of ambient turbulence, expressed as $\epsilon^{1/3}$ (see Chapters 3 and 4 for definition and discussions), atmospheric stability (γ')*, and of the crosswind, summarize the major meteorological factors which were studied during this program.

* γ' is the lapse rate of temperature relative to the adiabatic (neutral) lapse rate; in meteorology it is called the lapse rate of potential temperature. Mathematically, $\gamma' = \partial T/\partial z + [(\gamma-1)/\gamma]\, g/R \approx \partial T/\partial z + 1$ in degrees Celsius/100 m, where γ is the ratio of specific heats and R is the gas constant for air.

Table 2-2. Summary of Constant Test Parameters.

Vortex Generator Aircraft	
Type:	Aero Commander 560F
Wing Span, b :	14.9 m
Weight, W :	3000 kg
True Airspeed, U :	54 m/sec
Circulation (elliptic loading), Γ_e :	42 m^2/sec*
Vortex Spacing (elliptic loading), b_{ve} :	11.7 m*
Probe Aircraft	
Type:	Cessna Cardinal RG
Airspeed, U_p :	54 m/sec (approx.)
Field Elevation:	850 m

*Actual values deviated from these numbers. See the discussion in Chapter 4 for details.

Table 2-3. Summary of Test Conditions.

Date	Series	Run	Time	Altitude (m-AGL)	Heading	No. Wake Crossings	$\varepsilon^{1/3}$ ($cm^{2/3} sec^{-1}$)	γ' (°C/100 m)	Wind Direction	Crosswind (m/sec) (+ from right)
					Group I					
3/1/73	1	1	0657	150	015°	4	-	1.7	NE	-
		2	0703	150	015°	4	-	1.4	N	-
		3	0710	150	015°	5	-	1.2	N	-
	2	1	0828	150	015°	4	-	1.0	NE	-
		2	0836	180	015°	4	-	1.0	NE	-
		3	0842	180	015°	5	-	1.0	NE	-
4/6/73	3	1	0615	120	265°	3	-	1.0	-	0
		2	0622	180	265°	3	-	-1.3	-	2.9
		3	0626	180	265°	4	-	-1.4	-	1.2
	4	1	0710	90	265°	4	-	0.4	W	0.4
		2	0715	60	265°	4	-	3.2	W	-
		3	0722	30	265°	3	-	2.9	E	-
	5	1	0806	30	085°	5	-	1.5	E	-
		2	0812	15	085°	5	-	1.4	E	-
		3	0820	15	085°	5	-	1.1	E	-
	6	1	0859	15	315°	3	-	0	SE	-
		2	0905	10	315°	4	-	-1.7	SE	-
		3	0910	6	315°	3	-	-3.3	SE	-
5/2/73	7	1	0618	150	265°	5	0.4	1.3	-	0.2
		2	0625	150	265°	5	0.4	1.5	-	0.1
		3	0632	150	265°	5	0.5	1.6	NE	-
	8	1	0718	150	265°	5	0.5	0.9	N	-
		2	0725	150	265°	5	0.4	1.1	N	1.5
	9	1	0814	180	265°	3	1.3	0.3	N	-
		2	0819	180	265°	4	1.2	0.3	N	-
	10	1	0900	30	315°	3	1.4	0.4	NE	-
		2	0907	15	315°	3	-	0.8	E	-
	11	1	0938	15	265°	-	-	1.0	SE	-
		2	0946	8	265°	-	-	1.0	E	-
6/27/73	12-14		Special vortex dissipation tests; see Tombach and Bate (1973) for details.							

- Data missing or not defined

Table 2-3 (continued).

Date	Series	Run	Time	Altitude (m-AGL)	Heading	No. Wake Crossings	$\varepsilon^{1/3}$ ($cm^{2/3} sec^{-1}$)	γ' (°C/100 m)	Wind Direction	Crosswind (m/sec) (+ from right)
					Group II					
10/26/73	1	1	0725	150	360°	4	-	1.9	E	0.6
		2	0728	150	360°	5	-	1.6	E	0.4
		3	0736	150	360°	3	-	2.1	E	0.7
	2	1	0827	110	360°	3	-	2.4	E	-
		2	0835	110	360°	4	-	3.2	E	-
		3	0840	110	360°	1	-	3.8	E	-
	3	1	0931	250	360°	4	-	3.5	NE	4.1
		2	0938	250	360°	4	-	4.1	NE	-
		3	0945	250	360°	4	-	4.7	NE	3.3
	4	1*	1029	250	360°	1	-	1.6	NE	6.5
		2*	1038	250	360°	0	-	1.4	NE	-
		3*	1046	250	360°	0	-	-0.3	NE	3.3
12/18/73	5	1	0713	150	360°	5	0.9	1.3	E	4.8
		2	0719	150	360°	6	0.9	1.6	E	4.2
	6	1	0757	90	360°	5	1.7	2.2	E	2.6
		2	0802	90	360°	6	1.2	2.2	E	3.4
		3	0808	90	360°	5	0.6v	2.3	E	4.5
	7	1	0856	150	360°	4	1.6v	0.2	E	6.3
		2	0904	150	360°	4	2.1	0.5	E	-
		3	0910	150	360°	4	2.6	0.7	E	6.7
	8	1*	0957	230	360°	3	2.4	0.2	E	5.3
		2*	1005	180	360°	5	2.0	1.0	E	6.6
		3*	1008	230	Turn	6	2.3	0.3	E	6.6
12/19/73	9	1	0706	15	315°	4	1.8	17.2	NW	1.9
		2	0710	15	315°	4	1.7	16.0	NW	1.8
		3	0715	15	315°	4	1.6	16.3	NW	1.7
	10	1	0800	30	315°	4	2.2v	7.7	N	0.8
		2	0805	30	315°	4	2.4	8.3	N	0.6
		3	0811	15	135°	-	2.8	9.0	N	0.4
	11	1	0855	7	315°	4	2.0	3.3	SW	-0.2
		2	0858	7	135°	5	2.3	3.0	SW	-0.2
		3	0902	30	315°	4	2.0	2.5	SW	-0.7
	12	1*	0948	15	315°	4	2.3	-0.1	S	-0.5
		2	0953	15	315°	4	2.3	-0.3	S	-0.7
		3	0958	15	135°	1	2.3	-0.6	S	-0.9
	13	1*	1052	90	315°	3	2.6	0.9	E	-
		2*	1055	L&TO	315°	-	-	-	E	-
		3*	1101	90	315°	-	2.6	1.0	E	-

2/25/74	14	1	0755	150	345°	2	0.4	2.0	E	3.8
		2	0800	150	345°	3	0.5	2.1	E	3.8
		3	0805	150	345°	4	0.5	2.2	E	3.8
	15	1	0907	80	345°	4	1.5	5.1	E	3.7
		2	0914	80	345°	4	1.6	6.3	E	3.3
		3	0920	80	345°	4	1.7	7.2	E	2.9
	16	1	1010	110	345°	4	2.5	1.3	-	2.2
		2	1017	110	345°	4	2.5	0.9	-	2.0
		3	1020	140	345°	3	2.8	1.3	-	1.9
	17	1	1119	300	345°	4	1.8	0.5	-	-
		2	1123	300	345°	3	2.1	0.4	-	-
		3	1127	300	345°	3	2.3	0.2	-	-
2/26/74	18	1*	0738	90	345°	0	0.9	3.1	NW	0.2
		2*	0742	60	345°	0	-	-	NW	0.2
		3	0750	30	300°	4	-	3.6	NW	0.2
	19	1	0833	30	300°	5	1.3	4.7	NW	0.4
		2	0838	15	300°	4	1.3	3.9	NW	0.4
		3	0843	7	300°	5	1.3	3.1	NW	0.4
	20	1	0923	30	300°	4	2.3	-0.5	NE	2.5
		2	0928	15	300°	4	2.2	-0.5	NE	2.4
		3	0933	7	300°	3	2.2	-0.6	NE	2.3
	21	1	1017	L&TO	300°	4	-	-	SE	1.0
		2	1031	50	300°	4	2.4	1.9	SE	1.5
		3	1037	80	300°	3	2.6	0.7	SE	1.2

* Special test to observe effect of non-standard configurations (turns, climbs, descents, control motions, etc.)

v Variable

- Data missing or not defined

3. METEOROLOGICAL FACTORS

The three factors of turbulence ($\epsilon^{1/3}$), wind shear ($\partial U/\partial z$), and stability (γ') are all involved in the motion and decay of vortices. Thus they must be monitored in field experiments on wake evolution, as was the case in this study. Since their forecasting would become a necessity for operational application of a wake vortex predictive system at airports, it is desirable to understand them, their connection with gross meteorological parameters, and the coupling between them.

For vortex prediction, the altitude region of greatest interest is in the lowest levels, say below 70 m, where the simplifications of surface boundary layer theory sometimes aid in understanding and forecasting. However, the meteorological region of interest (i.e., that of longest wake lifetimes) emphasizes the strongly stable cases in light wind, for which no satisfactory theoretical framework is available; and the "real world" includes cases where there are local variations of surface roughness, and nearby mountains complicate matters.

Despite its complexity, the importance of the subject still dictates that we distill whatever information we can about meteorological factors from the present experiments. This chapter explores two facets: the correlation of turbulence and stability, and the prediction of turbulence intensity.

3.1 Turbulence vs Stability

In many of the test cases wind shear was apparently not important for vortex breakup, and so our attention focuses on $\epsilon^{1/3}$ and γ'

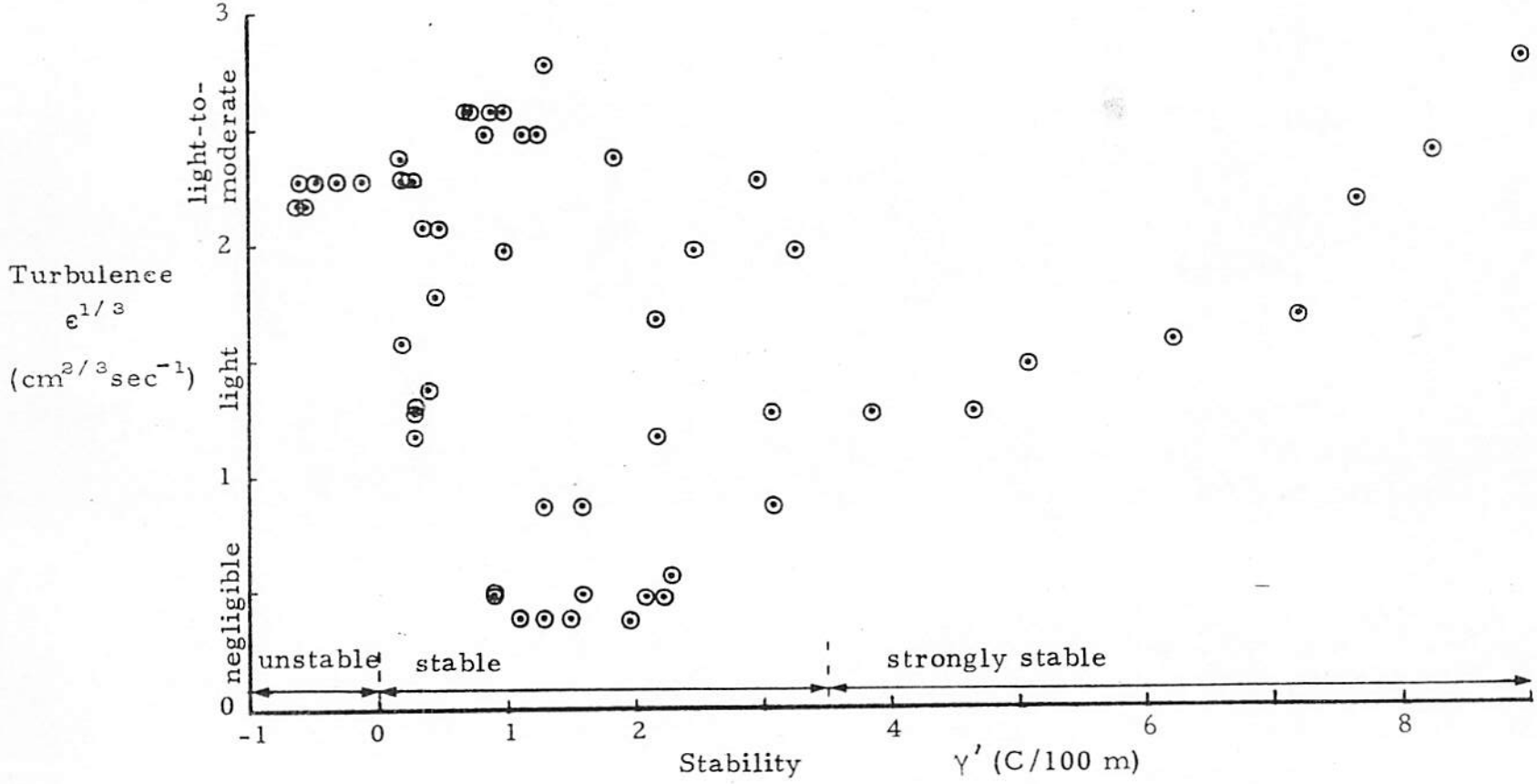

Figure 3-1. Correlation of Atmospheric Turbulence ($\varepsilon^{1/3}$) and Stability (γ'). The high turbulence levels at the far left are due to the overturning of unstable air; those on the far right are generated by shear in drainage flows, in spite of the strong stability. In the $0 < \gamma' < 3.5$ stable region various forcing functions give scatter.

and their correlation and coupling.* Figure 3-1 is a plot of the $\epsilon^{1/3}$ and γ' data from Table 2-3. It can be seen that the turbulence levels divide into three conditions: for $\gamma' < 0$ (unstable), the turbulence is never low and centers around the upper end of what is usually considered "light": for $0 < \gamma' < 3.5$ C/100 m (slightly stable), the turbulence values are widely scattered; for $\gamma' > 3.5$ the turbulence increases about linearly with stability.

The data on Figure 3-1 represent a very limited set, and yet cover a wide range of altitudes (7 m to 230 m) and wind speeds from negligible to moderate. Thus one should be cautious about generalizing to other altitudes, winds and topographies. Nevertheless, the data do stratify into groups in a manner which illuminates physical mechanisms and is consistent with certain other results.

When $\gamma' < 0$ the atmosphere is unstable and turbulence is generated by overturning of the air, as in the thermal plumes resulting from surface heating. On the other hand, when γ' is large, i. e., the extreme stability case, the turbulence appears to increase with stability, opposite to what is usually considered to be the case. The likely reason, as outlined by MacCready, et al (1974), is based on the local high mountains providing a temperature driving force through drainage winds. These winds, in the stable light wind conditions, induce horizontal movements and hence vertical shears which cause exceedances of the critical Richardson number (in all but the stablest conditions close to the ground), resulting in turbulence. The turbulence is generated aloft and then disperses from its originating altitude. This

---

* γ' is the lapse rate of potential temperature (i. e., the actual lapse rate minus the adiabatic lapse rate). $\epsilon^{1/3}$ is the rate of dissipation of turbulent energy in the idealized case of isotropic turbulence. An explanation of this concept is given by MacCready (1962).

concept of a stable temperature gradient being associated with turbulence in complex regions surrounded by high mountains is borne out by observations on a plume diffusion study near Page, Arizona, and by the extensive turbulence study by Boeing for the Air Force called LO-LOCAT, both cited in the above paper. It is also noted that Leahey and Halitsky (1972), studying plume diffusion in drainage flows, found the least dispersion in neutral cases. Again, stability was associated with the mechanism for inducing flows, which then caused turbulence.

For γ' in the intermediate range of slightly stable lapse rates, Figure 3-1 shows much scatter. Evidently sometimes the stability dominates and damps out the turbulence, while other times the generating mechanism, say mechanical friction at the ground, dominates and gives moderate turbulence.

Specifically, at the Mojave test site there are mountains within 20 to 100 km on three sides, some of which rise up to 300 m above the airport. The same conditions which are conducive to strong atmospheric stability also contribute to drainage flows of cold air down the mountain slopes and, in layers, through the valley below. The resulting shears are the source of turbulence -- and also are the shears which are of concern because of their effect on wake tilting (to be discussed in Section 4.2). Figure 2-9 gave an example of the relation between turbulence and stability at the test site. Early in the morning, at 0639, the lapse rate was stable and the turbulence aloft was stronger than that below 150 m, except for a peak in the turbulence level at the surface due to locally generated turbulence by surface roughness.

3.2 Turbulence Predictions

Operationally, one wants to be able to predict the temperature lapse rate, wind gradient, turbulence, and mean wind in the lowest

70 m or so enough ahead of time to permit air traffic controllers to alter landing/takeoff procedures -- say 10 minutes. It is desirable to do this with simple, local, ground-based equipment. Handling the total problem in the general case is beyond present capabilities of even very complex systems, but some partial studies can be of value in approaching the problem. Two of these partial studies were convenient to include in the present program and are reported here. For the first we utilize some meteorological measurements made during the course of the program to see how well wind speed measurements near the ground can be used to infer turbulence aloft in light wind conditions without stability information being used -- for this particular site and weather conditions. For the second we continue with the concepts of surface boundary layer theory and estimate the wind speed above which there is no wake turbulence problem at a particular site.

There were two field experiment periods with surface data at Mojave (December 19 and February 25-26) when wind and stability and turbulence profiles were also available. The following table shows the meteorological data available from these periods. The left side of each column relates to the December case, while the right side relates to the February case.

Height	Acoustic Radar	$\epsilon^{1/3}$ (turb.)	T (temp.)	U, θ (wind)	σ_w (turb.)	Shear (U profiles)
3 m		|		X|		
6 m					X|	
8 m				|X	|X	
10 m				X|	X|	
5-300 m		X|X	X|X			X|X
15-500 m	|X					

The meteorological portions of these tests represent a huge amount of data, which will not be duplicated here. Figure 2-9 gave a sample of some of the soundings for a brief period. We examined the December data in great detail and have drawn a group of conclusions from it which we present below. The February cases were not evaluated in detail since a cursory look suggested they would not alter the main conclusions.

The main conclusion is that the early winter morning meteorology in the Mojave desert is complex. Its details are likely not predictable, in the ordinary sense, but extrapolations in the vertical (say from 15 m to 50 m), and in time (say up to 10 minutes) seem at least marginally useful, with accuracies good enough to help with wake decay studies and operations as long as one is after qualitative information.

The observational techniques used on the program (surface measurements, aircraft soundings, pibals, and smoke-winds) do have small enough errors to give data adequate for correlation with vortex motion and decay characteristics. However, the complexity of the flows at low level precludes reliance on standard surface boundary layer theory for quantifying predictions.

The December 19, 1973 case, covering 0630-1100, showed strong stability at the start (20 C/100 m below 30 m, isothermal to 300 m), reaching neutral at about 0930 (when the 10 m wind reached a minimum). The minimum $\epsilon^{1/3}$ was 0.3 $cm^{2/3} sec^{-1}$ at 90 m at 0720. Below 15 m, $\epsilon^{1/3} > 1.5$ $cm^{2/3} sec^{-1}$. The $\epsilon^{1/3}$ soundings implied $\epsilon^{1/3}$ was being generated aloft and transported down, and also generated at the ground and transported up. The surface (say 5 m) quantities were always in the 1.7 to 3.5 $cm^{2/3} sec^{-1}$ range, and minimum values tended to be at 90 m prior to 0820.

Wind measurements at 5 m and 10 m showed no normal gradients (0600-0700, 3.3 mph at 5 m, 8.1 mph at 10 m; while later in some cases the 5 m and 10 m winds were identical). The profiles did not approach the conventional logarithmic wind profile even considering stability modifications.

For these light aircraft tests, the depth of interest is up to 30 m, with most interest probably in the 10-20 m range. For operational purposes with the landing of large aircraft, the region to 50 m is of primary significance.

To estimate $\epsilon^{1/3}$ from U at these low altitudes and surface roughness, one can start with the neutral condition formula

$$\epsilon^{1/3} = \frac{U_1 k^{2/3}}{z^{1/3} \ell n (z_1 / z_o)} \quad . \tag{3-1}$$

We tried this for the average 10 m wind and assumed z_o = 4 cm (the roughness scale of long mown grass). Results are given on Figure 3-2, compared to $\epsilon^{1/3}$ observations from the airplane -- for 15 m and 50 m heights. For near-neutral and slightly unstable, where the formula should hold in steady-state conditions with moderate wind, observed values are twice computed values. Apparently some $\epsilon^{1/3}$ source is from above, or surface roughness is <u>much</u> greater than the 4 cm assumed, or the meteorological situation is not treatable by simple equations. For strongly stable, observed is less than computed, as would be expected.

To estimate $\epsilon^{1/3}$ from σ_w, we examined the available data: σ_w from a sigma meter at 5 m and 10 m, and from w at 10 m. We utilized the w trace (deriving σ_w by taking 1/4 of the peak-peak variation of w within a 15 minute sample, with biggest peak omitted), since the σ_w values were mostly zero and threshold considerations caused uncertainty, and the short averaging times of the sigma meter

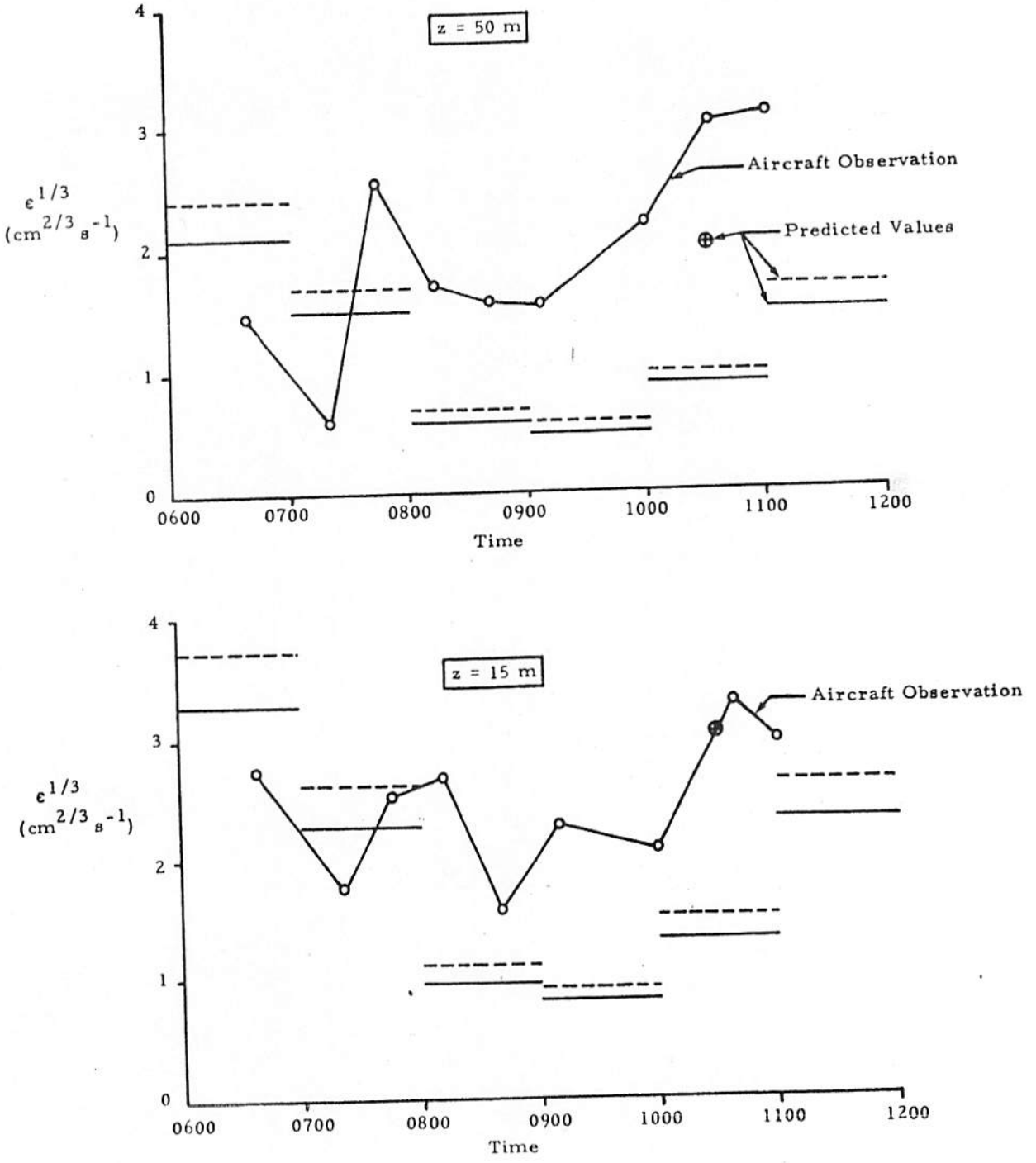

Figure 3-2. Comparison of Predicted and Measured Turbulence Values at Two Heights. Two surface roughness scales were used for the predictions -- z_o = 8 cm (---) and z_o = 4 cm (—) -- which were computed from neutral boundary layer theory using U at 10 m. The two points (⊕) were extrapolated from measured σ_w at 10 m.

limit the usefulness at low wind speeds. The results for the 10-11 o'clock period when σ_w was large enough for significance (average 0.25 m/sec) are shown in Figure 3-2, and are usably close to the observed values. The formula that was used for the computation was

$$\epsilon^{1/3} = \frac{\sigma_w}{L_w^{1/3}} \qquad (3\text{-}2)$$

with the assumption that σ_w is constant with height (valid for neutral atmospheres). L_w is taken as 40% of the height, z. The rationale for these assumptions is given in the report by Lissaman, et al (1973) and the paper by MacCready, et al (1974).

In summary, for our limited experiment, the concept of simply using low altitude wind and the neutral surface boundary layer equations for getting turbulence at 50 m, without considering stability, is adequate if one can sometimes accept an error (in the conservative direction, as far as vortex duration is concerned) of a factor of 3. Utilizing stability information would improve matters, but not very much. Using Eq. 3-2 and the sigma meter approach seems somewhat more effective -- as is to be expected because then we are starting with a quantity which included stability effects already. Note that the wind profiles show that sometimes, in these weak conditions in or near complex terrain, there are randomly-moving layers which cannot possibly be put into surface boundary layer theory developed for homogeneous conditions. Then the most one can hope to do is operate with categories rather than explicit predictions, categories established empirically for the site or for a comparable location.

To consider the easier problem of what wind would assure fast breakup of vortices at the Mojave site, first note that with stronger wind there is usually enough turbulence to keep the layers

below 50 m well "connected", and also to overpower somewhat the effects of stability. Then the neutral boundary layer equation can be used. If we choose a condition with a 7 m/sec wind, at 15 m, for an airport of $z_o = 4$ roughness (long mown grass),* Eq. 3-2 gives $\epsilon^{1/3}$

z(m)	$\epsilon^{1/3}(cm^{2/3}sec^{-1})$
15	6.2
30	4.9
50	4.1

At the 50 m height this $\epsilon^{1/3}$ can be taken as the $\epsilon^{1/3}$ to use in decay calculations. At lower altitudes the $\epsilon^{1/3}$ value needs some correction terms to let it be applied to the Crow-Bate instability theory (Lissaman, et al., 1973, and Section 4.3 of this report) because of attenuation of large eddies. In very strong stability there can be a suppression of such wavelengths too, but such stability is unlikely near the ground in such strong winds.

Such turbulence magnitudes as shown above give less than 30-second linking times for vortices from all aircraft. Adding 20 seconds to account for decay after linking still gives safety with 1-minute spacing. Thus a 15 kt (7 m/s) wind speed rule for safe airport operation without concern for wake turbulence seems reasonable, for conditions similar to those prevailing at Mojave during these tests.

*Probably the smallest roughness to be expected at an airport. Buildings and topography would cause higher values.

4. WAKE BEHAVIOR

The behavior of aircraft wakes is strongly governed by the prevailing meteorological conditions, particularly winds, atmospheric stability, and turbulence. Although not a meteorological factor itself, the influence of the ground plane also significantly affects the local meteorology, as well as the vortex dynamics of those wakes generated in, or moving into, ground effect. These meteorological factors are all intimately coupled, hence the ultimate fate of an aircraft wake generated in the atmospheric environment is a result of a complicated combination of all of them.

The specific effects of each of these factors would be expected to exhibit varying levels of relative importance at different times and under different situations. This is true under operational flight conditions (such as at airports), as well as for the conditions which existed during the experiments reported herein. Thus, a significant factor involved in performing these experiments was that of making measurements which would allow meaningful data to be obtained with all of the normally coupled meteorological effects properly isolated.

Significant wake properties or parameters of its motion which were measured in these experiments were the temperature and size of the wake, its descent and banking, the spacing of the vortices, and the decay of the organized vortex structure. The results of these measurements are presented below.

4.1 Wake Descent

The descent of an aircraft wake is influenced by several factors including principally the mutual induction of the vortex pair, atmospheric convection, possible atmospheric turbulence and stability, and

the proximity of the ground plane. To define the magnitude of influence of these various factors, wake descent was measured photogrammetrically from the pictures taken generally by the Site 2 cameras. Also, in Group II, direct measurement of the vertical position of the probe aircraft while crossing the wake was recorded by the on-board altitude sensing unit. These two sets of measurements provide somewhat different descent data: the on-board indication provides a direct measure of conditions at the point of each vortex crossing, while the photographs allow localized motions due to turbulence and to the sinuous instability to be smoothed out to obtain average wake descents. Thus the localized measurements were useful for the discussion of wake buoyancy presented in a later section of this chapter; only the photographic measurements will be considered for this discussion of wake descent.

The sequence of photographs in Figure 4-1 illustrates the type of records from which descent was obtained. Although this particular test was a low level one (h_o = 30 m) and the site and camera placement were not the same as those described in Section 2.1, the technique of data reduction was the same as in the higher altitude tests. These photographs show a deceptively simple behavior, with a straightforward descent at constant speed for the first 30 seconds. Between 30 and 45 seconds, however, the two vortices separated vertically by a considerable distance and the upper vortex then broke down and disappeared. The beginnings of this vertical separation are visible at 30 seconds; the residual smoke from the decayed vortex can barely be seen above the intact vortex at 45 seconds. At 60 seconds the remaining vortex is also seen to be breaking down.

In the next section it will be shown that this asymmetrical behavior is coupled with wind shear. Here, the absence or presence of vertical separation will be used as a factor for classifying the descent behavior of wakes, since unbanked wakes can be expected to behave differently than those which are rolled well over onto their sides. To

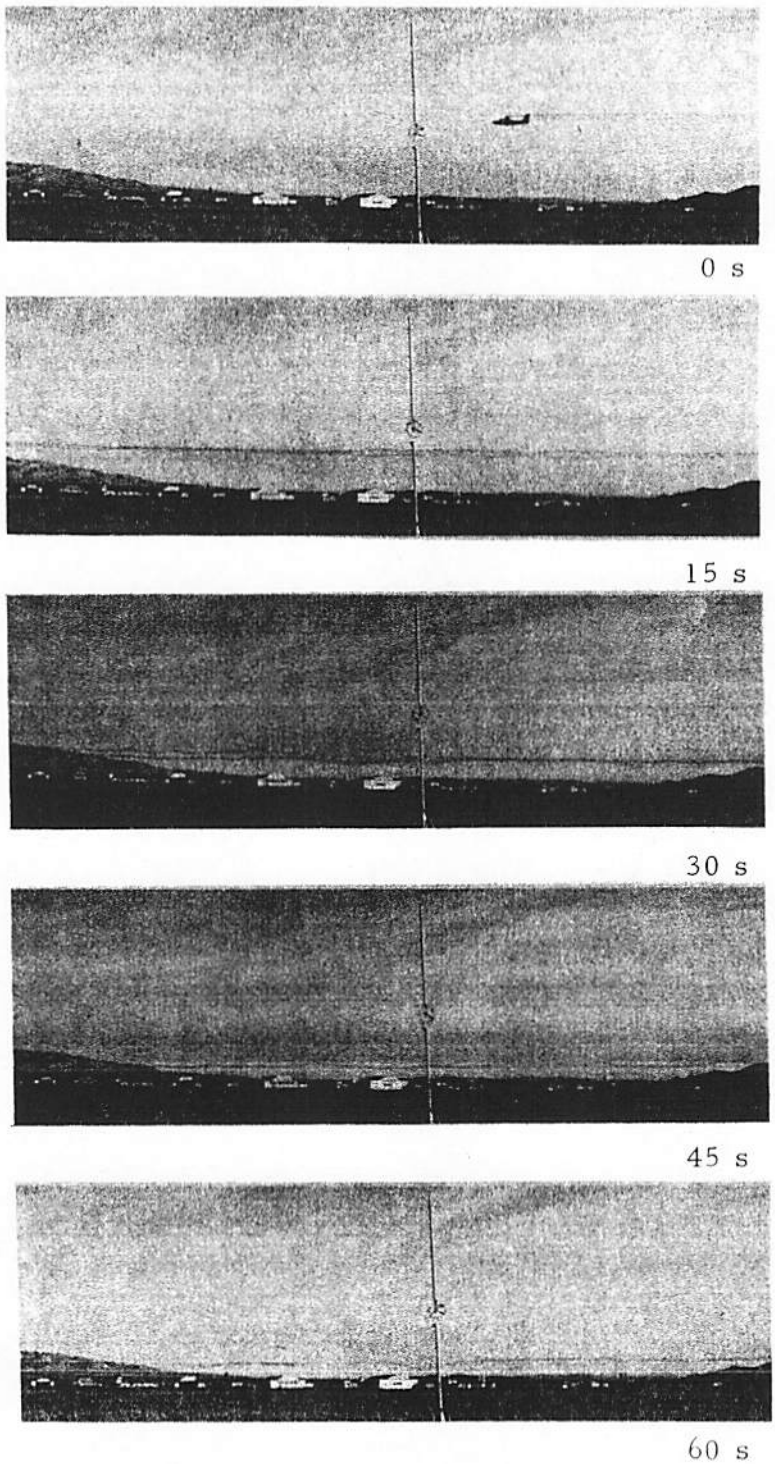

Figure 4-1. Side View of Descent of Wake Generated at 30 m. (Group II, Series 10, Run 1).

avoid the complicating influence of ground effect, only the descent of wakes generated at least 60 m above the ground will be considered.

Considering first only wakes for which the magnitude of the vertical vortex separation, Δd, never exceeded 4 m (i.e., those for which the tilt angle never exceeded about 25°), photogrammetry shows the descent trajectories plotted in Figure 4-2 for unstable and neutral stratifications and in Figure 4-3 for the stable isothermal and inversion conditions.

In Figure 4-2 the wakes actually rose in the two unstably stratified cases shown, probably due to being carried upward by the considerable vertical currents which accompany instability. The high turbulence which naturally occurs in such an unstable atmosphere resulted in very brief lives for these wakes.

On this same figure, the wakes in a neutral atmosphere show a fairly rapid descent, with initial speeds of 80 to 130 meters per minute. After 20-30 seconds the descent has slowed noticeably, to 60 to 80 m per minute. All of these speeds well exceed the descent rate computed from

$$w = \frac{Wg}{2\pi \rho U b_v^2} \qquad (4\text{-}1)$$

where substitution of $W = 3000$ kg, $\rho = 1.11$ kg/m^3, $U = 54$ m/s, $b_v = 0.78\, b_{ve} = 9.1$ m*, and the acceleration of gravity, $g = 9.8$ m/sec^2, give $w = 0.94$ m/s = 57 m/min. (Note that if b_{ve} had been used in this formula, the value of w would have been 39% slower.)

---

*b_v is the actual vortex spacing given in Section 4.5; b_{ve} is the predicted vortex spacing for an elliptically loaded wing.

Wake descent trajectories in more stable atmospheres are presented in Figure 4-3. Here the range of initial descent speeds is between 45 and 75 meters per minute -- which neatly bracket the computed value of 57 m/min and are within about 25% of it. Although the wake lifetimes in this figure are considerably longer than those in the less stable conditions of Figure 4-2, the slower descent speeds here result in total descent distances which are comparable or slightly less than those in the previous figure. As before, there is often slowing down of the speed of descent after 30-40 seconds, with descent speeds at 50 seconds typically about 1/2 to 3/4 of their initial values. Some wakes actually reverse direction and ascent in the last moments of their lifetimes; a few descend at relatively constant speed until they break up.

The difference in descent speeds of the long-lived neutral wakes in Figure 4-2 and the stable wakes of Figure 4-3 is quite dramatic and suggests that wake buoyancy may play a role in governing wake descent. The effect of turbulence on the descent rates seem to be considerably less significant, since the difference in descent rates is established very quickly ($t \lesssim 10$ s), before any turbulent effects would be likely to manifest themselves.

Buoyancy is a plausible mechanism which could have an effect on wake descent, with an increased retarding tendency in a more stable atmosphere.* But, it is difficult to explain why the neutral case, in which there is no buoyancy, shows wakes descending much faster than would be predicted by theory, while the more stable cases give descent speeds within reasonable tolerances of the theoretical values. Perhaps the two long-lived neutral cases in Figure 4-2 were singularities -- wakes in a downward moving air mass. Only more data can settle this question. Unfortunately, long-lived wakes in neutral condi-

*But, there is not even agreement on whether buoyancy accelerates or retards vortex descent. See Lissaman, et al (1973) for a comprehensive discussion of the various theories.

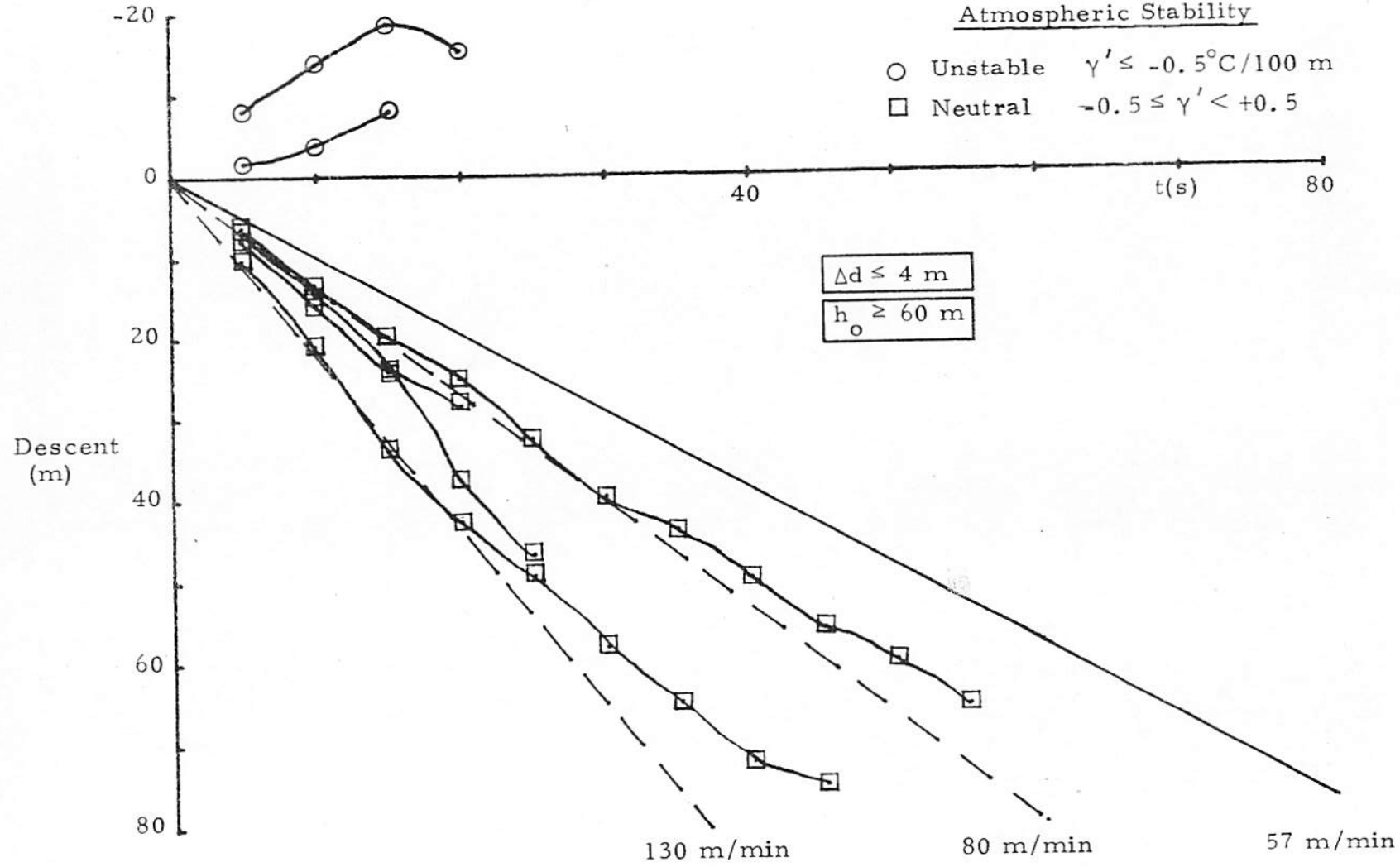

Figure 4-2. Wake Descent Trajectories Under Unstable and Neutral Atmospheric Stratification, for Wakes Out of Ground Effect Which Remain Relatively Level During Descent. The calculated descent speed of 57 m/min (see text) is represented by the heavy line; two other descent rates are indicated by the broken lines. Each data point is the average descent for about 200 m of wake length (the amount visible in one frame of film).

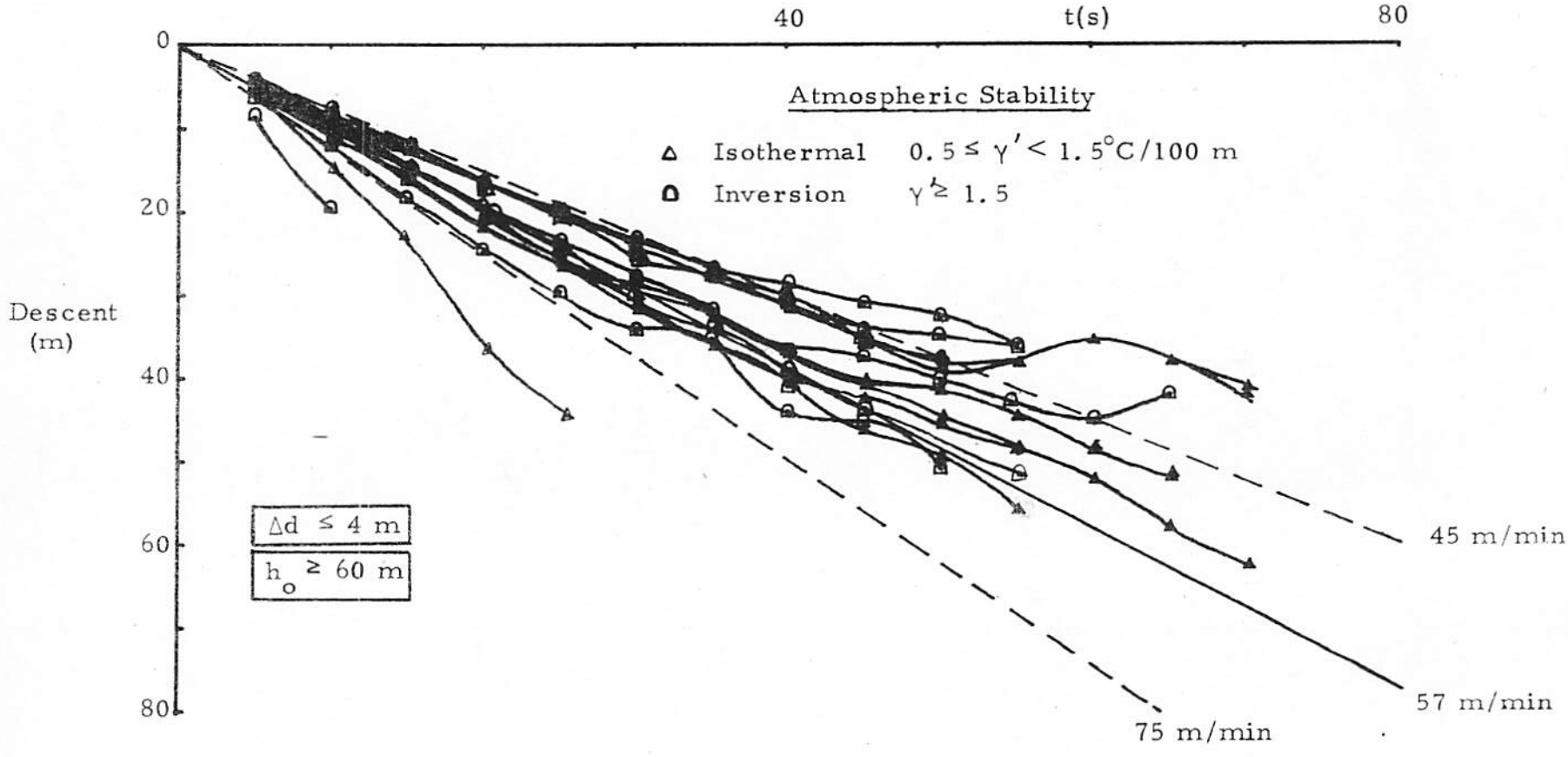

Figure 4-3. Wake Descent Trajectories in Stably Stratified Atmospheres, for Wakes Out of Ground Effect Which Remain Relatively Level During Descent. The solid line is the descent rate calculated from the aircraft weight and initial vortex spacing (see text); two other arbitrary rates of descent are indicated by the broken lines.

tions are hard to find because seldom is a neutral lapse rate accompanied by low turbulence, except possibly over the ocean. *

Theoretical models of wake descent in a stratified atmosphere indicate either increasing descent speed with time if no mixing between the wake and its surroundings (or detrainment only) is assumed, or decreasing speed if entraining mixing is postulated. The data presented here tends to support the models with mixing. However, the change in descent speed (either increasing or decreasing) predicted by most models to take place over a one-minute period is not very great and thus the assessment of modeling techniques using measured descents is not definitive. Data for longer-lived wakes, under calmer atmospheric conditions than those which prevailed during the current tests, might yield a more satisfactory assessment of the effects of stability alone on wake descent; the answer might only be of academic interest, however, since other factors (for instance turbulent mixing) appear to cause the wake descent speed to slow down by a significantly greater amount than the speed change predicted by these models.

Most of the runs in Figures 4-2 and 4-3 were flown either into the wind or downwind, and there was little or no crosswind component. In the Group II tests, the generator aircraft flight path was intentionally aligned perpendicular to the wind, which resulted in more pronounced vertical separations between the vortices, as will be discussed in the next section. Such wakes, in which the vertical spacing between the two vortices was more than 4 m at some point in their lifetimes

---

*The hazards of making inferences based on limited data are well displayed by comparison of this discussion with that in the Tombach and Bate (1973) preliminary report. There, a considerably smaller data base suggested that increasing stability resulted in increased descent speed; exactly contrary to the observations presented here.

(corresponding to bank angles in excess of about 25°) have been considered separately here. Their descents are shown on Figure 4-4. The range of initial speeds is again 45 to 75 m/min, as would be expected before significant banking had taken place. Surprisingly, banking does not change these speeds much as the wake ages and the trajectories do not look much different than those for unbanked wakes. The two neutral cases open the entire range of descent speeds, from the slowest to the next to the fastest, with the longer-lived one descending faster than most of the more stable wakes, in accord with the results of Figure 4-2.

The considerable slowing down of wake descent speed which manifested itself in previous experiments with a Cessna 170 wake (Tombach, 1973), and which was ascribed to wake tilting, is not apparent in Figure 4-4. For the cases shown, the average vertical separation at the latest times when both vortices of a given wake were still intact was 7.2 m -- about 80% of the measured initial vortex spacing, or a bank angle of about 50°. This value should be compared with the average of 5.2 m* for all of the Cessna 170 tests, which corresponds to about 60% of its measured initial vortex spacing. This gives an average bank angle of about 35° for all of the Cessna 170 runs out of ground effect; many were much more severely banked, and some had rolled past the vertical. Such extreme bank angles for wakes out of ground effect were not observed in the current test program, and thus the effect of wake tilting on wake descent might be expected to be less than for the earlier experimental program.

*This is an unpublished figure calculated from the raw data of that experiment.

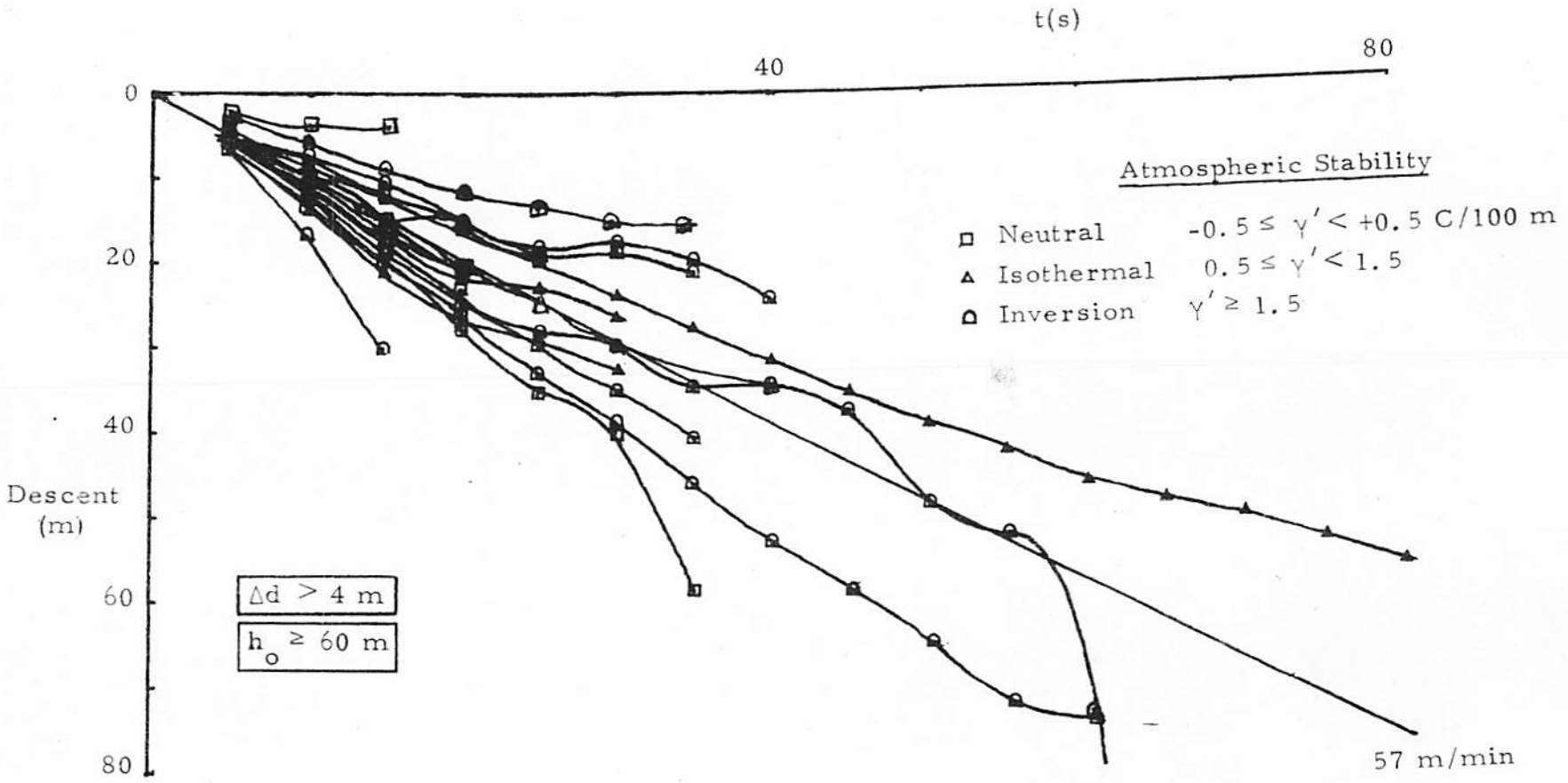

Figure 4-4. Descent Trajectories for Banked Wakes. The theoretical descent rate for unbanked wakes is indicated by the solid line.

In general, the following points emerge from this discussion:

1. The initial rate of descent of a wake is usually within 25% of the theoretical value (computed using actual vortex spacing) in a stably stratified atmosphere. Descent in an unstable atmosphere is unpredictable, and ascent is possible. In this experiment, the most rapid descents (50% faster than theory) were recorded by wakes in neutrally stable conditions.

2. The descent speed slows down after some 30 seconds, and is usually 50 to 75% of its initial value by 50 seconds after generation.

3. Wake tilting to angles of up to about 50° seems to have little discernible effect on wake descent rates.

4. The descent distances in stable conditions were at most 50-60 m, while in neutral conditions 60-75 m descents were attained.

4.2 Wake Tilting

Significant tilting of the plane of the wake as a regular feature of wake behavior was first noted by Tombach (1972, 1973). The direction of tilt was correlated with the direction of the component of the wind which was perpendicular to the wake, and it was found that the upwind vortex descended below the downwind one in 73% of the cases. It was speculated that shear in the atmospheric boundary layer could be the cause of the tilting. Burnham (1972) also reported a similar phenomenon with transport aircraft wakes near the ground and developed a simple ad hoc model for computing the behavior. Lissaman et al (1973) explored analytically the effect of shear on a wake and computed that, with shear in the sense of a wind flow in a boundary layer, the recirculating cell about the upwind vortex was enlarged and the downwind cell contracted. No mechanism was found to explain wake tilting, however.

Expanding on the work by Lissaman, et al, a model for the streamlines associated with a vortex pair in wind shear near the ground was developed by Brashears, et al (1974). Their model indicates that banking of the wake does occur, but in a more complex manner than presumed by Tombach. They conclude that the upwind vortex descends (relative to the other vortex) in weak shear, in agreement with the Tombach results, but that it rises in strong shear; and they present experimental data which appears to support the model prediction. They also suggest that atmospheric stability may be an additional factor influencing the tilting.

To provide additional experimental data on this phenomenon, most of the Group II tests were intentionally flown in a crosswind. A flight level at which substantial wind shear was present was sought out, using as a guide the visual observation of the smoke grenade drops before and after each sortie. Figure 4-5 shows one such smoke grenade drop and illustrates the approach used.

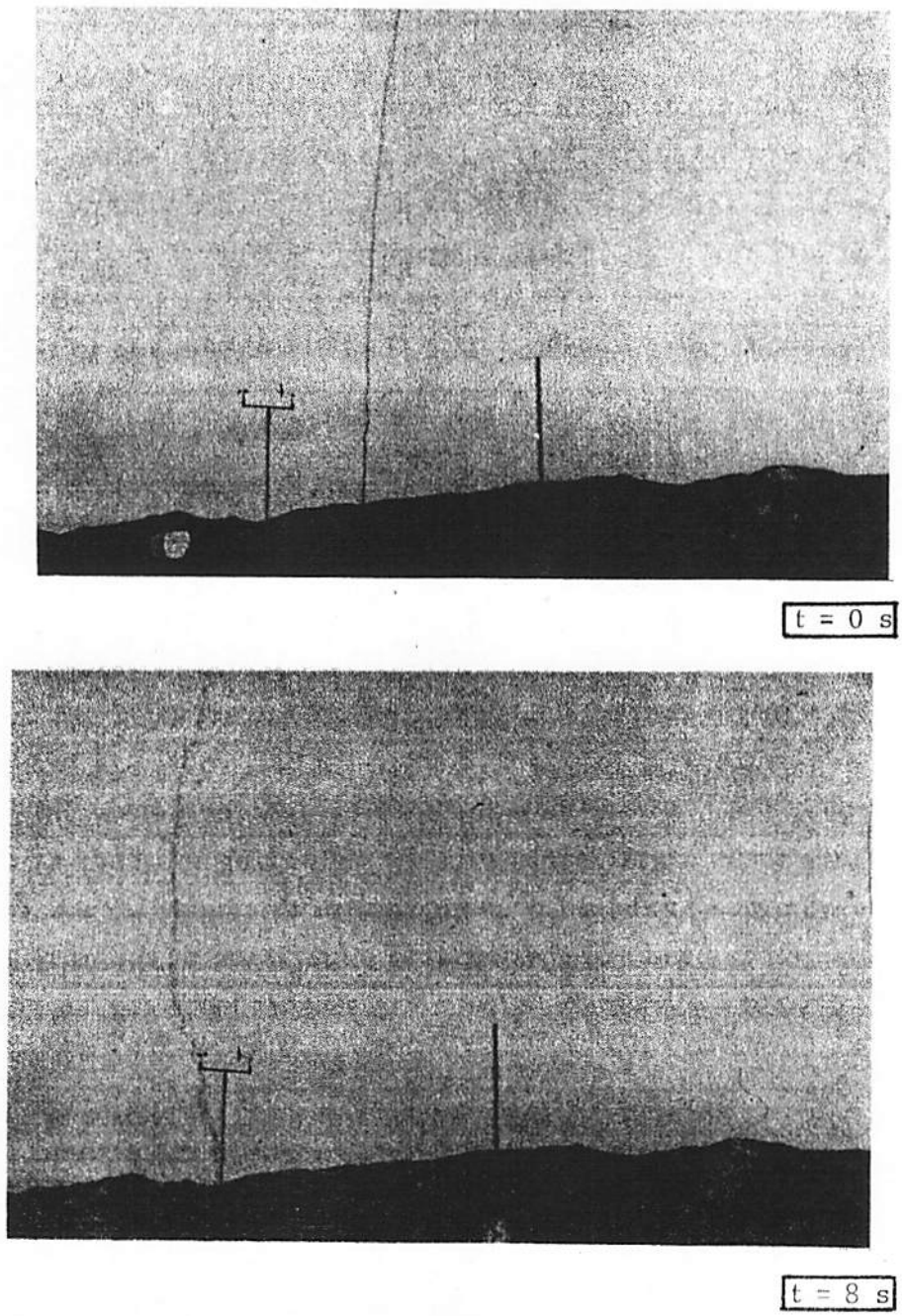

Figure 4-5. Smoke Grenade Drop Preceding Series 9 (Group II). The camera is pointed along the flight path direction (315°) so that the smoke drift indicates the shear component across the wake. The wind vane shows the surface wind to be a head-wind with a slight crosswind component from the right. Two levels of shear, with opposite signs, are present at the two heights indicated by the arrows on the lower photo. All of the Series 9 runs were flown in the lower shear region, which had a strength of $\tau = 0.10\ s^{-1}$ ($\sigma = 0.24$) at the time of this smoke drop. (σ is defined on the next page.)

The degree of vertical separation of the two vortices as a function of wind shear, for wakes generated more than 100 m above the surface, is plotted in Figure 4-6. Positive shear corresponds to counterclockwise vorticity from the perspective of the pilot of the vortex generator aircraft, or to vorticity in a boundary layer flow from the pilot's right. The shear is expressed in terms of a non-dimensional form

$$\sigma = \frac{\pi}{2\Gamma_0} b_v^2 \tau \ ,$$

where τ is the shear in units of meters per second per meter. For the conditions of these experiments the measured values are $\Gamma_0 = 52.6\ m^2/s$ and $b_v = 0.77\ b_{ve} = 9.01$ m so $\sigma = 2.42\ \tau$. The vertical separation Δd is positive when the left vortex is lower than the right one, i.e., when the wake rotates counterclockwise. In the figure there is no significant tendency for tilting to occur in one direction or the other, a probable consequence of the weak shears encountered. Also, the magnitude of the vertical separation of the vortices is, with one exception, always less than 5 m so that bank angles remain less than about 35°.

Stronger shears can be found closer to the ground, but the proximity of the ground itself introduces complicating effects. The plots in Figure 4-7 show the situation here. This time there is a slight preference for Δd to have the opposite sign than σ when $\sigma < 0.12$, and this trend is quite definite for $\sigma > 0.12$. Such a behavior, corresponding to the descent of the upwind vortex in a boundary layer, corresponds with the prior observations of the Cessna 170 wakes.

In order to ascertain whether some aircraft characteristic, such as the normally clockwise (when viewed from the tail) propeller rotation, could cause this preference for what was generally clockwise

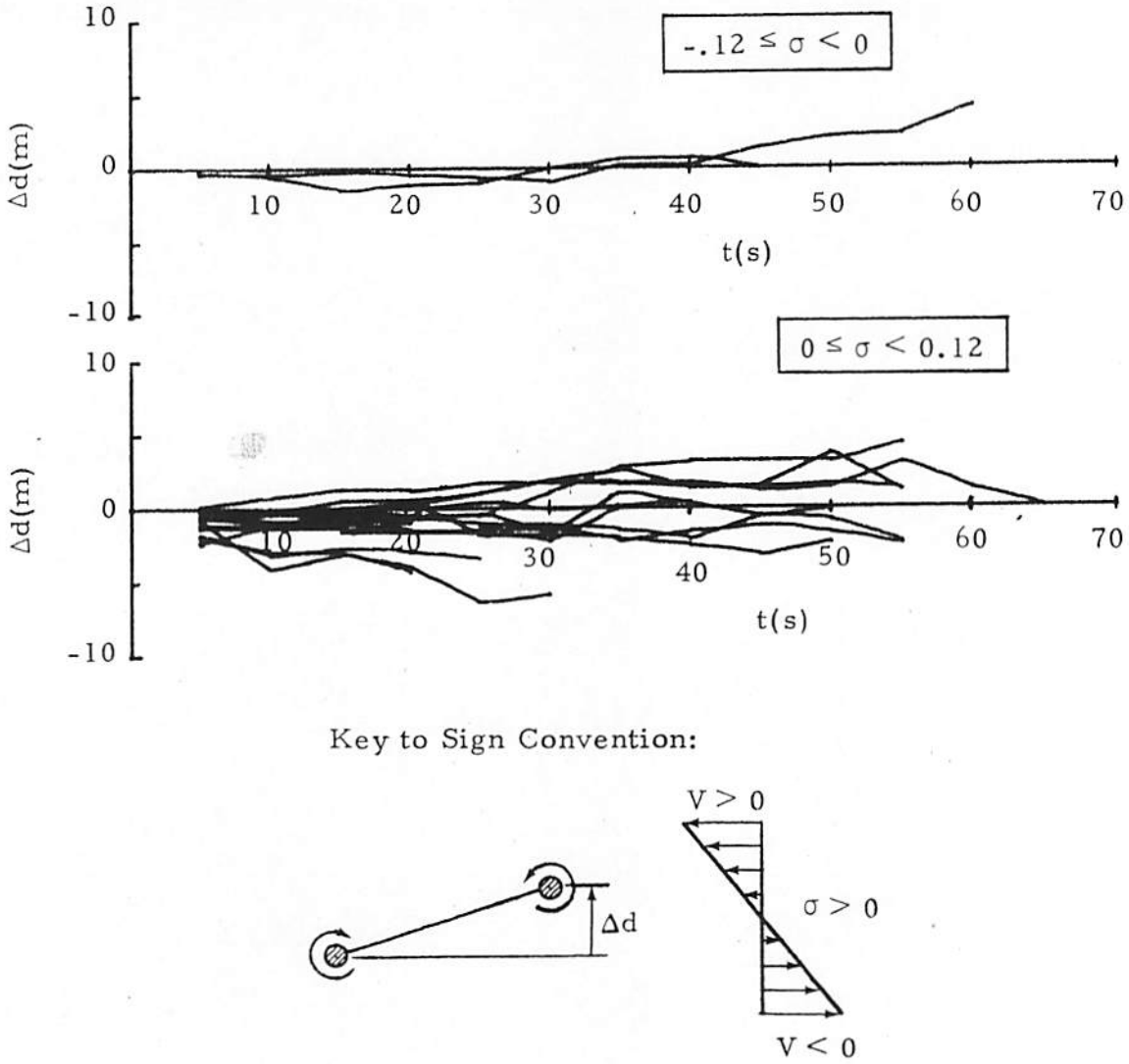

Figure 4-6. Vortex Height Mismatch Evolution in Weak Shear for Wakes Generated More than 100 m Above the Ground. The shear is defined as $\tau = \partial V/\partial z$, where V is the crosswind component with the sense shown.

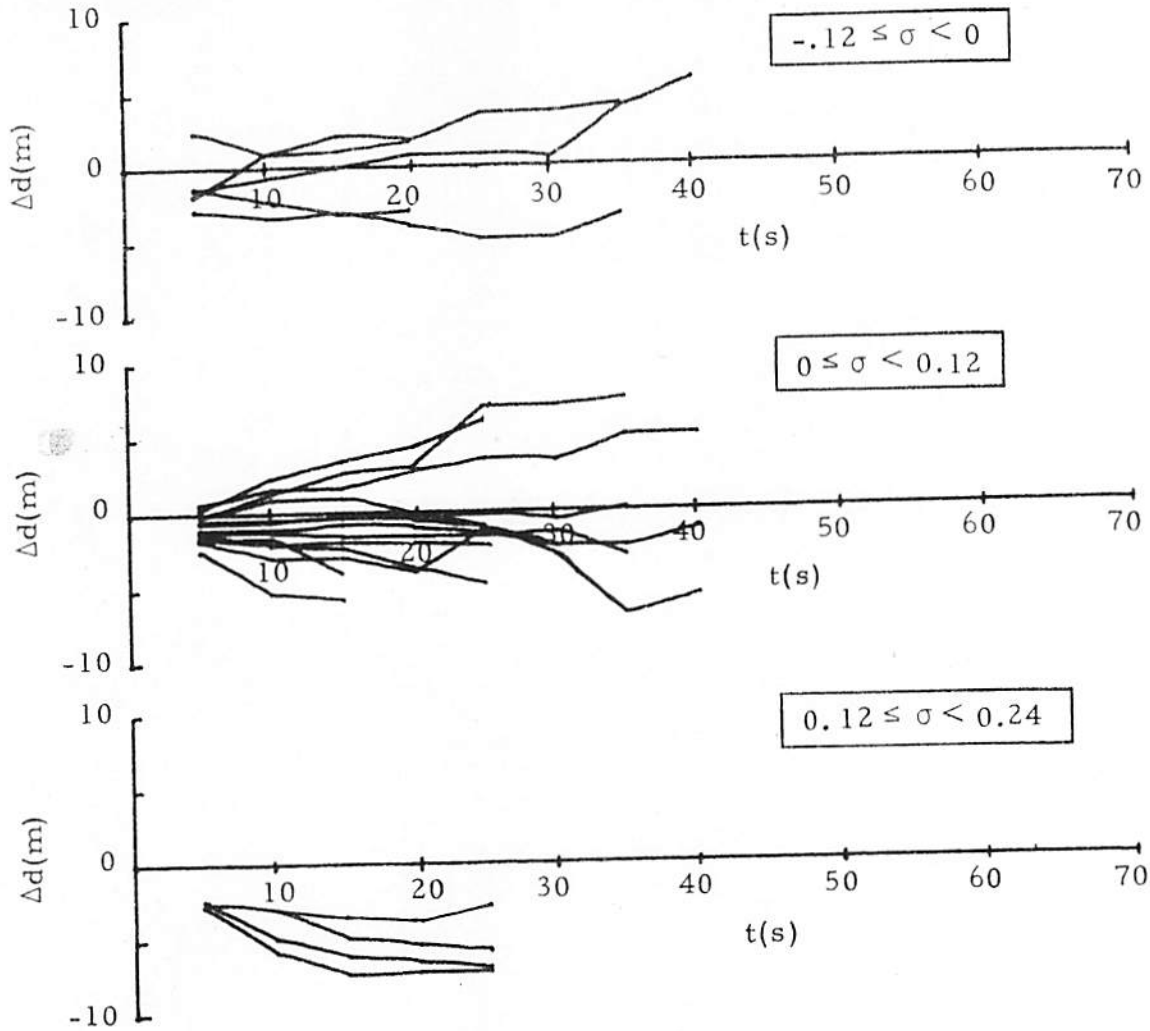

Figure 4-7. Vortex Height Mismatch Evolution in Shear for Wakes Generated at 100 m or Less Above the Ground.

banking, a number of test sorties contained consecutive pairs of low-level ($h_o \leq 15$ m) runs with the aircraft flying in opposite directions in the two runs. When $\sigma > 0.05$, the direction of banking, relative to the direction of the shear, was the same on both runs, i.e., the upwind vortex behaved in the same manner regardless of aircraft flight direction. When $\sigma < 0.05$, the results were inconclusive, possibly reflecting the imprecision of the measurement of small wind shears. It appears, though, that any aircraft-induced effects are small and negligible.

To further explore the qualitative observations thus far presented, the altitude mismatch of the vortices at a wake age of 20 seconds is plotted as a function of wind shear in Figure 4-8. Since the bank rate is hypothesized to correlate with the wind shear strength, the total bank angle should increase approximately linearly with time. Thus the appropriate plot of banking should have $\Delta d/t$ along the ordinate in order to eliminate explicit time effects. By choosing all data points at one age (taken as 20 seconds to give measurable bank angles before wake breakup begins) this time dependence is also eliminated. *

The data in Figure 4-8 show a strong tendency for $\Delta d < 0$ when $\sigma \gtrsim 0.10$ and suggests the possibility that $\Delta d \propto (-\sigma)$. No strong correlation with height of wake generation is apparent, except that the stronger shear points all occurred for wakes generated at or below 30 m above the ground. (The two points generated at 7 m will be discussed specially later in this section.)

---

*Since the descent generally increases linearly with time, a plot with $\Delta d/d$ along the ordinate has some appeal and was used in the previously mentioned work by Brashears, et al (1974). Local air currents and ground effect caused considerable data scatter when this was tried here, because occasionally especially small values of d after 20 seconds gave very large values of $\Delta d/d$.

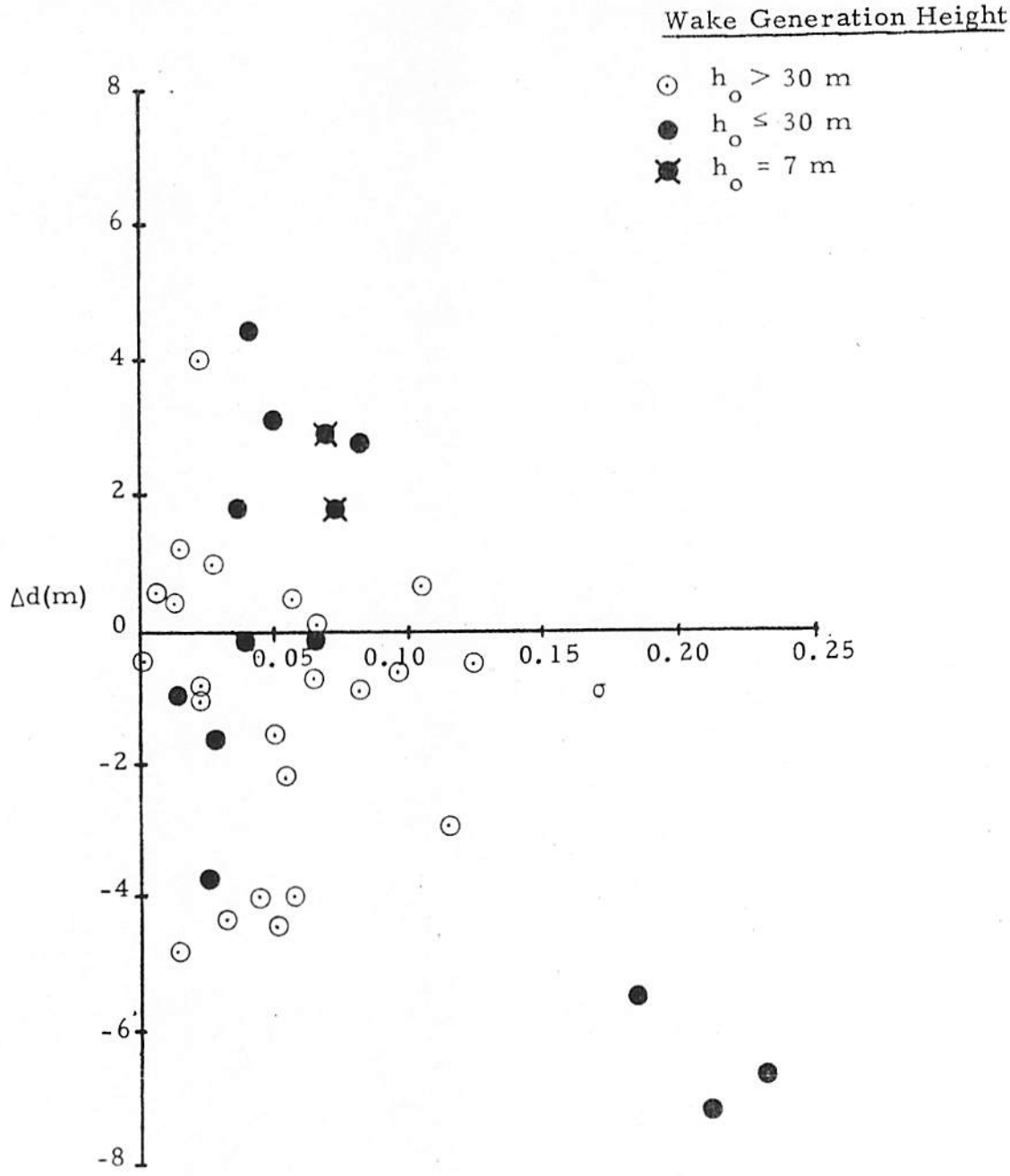

Figure 4-8. Observed Values of Vortex Height Mismatch at a Wake Age of 20 Seconds, Plotted versus Non-dimensional Wind Shear and Categorized by Height of Wake Generation. All data has been reconstructed so that $\sigma > 0$. $\Delta d > 0$ means that the upwind vortex would rise in shear in the sense of a boundary layer flow.

The statistics of the wake tilting observations are presented in Table 4-1, where the probability of wake tilting in the "upwind-vortex-descends" sense is correlated with generation altitude and shear strength. The general conclusion to be drawn from this table is that the stronger the shear the more definitive this correlation. In fact, deleting the weakest shear cases ($\sigma < 0.05$), 72% of the cases show behavior of the form described (vs. 73% of the Cessna 170 cases mentioned earlier). Although strongest correlation occurred for generation heights between 30 and 100 m, the number of points in this altitude range is small enough to make generalization of this observation suspect. Also, the correlation does appear stronger at lower altitudes, but a clear conclusion to this effect cannot be drawn.

Table 4-1. Frequency of "Upwind" Vortex Descent Below "Downwind" Vortex for Various Shear Strengths and Vortex Generation Altitudes. Wake Age = 20 Seconds.

Generation Altitude	Shear			
	$\lvert\sigma\rvert < 0.05$	$0.05 \leq \lvert\sigma\rvert < 0.10$	$0.10 \leq \lvert\sigma\rvert < 0.25$	All σ
$h_o \leq 30$ m	67% (6)	33% (3)	100% (3)	67% (12)
$30 < h_o \leq 100$ m	67% (3)	100% (2)	100% (1)	83% (6)
$h_o > 100$ m	43% (7)	71% (7)	50%(2)	56% (16)
All h_o	56% (16)	67%(12)	83%(6)	61% (36)

KEY: X%(Y) -- X = percentage of samples in class behaving as described (viz., sign of Δd opposite to sign of σ).

-- Y = total number of samples in class.

A further stratification of the same data by atmospheric stability, in terms of the stability classes used in the previous section, was unsuccessful in demonstrating any correlation between stability and wake tilting.

A more illuminating correlation, showing the relationship between the degree of tilt and the shear strength appears in Table 4-2. There the increase in expected tilt (with Δd becoming more negative) as shear increases shows clearly, and the fact that $\sigma > 0$ correlates with $\Delta d < 0$ is also displayed since $\overline{\Delta d}$ is never positive.

Table 4-2. Relationship Between Shear Strength and Average Vortex Height Mismatch at Wake Age of 20 Seconds.

Generation Altitude	Shear			
	$\lvert\sigma\rvert < 0.05$	$0.05 \leq \lvert\sigma\rvert < 0.10$	$0.10 \leq \lvert\sigma\rvert < 0.25$	All σ
$h_o \leq 30$ m	0.0 (6)	0.0 (5)	-6.3 (3)	-1.6 (12)
$30 \leq h_o \leq 100$ m	-0.3 (3)	-3.3 (2)	-0.5 (1)	-1.3 (6)
$h_o > 100$ m	-1.0 (7)	-1.0 (7)	-1.2 (2)	-1.0 (16)
All h_o	-0.5 (16)	-1.1 (12)	-3.7 (6)	-1.3 (14)

KEY: X(Y) -- X = $\overline{\Delta d}$ = average vortex height mismatch in class.

-- Y = total number of samples in class.

An effect of generation altitude on the degree of wake tilting is also shown in Table 4-2, with greater height mismatching corresponding to lower generation altitudes. When looked at within each shear strength class, however, it is seen that three points in strong shear at $h_o \leq 30$ m control this conclusion and that, in fact, no such conclusion can be drawn for weaker shear. Thus the possibility remains that more data would show the apparent Δd vs h_o correlation to be a myth.

Excluded from the previous discussion were two consecutive runs made at 7 m above the ground, in directions opposite to each other, both of which showed strong tilting in the opposite direction ($\Delta d > 0$ for $\sigma > 0$) than the preferred mode above. This particular generating altitude is so close to the equilibrium altitude of the vortices in ground effect that there was less than 0.2 m of descent in 20 seconds, but there was considerable tilting (1.8 and 2.8 m mismatch at 20 s). The shear for these two cases was $\sigma = 0.08$, and there was a strong temperature inversion present. Whether these two points indicate that a different behavior occurs very close to the ground than further aloft cannot be determined on the basis of only these two pieces of data, however.

With the exception of the two points just discussed, the behavior of the wakes in shear agrees in a general way with that described by Brashears, et al (1974). All of the shears in the present experiments were weak enough ($\sigma < 0.25$) that the Brashears, et al, formulation would predict $\Delta d < 0$, in agreement with the experiments. Their interpretation of their streamline diagrams leads them to predict $\Delta d > 0$ (for $\sigma > 0.5$ and thus, obviously, somewhere in the range $0.3 \lesssim \sigma \lesssim 0.5$, one must also have $\Delta d \sim 0$), but this contrary behavior was not investigated here because of insufficiently strong shear.

Based on these experiments, as well as on data presented by Brashears, et al, it should be noted that any tilting model predictions

are going to be probabilistic, not deterministic -- the precise details of motion of any given wake still cannot be predicted, only the most likely direction of tilting can.

In addition to the tilting, another dramatic aspect of wake behavior in wind shear became quickly apparent. Regardless of generation altitude, whenever the wake banked in wind shear the upper (generally downwind) vortex always broke up well ahead of the other vortex, often leaving one vortex drifting alone for an additional 30 seconds or more until it also decayed. In the overhead view in Figure 4-9, the upper vortex shows signs of instability at 15 seconds and has completely broken down by 30 seconds. A side view of a similar case is shown in Figure 4-10. In the latter sequence the upper vortex is becoming unstable at 20 seconds and is no longer visible at 30 seconds. The sole remaining vortex rises slightly until it is 60 seconds old, and then is breaking down at 70 seconds. These wakes were generated only 15 m above the ground and the lower vortex descended to within less than 10 m of the ground. Interestingly, the single remaining vortex did not attempt to link with its image below the ground, as has been observed when both vortices approach the ground (Dee and Nicholas, 1969) but rather invariably underwent a vortex breakdown. Another case with similar asymmetric behavior, but generated at a higher altitude, was shown previously in Figure 4-1.

Several investigators have reported observations of extremely long-lived single vortices. Tombach (1973) photographically tracked one smoke-marked Cessna 170 vortex for 193 seconds, some three times the normal persistence under similar atmospheric conditions. MacCready (1971) reported observing a single contrail behind a turning B-52 for some six minutes. And Burnham, et al, (1972) have acoustically tracked a Boeing 747 vortex near the ground for at least three minutes. All of these may be similar to the cases just shown in the figures, with wind shear (or possible asymmetrical effects due to the

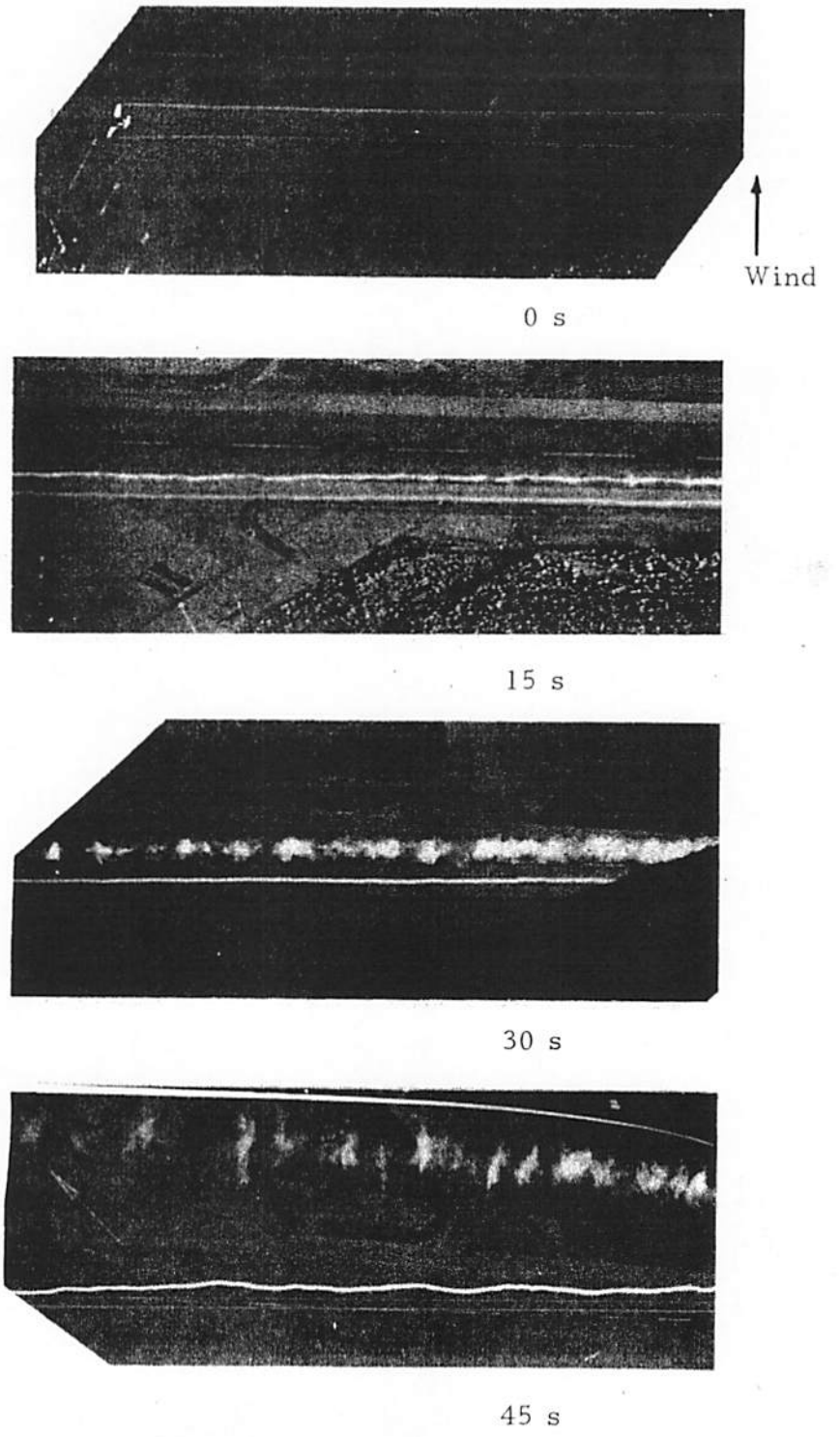

Figure 4-9. Overhead Views of Wake Behavior in Wind Shear - Group II, Series 9, Run 2. Wake generated 15 m above the surface; $\sigma = 0.22$. One vortex descends toward the ground; the other remains aloft and breaks up. The photographs were taken from an aircraft circling overhead, thus the angle of observation is slightly different in each picture.

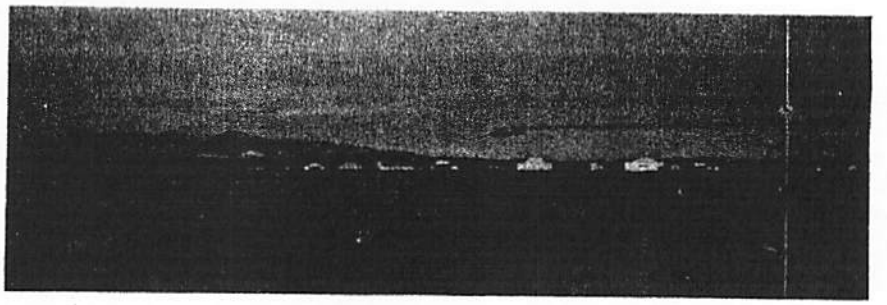

0 s

10 s

20 s

30 s

Figure 4-10. Side View of Wake Behavior in Shear Near the Ground. Generation altitude was 15 m; σ = 0.24 . Considerable banking takes place at 10 s, the upper vortex becomes unstable at 20 s, and has vanished by 30 s.

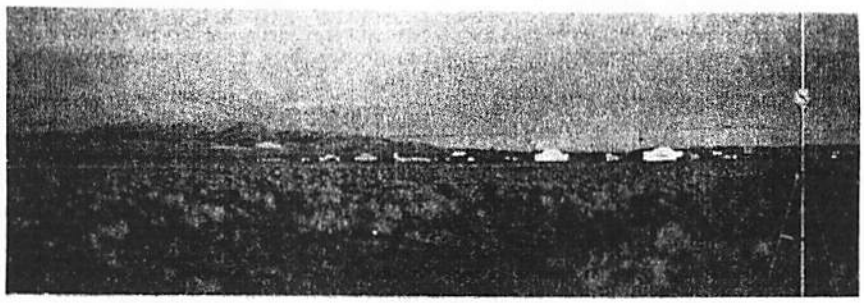

40 s

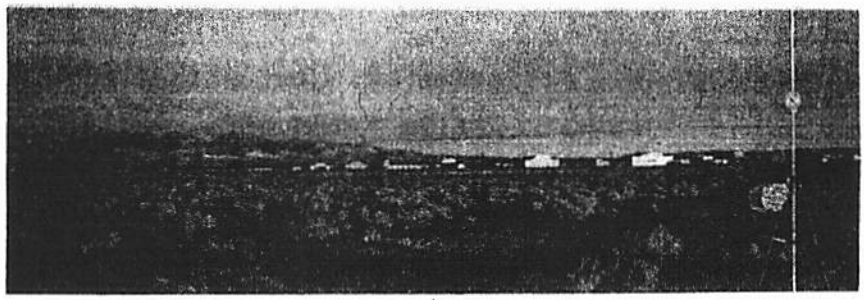

50 s

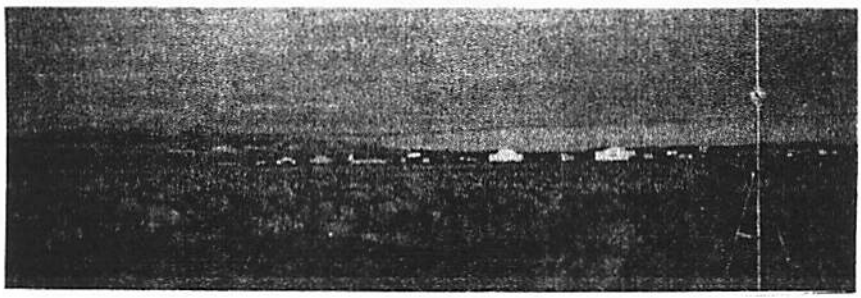

60 s

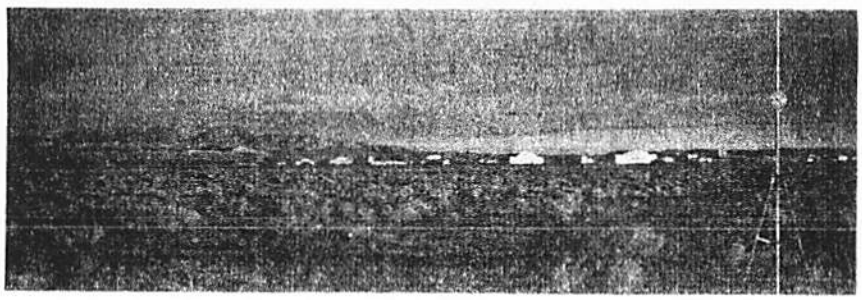

70 s

Figure 4-10, continued. The single vortex rises between 40 s and 60 s, and vortex breakdown is taking place at 70 s. (Group II, Series 9, Run 1.)

B-52 turn) causing one vortex to decay well ahead of its then more stable mate. An explanation for this behavior has yet to emerge, however.

Whenever tilting occurred in ground effect, the upper vortex rose upward more than the lower vortex descended, so that the net motion of the wake was upward. At generation altitudes of about 15 m, this meant the wake descended initially and then rose slightly as it tilted. In two cases generated at 7 m there was no wake descent after the first few seconds, and the wake was higher than its generation altitude after 20 seconds. When generated at higher altitudes, tilting probably slows wake descent, but other factors mask explicit correlations of tilting with slowing of descent, as was discussed in the previous section. On the other hand, in studies with a Cessna 170, Tombach (1972) concluded then that wake tilting was the dominant factor causing a slowing of the descent of the weaker wakes of those experiments.

To summarize the observations of the effects of wind shear in these tests:

1. Wind shear and wake tilting are well correlated, with the sense of the tilting being opposite to that of the shear. Interpreted for boundary layer shear, the upwind vortex descends relative to the downwind one. This correlation improves as the shear strength increases.

2. In this shear range, the <u>average</u> amount of tilt is roughly proportional to the shear strength, but in any given case the amount of tilt in weak shear is highly variable.

3. The upper vortex in such a tilted wake breaks down first, leaving behind a single vortex which often persists for an extended period before it breaks down.

4.3 Wake Decay

Both of the common types of decay of the organized motion by instability were regularly observed in these tests. Breakdown of a single vortex, an example of which is shown in Figure 4-11, was frequently observed in all meteorological conditions, while the linking of vortices into vortex rings (Figure 4-12) was observed in relatively calm conditions (which allowed time for the instability to carry through to the linked state before the vortices had been broken up). Another form of breakup, consisting simply of a tearing apart of the vortex system by turbulence, with no identifiable instability occuring, was observed in more turbulent conditions.

These modes of decay were observed from various orientations and under various conditions. Some photographs of interesting aspects of the linking mode of breakup are shown in Figures 4-13 and 4-14.

Quantitative data on wake breakup was obtained from the motion pictures and still photographs. Among the factors recorded were the type of instability, the wake age at time of occurrence, and the speed of motion of the instability.

The time to breakdown, as a function of atmospheric turbulence, $\epsilon^{1/3}$, is plotted in Figure 4-15. Both linking and bursting types of instabilities are shown. The time of impact of each instability was selected as the moment at which a clear, nearly smoke-free, spot appeared in a vortex line due to either the formation of a link or

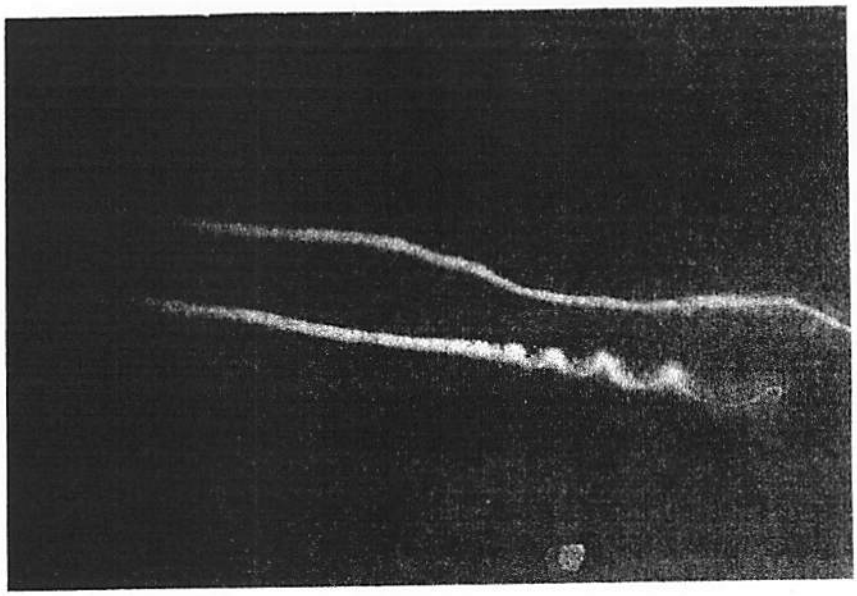

Figure 4-11. Breakup of Vortices by Vortex Breakdowns. Note the helical structure and the fine filament of smoke which remains on the lower vortex. A more diffuse breakdown is beginning in the upper vortex at the right edge of the photo.

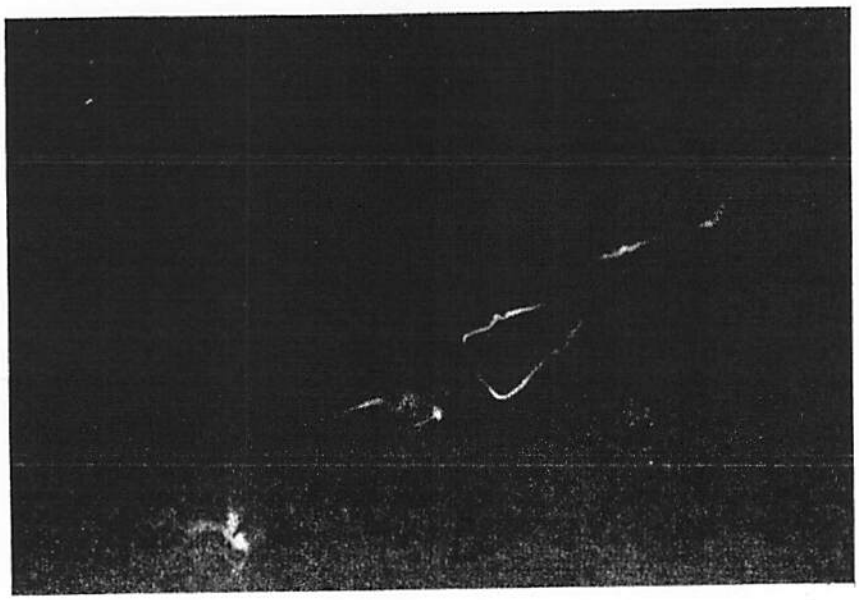

Figure 4-12. Breakdown of a Wake by Linking into Vortex Rings. Note the different forms the rings take, with vortex breakdown occurring in some. This upward view shows one of the clocks used for data synchronization. The wake age is 40 seconds. (Group II, Series 8, Run 3. An earlier photo of the same sequence appears in Figure 4-21.)

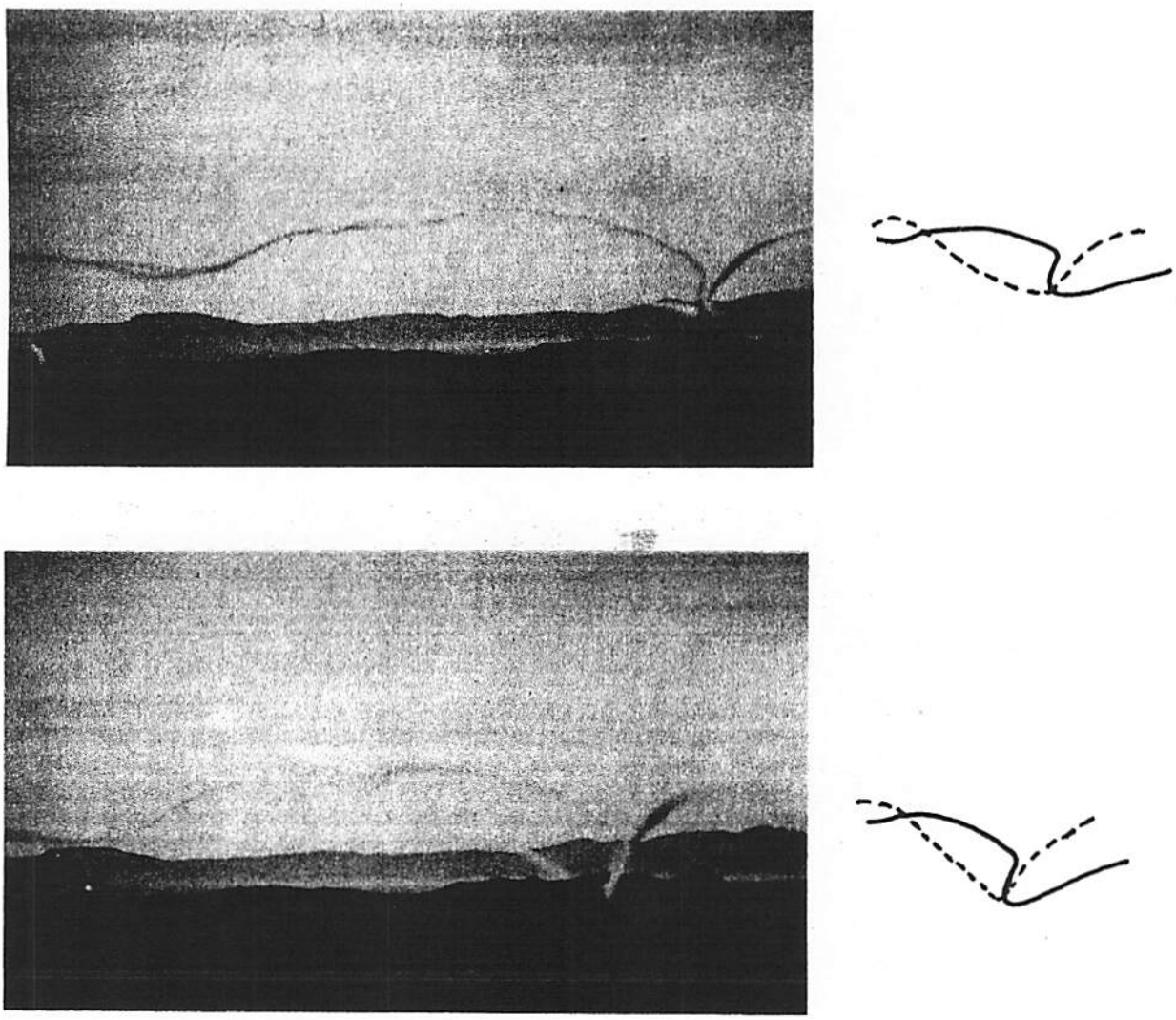

Figure 4-13. Side View of Final Stages of the Sinuous Instability. Top: The well defined vortices begin to converge on the right edge of the photo. The sketch sorts out the vortices. Bottom: About 5 seconds later, linking is imminent on the right. The smooth vortex structure is breaking up. Another point of linking is beginning to form on the left.

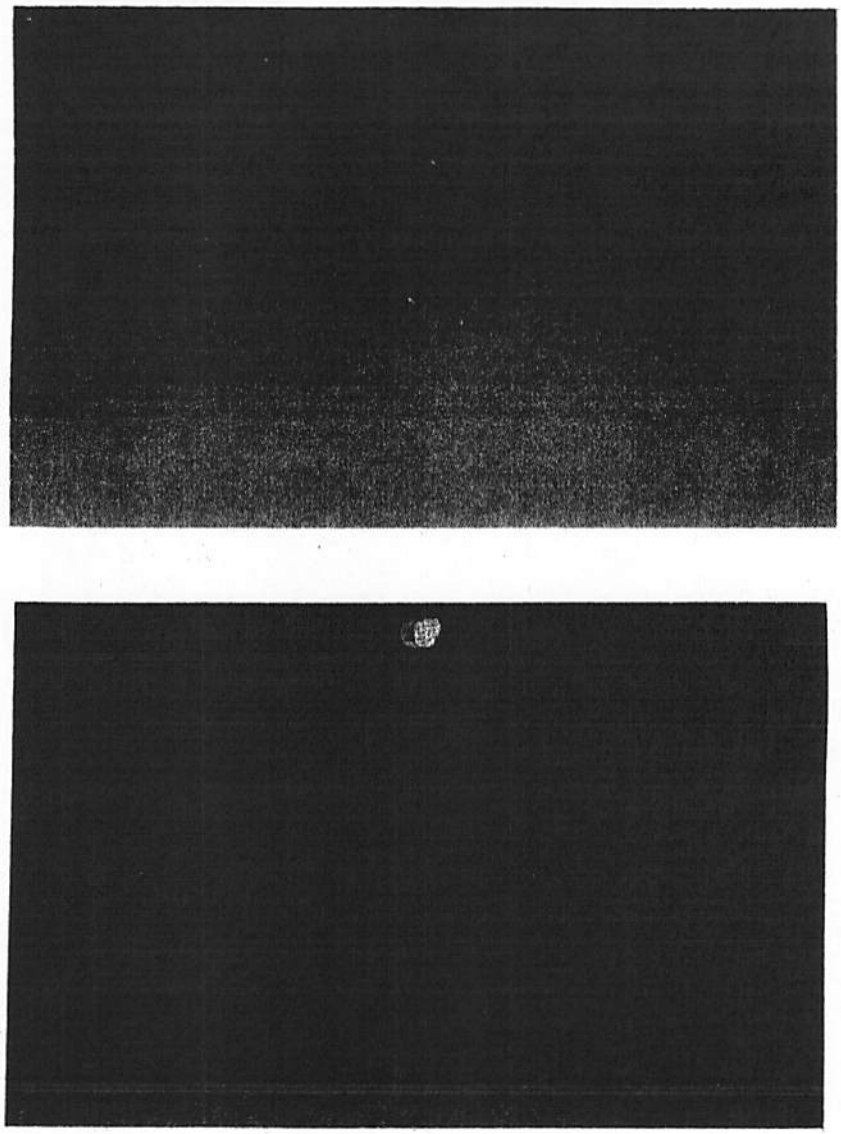

Figure 4-14. Evolution of Decay Within a Vortex Ring Formed from a Vortex Pair. Top: A vortex ring has been formed with smoothly curved ends where the two vortices linked and with a rather ragged region where the original parallel sections still remain. This side view from below makes it look as though the ring is a figure-8, an illusion of the perspective. The adjacent vortex segments have undergone breakdowns and are not as well defined as the ring. Bottom: Some 10 seconds later the smooth right end has small wiggles in it and a puff of smoke has appeared at the sharpest kink in the vortex.

the localized breakdown of the core flow. The atmospheric turbulence is characterized by $\epsilon^{1/3}$, the rate of dissipation of turbulent energy in the inertial subrange of isotropic, homogeneous turbulence (which is often approximated by the atmosphere).*

The linking and bursting data points lie generally in the same locations, especially for $\epsilon^{1/3} < 1$, with linking points showing a tendency to lie above bursting points for $\epsilon^{1/3} > 1$. This is consistent with the previously mentioned observation that linking was not observed when turbulence was sufficiently high, because the bursting tended to destroy the vortices before linking could take place. A similar trend can be found in the Cessna 170 data of Tombach (1973), although it was not explicitly noted then.

Two lines which bracketed most of Tombach's Cessna 170 data are drawn on Figure 4-15. Most of the current data, with the noticeable exception of some of the linking points, also lie within the same lines, suggesting again a $1/\epsilon^{1/3}$ nature to the wake lifetime. In the current tests, as well as in the Cessna 170 tests, bursting was the prevailing mode of decay.

The data concerning the sinuous instability alone has been plotted separately on Figure 4-16, in dimensionless form, along with the theory of Crow and Bate (from Lissaman, et al, 1973). The theory has been modified from that in the referenced report by the addition of a small time solution and appropriate fairing between the small and long time solutions. Also, the dimensionless turbulence function, η, has been re-defined slightly.

---

*For an explanation of these concepts see Chapter 3 and MacCready (1962).

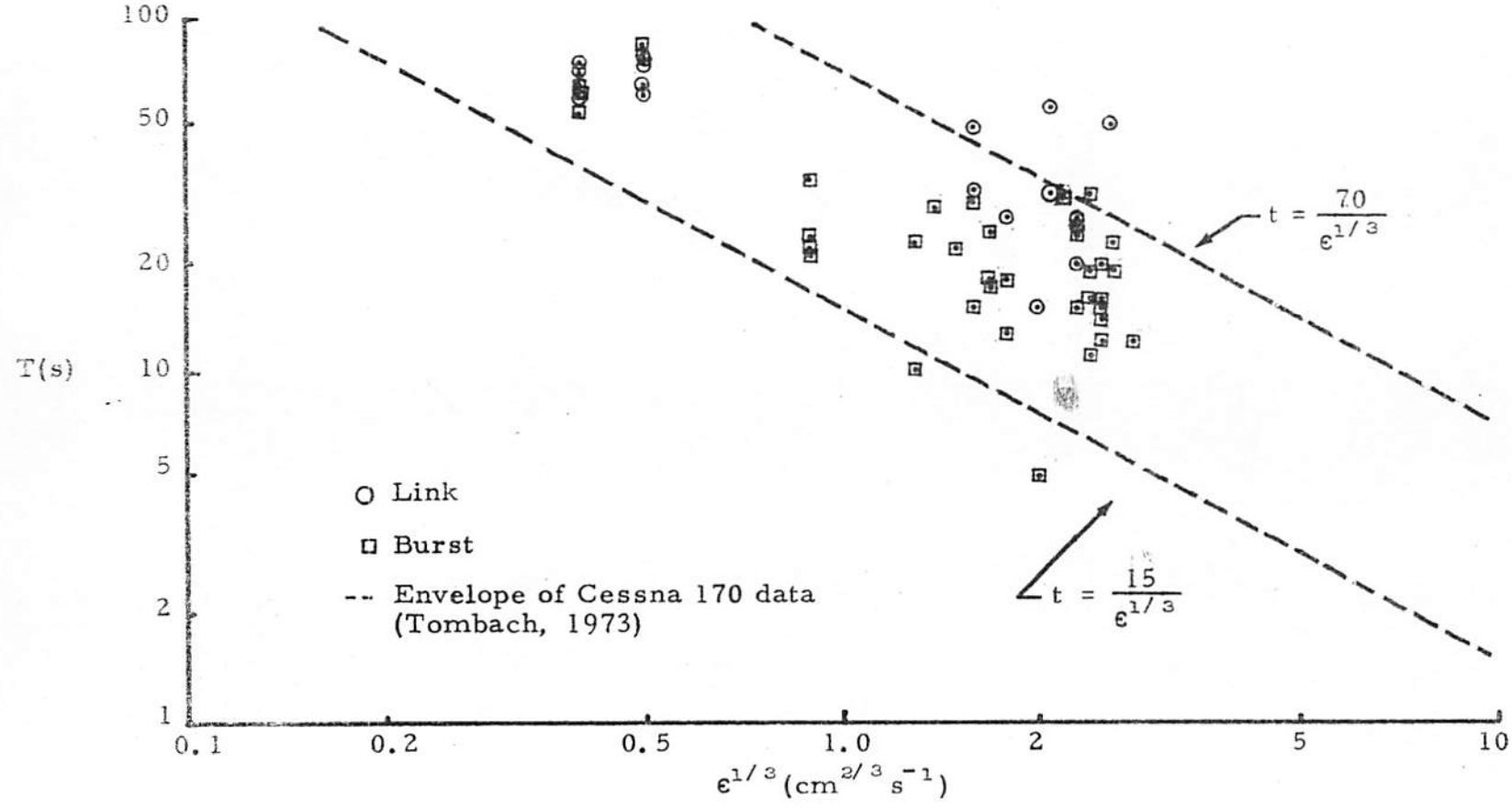

Figure 4-15. Lifetimes of Aero Commander Wakes as a Function of the Atmospheric Turbulence.

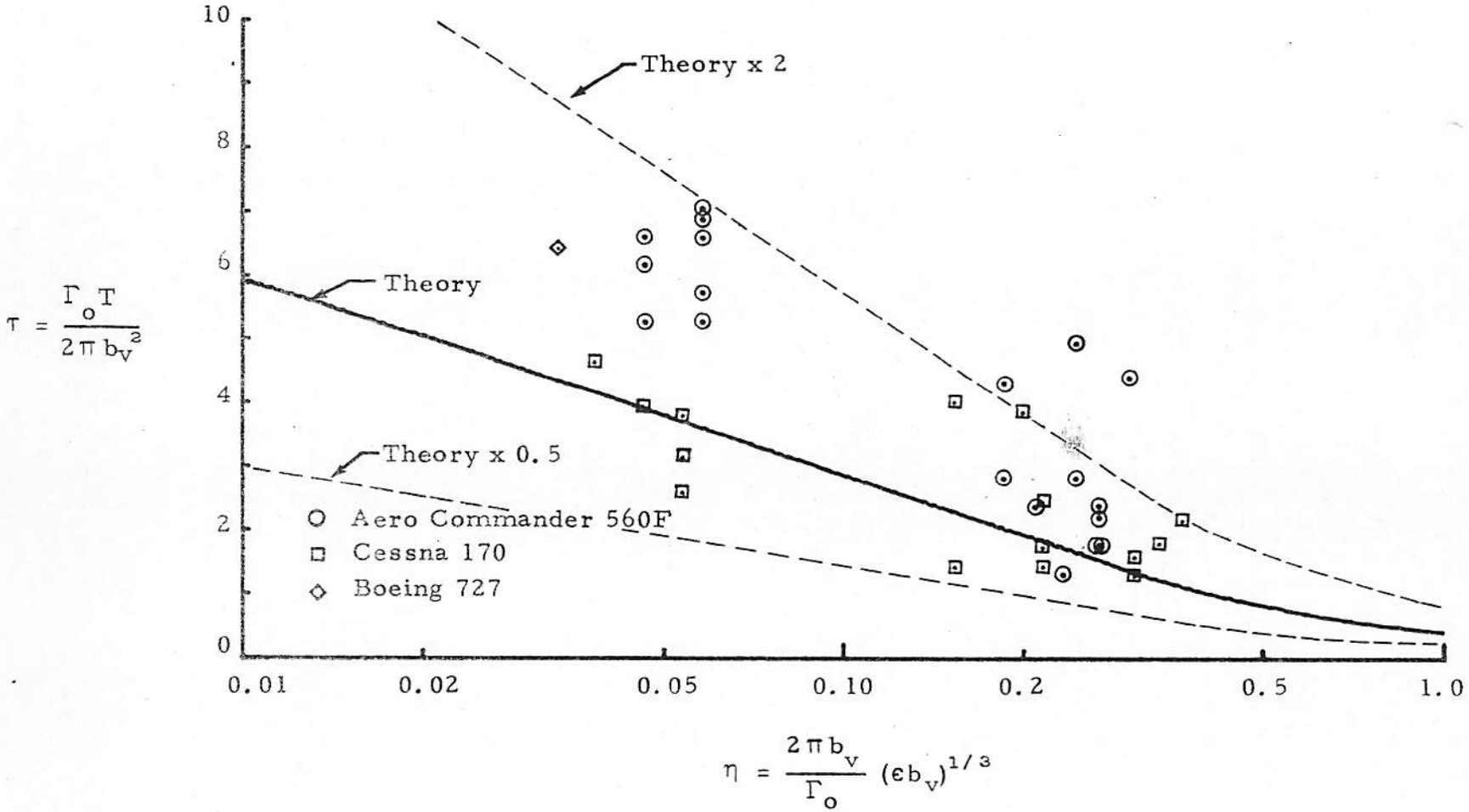

Figure 4-16. Dimensionless Relationship Between Wake Lifetime and Atmospheric Turbulence for the Sinuous Instability. Experimental data is shown for three aircraft and is compared with the theory of Crow and Bate.

In addition to the data from the present experiment, Figure 4-16 also contains the data from Tombach's Cessna 170 tests, along with one point obtained during flight tests conducted by NASA and FAA with a Boeing 727 in late 1973.* The vortex spacing, b_v, used to calculate both the dimensionless time, τ, and turbulence, η, as well as the circulation, Γ, is the actual vortex spacing in all cases.

There is a good deal of data scatter evident in the figure, with the Cessna 170 data providing a closer fit to the theory than either the Aero Commander or B-727 data. In some cases the data indicates linking times in excess of twice those predicted by the theory. However, all of the Cessna 170 data, the one B-727 point, and all but three of the Aero Commander points lie within a factor of 2 of the theory, as indicated by the broken lines.

An understanding of the significance of this data spread would be desirable, and some possible causes can be presented. It may simply be a consequence of the statistical nature of turbulence, it might be a result of the difficulty of making precise measurements of the turbulence quantities of interest, it might come about because the assumed isotropy of the ambient turbulence does not hold, or it might result from the fact that all three aircraft tests were under different types of conditions.

On the other hand, it might be that effects due to aircraft scale, or due to the differing geometries of the three aircraft, are the causes for the differences. Since the data points for both the Aero Commander

*The B-727 tests are described in Barber, et al (1975). The one data point is unpublished, and was extracted by AeroVironment from photographic sequences it made during those experiments.

and the B-727 indicate fairly consistently longer wake lifetimes than those for the smaller Cessna 170, there is some support for this idea. Such factors could result in differing amounts of turbulence in the vortices, for example, and in differing rates of decay of circulation (see, for example, Section 4.6 below and Bate, 1974, for some data on vortex strength decay), which then would alter the rate of growth of the instability.

It seems reasonable then that the scatter in the data is indeed a consequece of turbulence (and experiment) statistics while some as yet unknown scale or geometry effects could contribute to the apparent systematic differences in the data.

Considering now the vortex breakdown mode of instability, some study was made of the speed of propagation of the smoke burst along the vortex. Both natural bursts and those which were created when the wake was cut by a probe airplane were measured.

Considering first the natural bursts, the typical speed of travel of one of the bursts was generally $3.0 \pm .5$ m/s, so the bursts are diverging at about 6 m/s. There seemed to be no difference in the travel speeds whether the burst moved toward the aircraft or away from it, after allowance is made for wind.

After the Cessna Cardinal penetrated the wake of the Aero Commander, the vortices appeared broken apart in much the same way as they appeared a few seconds after a natural burst. Direct penetration of the vortices was not required; a similar effect was observed whenever the velocity fields of the Cessna and Aero Commander wakes interacted. The initial burst speed of a cut wake sometimes deviated considerably from the 3 m/s value (both faster and slower cases were observed) but soon stabilized at the same speed of travel as that for the natural burst. Thus there appears to be a characteristic speed of travel of the instability.

To summarize the main results of the present experiments regarding wake decay:

1. Wake decay at the scale of the present experiments occurred due to both core bursting and the sinuous instability, with core bursting being the more common.

2. There is a relationship between wake lifetime and the level of atmospheric turbulence. In general, this relationship exhibits a $1/\epsilon^{1/3}$ trend, with wake lifetimes much the same whether terminated by linking or bursting.

3. The theory of Crow and Bate for the linking breakup of vortex pairs appears to generally correlate with the data (within a factor of 2).

4. Core bursting is a regular form of vortex breakup, but very little is still known about its mechanisms or its coupling to the ambient atmosphere.

4.4 Wake Buoyancy

After formation, the wake descends due to the mutual induction of the vortex-pair. The steady-state inviscid representation of this motion (Lamb, 1945) shows that the vortices are accompanied by a body of fluid which is separate from the surrounding fluid and does not mix with it. The temperature of the fluid in this "wake oval" will thus increase adiabatically as the wake descends and, in a stably stratified atmosphere, the wake will acquire buoyancy and be subjected to a buoyant force.

In actual wakes some mixing takes place between the wake oval and the atmosphere, due to the turbulence present in the atmosphere plus that left in the wake by the aircraft. In these experiments the temperature of the wake was measured by the probing aircraft to ascertain the degree to which such mixing occurs. On one extreme, with no mixing, the wake would differ in temperature from the ambient air at the same level by an amount ΔT equal to $\gamma' d$ where γ' is the lapse rate of potential temperature and d is the distance the wake has descended since generation. At the other extreme, with complete mixing, ΔT would be zero always. Real cases will fall between these extremes.

Whether either of these extremes, or something in between, occurs is of considerable interest in understanding some aspects of wake behavior. Since a buoyant force alters the equations of wake transport, any acquired buoyancy should influence wake parameters such as descent speed and vortex spacing. This influence has been modeled analytically by a number of investigators, with a variety of conclusions, some contradictory. Lissaman, et al (1973) compared the various theories; a lack of detailed corresponding experimental information made an assessment of their validity difficult.

A major objective of the AFOSR-sponsored portion of the flight test program was an experimental study of wake buoyancy effects. Detailed results of this program were presented by Tombach (1974), thus only the key points of that study, supplemented by some data acquired subsequent to that report, will be presented here.

To demonstrate the nature of the measurements made, Figure 4-17 shows a set of temperature profiles through one wake at four different distances behind the generating aircraft. The wake generally is well defined by its temperature profile, is usually fairly uniformly mixed until the later stages of its life, and acquires buoyancy monotonically until late in its life. Study of many such profiles showed that: (1) Only $\Delta T \geq 0$ is observed, except at very young wake ages, since the atmosphere is usually stable and wakes in the more turbulent unstable atmospheres do not last long, (2) ΔT generally increases for a period of time (of the order of 50 seconds) and then begins to decrease, (3) There is no obvious correlation between ΔT and γ' at any given time, contrary to the expected result of increased buoyancy in more stable conditions.

The temperature excess acquired by the wake can be represented by $\Delta T = \beta \gamma' d$, where β is an index of mixing, with $\beta = 0$ representing total mixing and $\beta = 1$ representing no mixing at all.* The quantity $\Delta T/\gamma' = \beta d$ contains no explicit appearance of γ' on the right side, thus is independent of explicit lapse rate effects. Figure 4-18 displays the experimentally observed values of $\Delta T/\gamma'$. For $\beta = 1$, these points would just represent the distance of descent, d. The actual range of measured descents, from Figures 4-2 and 4-3, is in the shaded region. Since most of the data lies well below this region, the corresponding values of β are less than unity.

---

*Note that this definition of β differs from that used in the report by Tombach and Bate (1973).

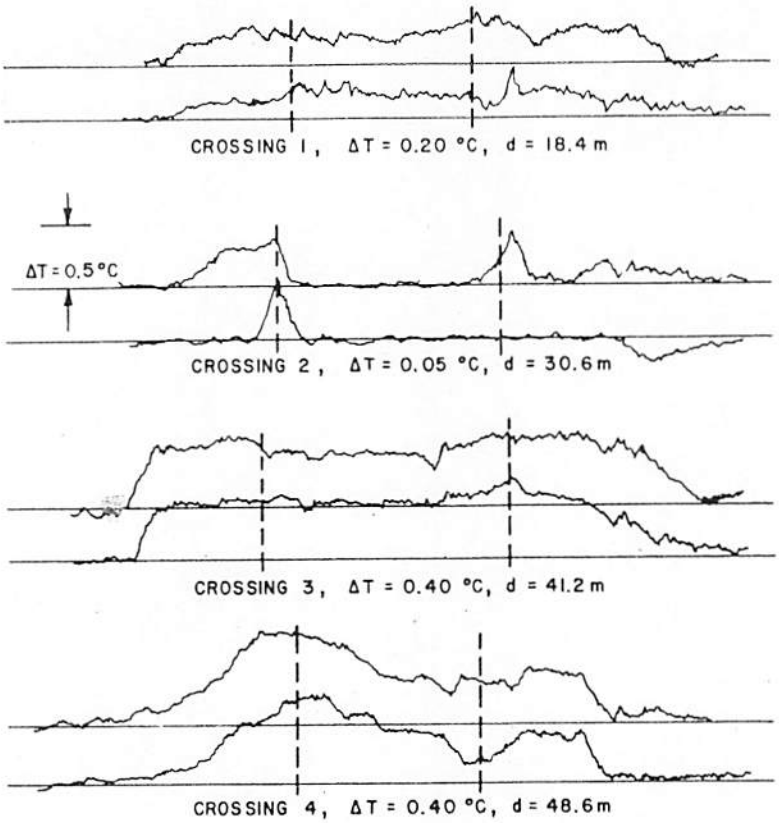

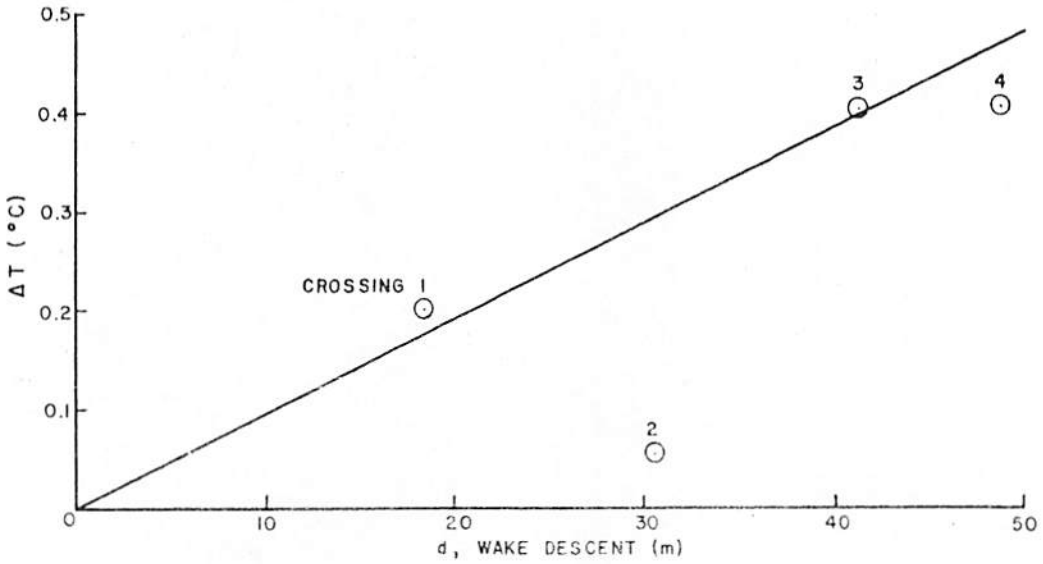

Figure 4-17. Top: Temperature Profiles for Four Successive Wake Crossings. (ΔT = average wake temperature excess, d = wake descent). Bottom: Increase of wake buoyancy with descent in a stable atmosphere. (Group I, Series 7, Run 1; $\gamma' = 1.3$ C/100 m.)

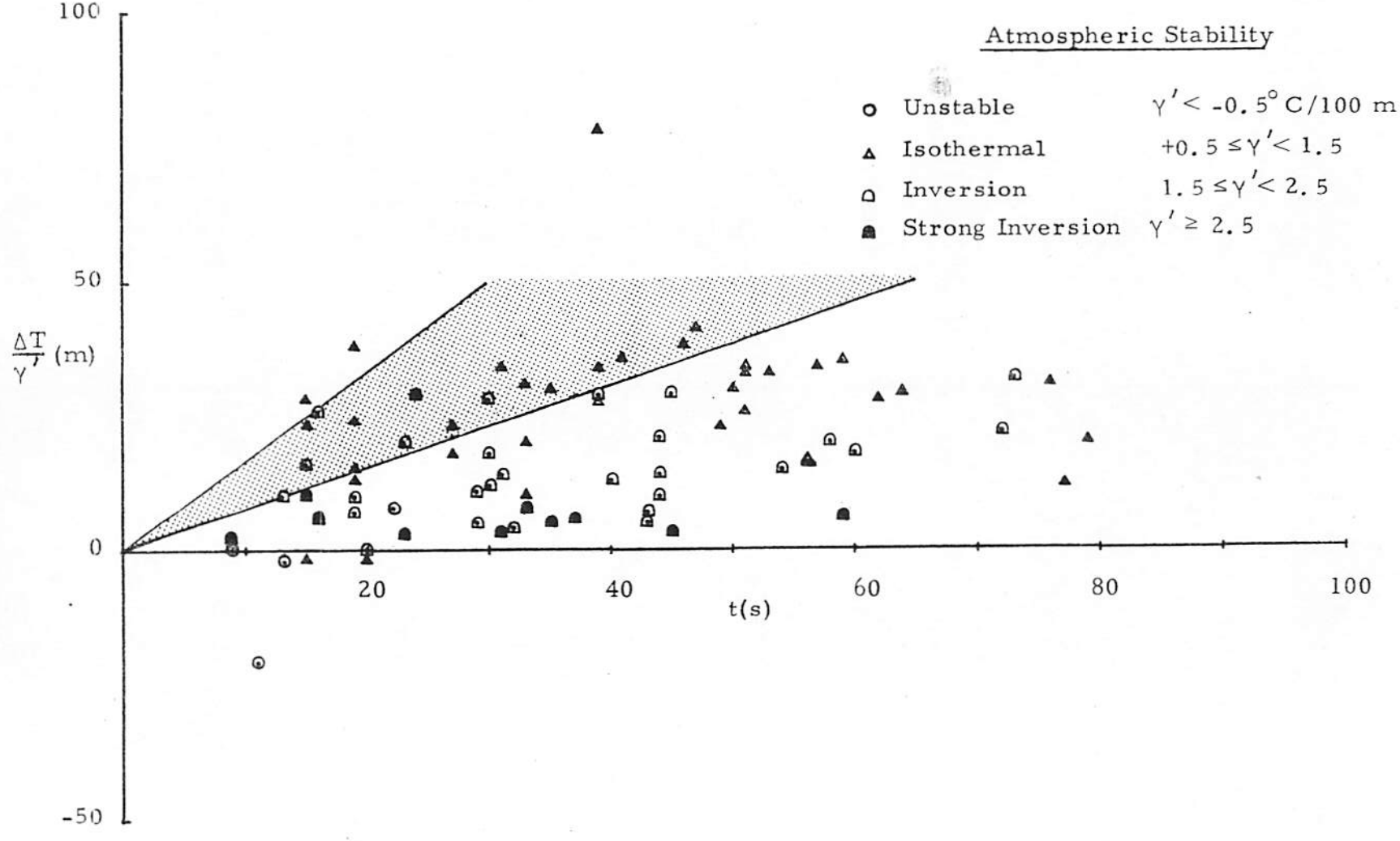

Figure 4-18. Average Temperature Excess Through Various Wakes, Normalized by the Lapse Rate of Potential Temperature. The shaded band indicates the range of temperature which would be expected from non-mixing wakes descending at the initial rates shown in Figures 4-2 and 4-3.

An explicit display of β versus time for a number of wakes appears in Figure 4-19. The number of points is considerably less than in Figure 4-18 because the simultaneous reliable measurements of d and ΔT required to compute $\beta = \Delta T/(\gamma' d)$ were less frequent than measurements of d or ΔT alone. There is considerable scatter because of this, but a number of cases, three of which are marked with trajectories, show a consistent decrease of β with time. (There is no physical significance to points where $\beta < 0$ or $\beta > 1$ unless a wake undergoes some unusual oscillatory motions during which it entrains at some times and not at others. The error in β becomes less severe for the older wakes since the uncertainty in d becomes less significant as d itself increases with time, and also because ΔT generally becomes larger and easier to measure until the vortex motion begins to break down. In most cases, β is probably within 0.1 of the correct value.)

This trend of decreasing β with time indicates a progressively increased rate of mixing between the wake and its surroundings as the wake ages. At some sufficiently long time all points must lie on the $\beta = 0$ line, but it might require destruction of the organized wake motion to achieve this. Since all of the data on Figure 4-19 corresponds to wakes with organized vortical motion (which is necessary to enable identification of the wake location by the velocity signature whenever the temperature profile is ill defined), the fact that the pattern of points never reaches $\beta = 0$ indicates that the organized wake always seems to retain some buoyancy and that entrainment is not strong enough to eliminate it.

In both Figures 4-18 and 4-19 the careful reader will find that many of the points corresponding to the most stable atmospheric conditions show less buoyancy and more mixing than those for less stable conditions. As was explained in Chapter 3, this is an anomaly caused by the test site location, where the drainage flows produced

in the most strongly stable conditions were more turbulent than the weaker flows occurring in more neutral conditions.

This result is illustrated in Figure 4-20, where that portion of the data in Figure 4-19 for which turbulence measurements also were available has been replotted with the symbols indicating the turbulence levels and the stability. Two conclusions are obvious: (1) All but one of the points with $\epsilon^{1/3} > 0.6$ were in inversion conditions, while 10 of the 17 points with $\epsilon^{1/3} \leq 0.6$ were in isothermal conditions, i.e., the turbulence was greater in the more stable conditions; and (2) Almost all of the data points with $\epsilon^{1/3} > 0.6$ lie below those obtained in less turbulence, thereby displaying the expected tendency toward increased entrainment with higher levels of turbulence.

The behavior that one might infer from the data in Figure 4-19 and 4-20 is sketched below. Because of data scatter and a limited number of points, some conjecture is involved, but it is likely that wakes start out with no mixing ($\beta = 1$) and that at a later time, which appears to be correlated with ambient turbulence and may be connected

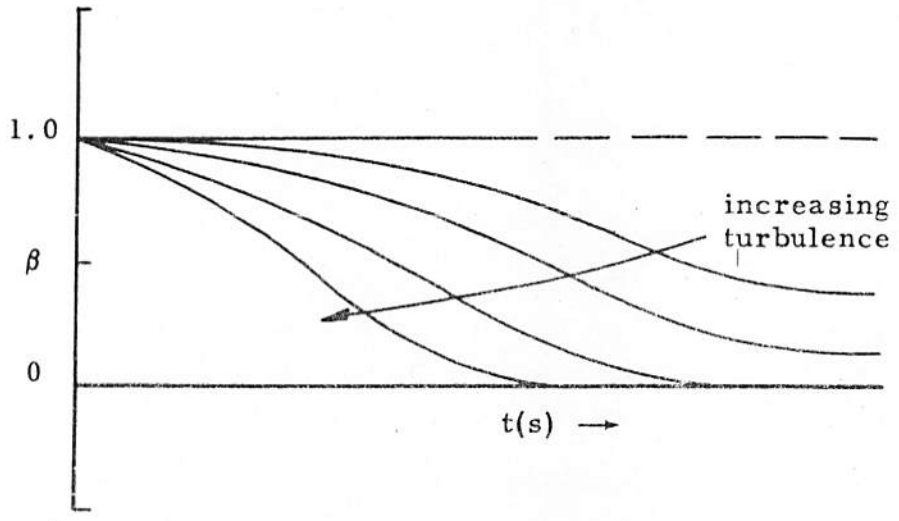

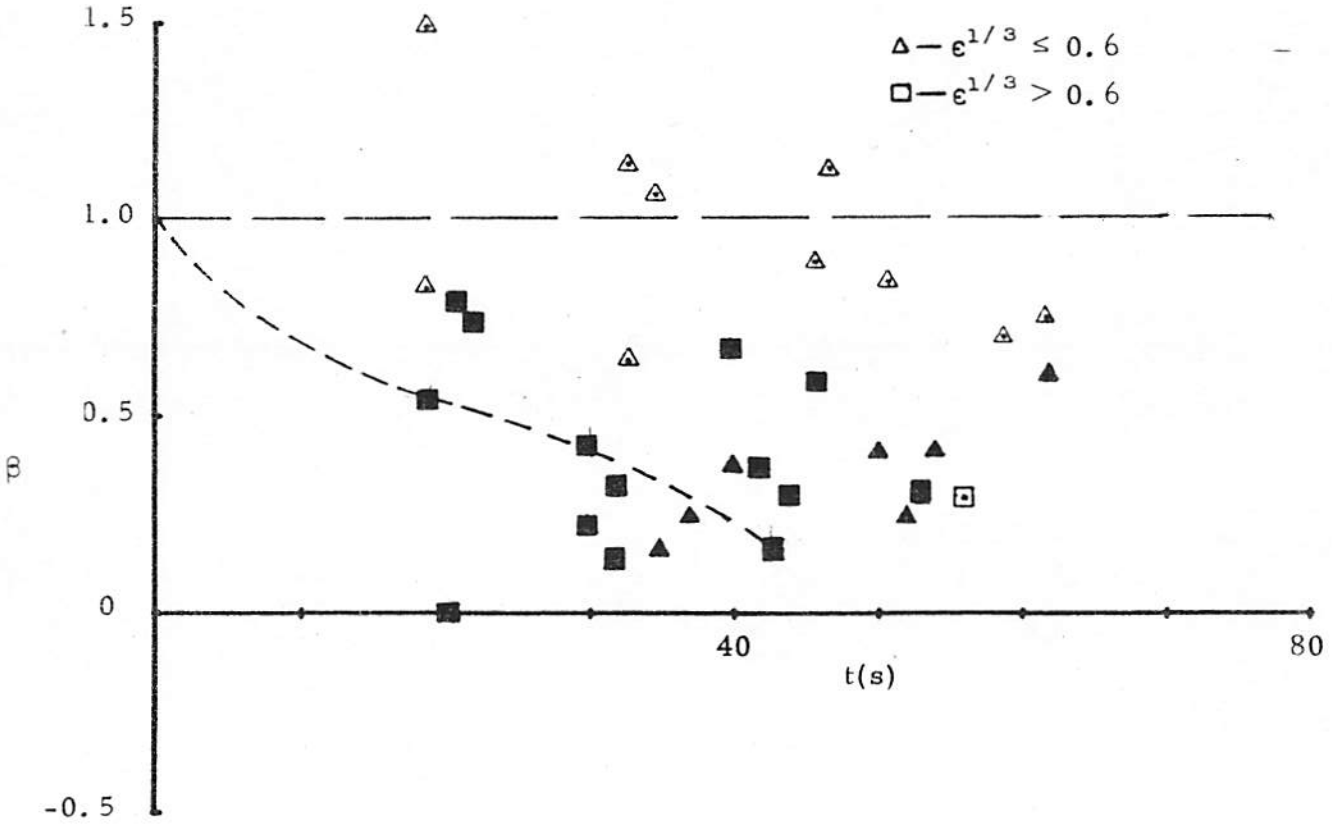

Figure 4-20. Non-Dimensional Mixing Index Versus Time, with Data Classified by Turbulence and Ambient Stability. Open symbols correspond to isothermal conditions; solid symbols to the more stable inversion conditions.

with turbulence in the wake, they begin to mix with their surroundings ($d\beta/dt < 0$). Eventually they have mixed so thoroughly that $\beta \rightarrow 0$, although an instability may bring this on catastrophically at an earlier time than would occur under normal decay.

This cycle of behavior has been postulated earlier by Lissaman, et al (1973), who in turn were inspired by similar behavior in laboratory vortex ring experiments performed by Maxworthy (1972). The three stages of vortex cell evolution just discussed were described by Lissaman, et al, as the inviscid cell (corresponding here to $\beta = 1$), the entraining cell ($d\beta/dt < 0$), and the decaying cell ($\beta \rightarrow 0$). An implication of this form of observed wake behavior is that those models of buoyant wakes which assume either that no mixing takes place or allow only detrainment of wake fluid are unlikely to be valid representations of actual wakes in an actual atmosphere. It is quite possible that the behavior they postulate may be fluid dynamically correct in some sort of an ideal medium (including possibly in a less turbulent atmosphere than that encountered here) but it appears that buoyancy and mixing have to be treated together in the most general representation of wake behavior.

To summarize the various observations of wake buoyancy measurements, as detailed in Tombach (1974):

1. Wakes acquire buoyancy as they descend through a stratified atmosphere;

2. The relative buoyancy (i.e., the fraction of the maximum possible buoyancy a wake could have after a given descent distance through a given atmosphere) decreases as the wake ages, although the total buoyancy may continue to increase (or decrease at a lesser rate than the relative buoyancy) as long as organized vortical motion is present;

3. Increasing ambient turbulence decreases the rate of increase of buoyancy and the maximum buoyancy acquired by the wake;

4. Atmospheric stability, per se, does not appear to play a role in the timing of and rate of loss of buoyancy.

4.5 Wake Size

Two sets of measurements characterizing the horizontal extent of the wake were made during the experiments -- measurements of the vortex spacing and of the size of the wake oval. The wake penetrations with the Cessna Cardinal gave direct information about both vortex spacing and the size of the wake oval. Vortex spacing was obtained by measuring the time between the positions of peak velocity for the two vortices from the high frequency velocity traces. The width of the wake oval was determined by measuring the length of the region of non-ambient temperature indicated by the high frequency temperature traces.

The wakes which were probed were seldom straight like those shown in textbooks or even in Figure 2-7. More typical was a distorted wake with vertical displacements of the vortices (such as in Figure 2-8) and irregular vortex spacing. The photographs in Figure 4-21 gave a hint of the sort of vortex spacing data to be expected. The probing of one cross section of the wake can result in a large range of vortex spacings, depending on the exact location of the interception.

The effect of such irregularities is apparent in Figure 4-22, where the vortex spacings measured by the Cessna Cardinal are plotted, normalized by the spacing which would prevail for a wake generated by an elliptically loaded wing of the same span and lift. The data is classified on the basis of atmospheric stability; an obvious observation is that there appears to be no correlation between lapse rate and the vortex spacing. The average spacing b_v for all of the wakes generated more than 30 m above the ground, and of age less than 20 sec, is 0.78* of the eliptically loaded value b_{ve}.

*The values presented here are somewhat less than those in the Tombach and Bate (1973) report. The reason is an airspeed system calibration error in the earlier data, which was not discovered until later on in this program.

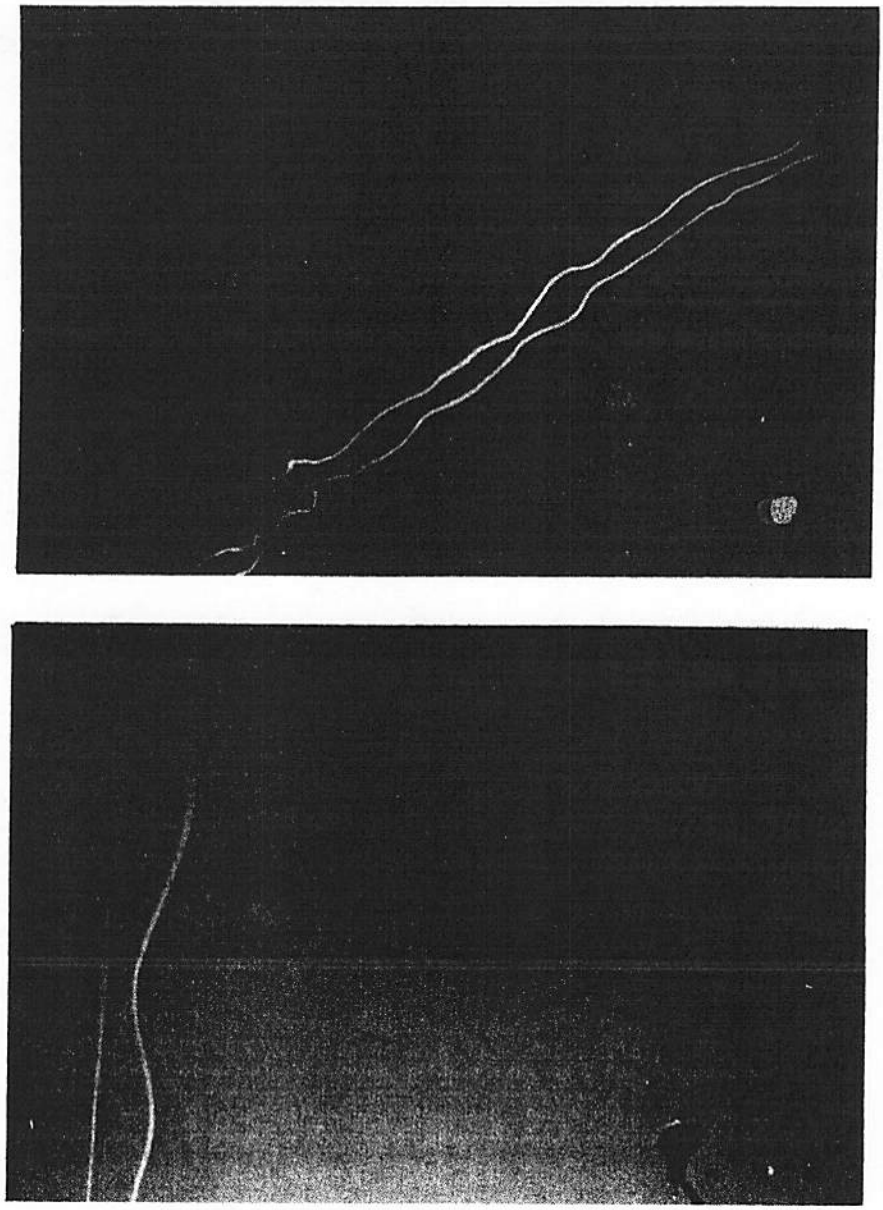

Figure 4-21. Two Examples of Common Wake Appearances. Top: In light-to-moderate turbulence ($\varepsilon^{1/3}$ = 2.3 $cm^{2/3}$ s^{-1}), 20 seconds after generation the wake displays the highly irregular spacing characteristic of the evolution of the sinuous instability (Figure 4-12 shows another photo taken 20 seconds later). Bottom: Sometimes one vortex remained straight while the other became distorted. Note the vortex breakdowns at the top.

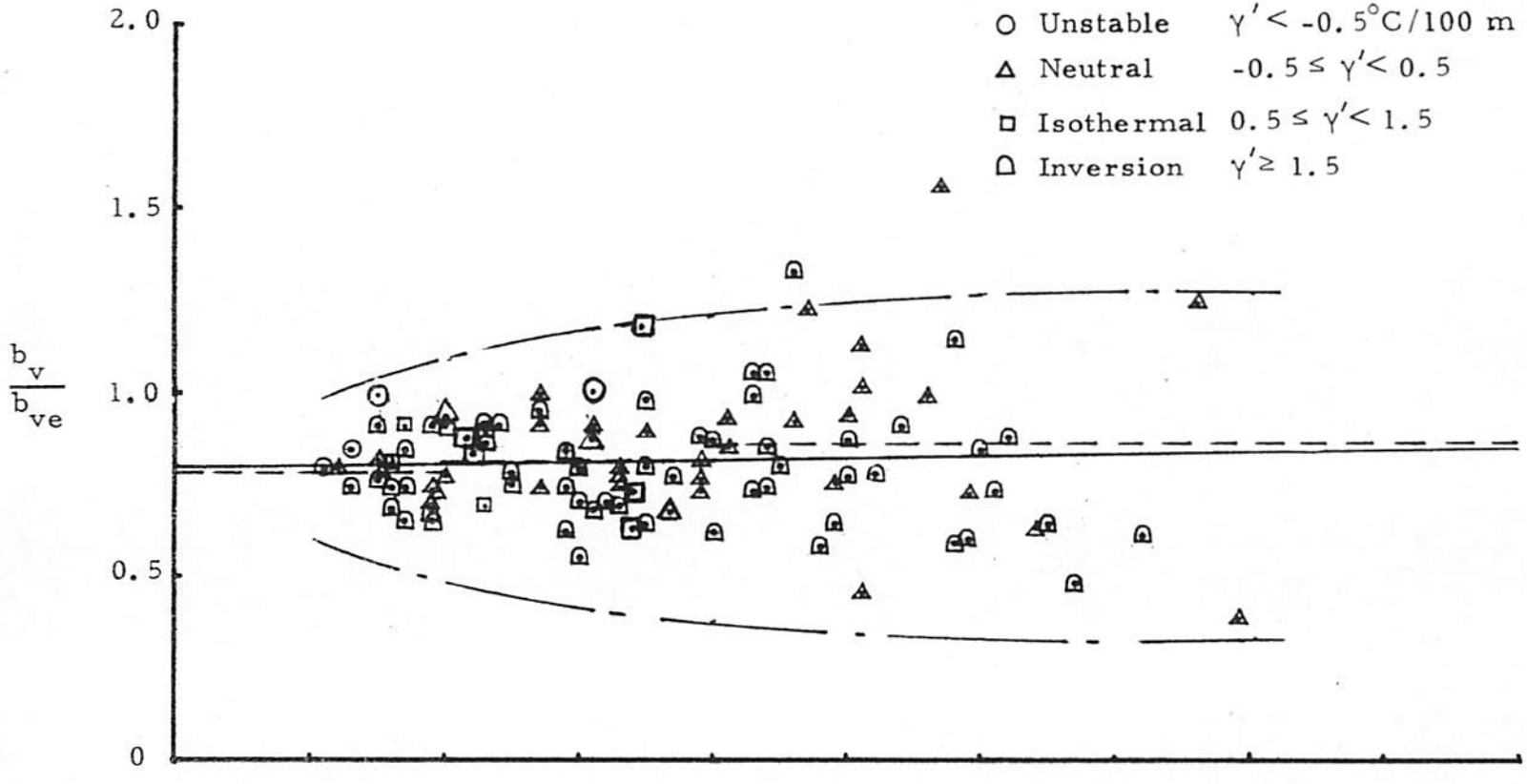

Figure 4-22. Vortex Spacings, b_v, Normalized by the Spacing for Elliptical Span Loading, b_{ve} (= 11.7 m), Measured by the Probing Aircraft in Wakes Generated at Least 60 m Above the Ground. Averages of b_v/b_{ve} for $0 < t \leq 20$, $20 < t \leq 40$, and $t > 40$ s are shown by the broken lines. The solid line is the linear regression line. Note the "parabolic" growth of the data spread.

The most likely reason for this difference from the theoretical value is non-elliptic lift loading of the wing. (The wings of the Aero Commander are not clean. Wing-mounted engines in large pods in the inboard portion of each wing and their propeller slipstreams affect a significant fraction of the wing area. Both the nacelles and the fuselage could contribute some lift at the angles of attack flown during these slower-than-cruise tests). For ages between 20 and 40 seconds the spacing is 0.80 b_{ve} and for ages greater than 40 seconds it is 0.85 b_{ve}. The best fit linear regression line through the data has the equation*

$$\frac{b_v}{b_{ve}} = 0.80 + .0004\, t \quad ,$$

for t in seconds. This equation obviously is not valid at t = 0, where the vortex spacing should approximate the wingspan (1.27 b_{ve}), but can be applied a few spans behind the generator, after the vortices have established their initial spacing. Both this equation and the averages for each 20-second interval indicate that the vortex spacing increases slightly as the wake descends, by an amount which is of the order of 3% in 1 minute.

The previously discussed instability of a vortex pair (Crow, 1970), results in distortion of the vortex filaments on planes which are inclined at about 45° to the plane which originally contained both undisturbed vortices. Since the vortices eventually make contact at the bottom, where these inclined planes touch, it would have been reasonable in Figure 4-22 to expect an occasional point with b_v near zero. Although such vortex "linkings" were probed, an identifiable vortex spacing of less than about 0.4 b_{ve} could not be obtained. The

*The numbers here are slightly different from earlier results by Tombach (1974), as a consequence of an increased data base.

reason for this becomes apparent if the linking photo in Figure 4-12 is studied. Since the hot wire probes were mainly sensitive to the longitudinal* velocity component, they would not respond when the probe aircraft was flying along the vortex, as it would have to do when penetrating the linked portion of a wake. Thus $b_v \approx 0.4\ b_{ve}$ simply represents the smallest observed spacing for which there was sufficient longitudinal velocity component to show up on the oscillograph traces.

A corresponding growth of vortex spacing to about twice the normal spacing, or about $1.5\ b_{ve}$, could also be expected at the uppermost (and most separated) portions of the sinuous wake. No value larger than about $1.3\ b_{ve}$ was observed, however. This value is probably real, since neither Figure 4-22, nor Figure 1 of Crow's 1970 paper (showing a B-47 wake), show a substantial increase in the greatest vortex separation before linking takes place and discrete vortex rings have been formed. Since the theory by Crow is a linear theory, valid for small displacements only, the symmetry (about the equilibrium position) required by it for the lateral and vertical motion of each vortex need not necessarily occur when the displacements become large.

Vortex separation was also measured photographically, with the results shown in Figure 4-23. These measurements were made by selecting one point of wake cross section in space and observing the vortex spacing at that point. There are a few differences between this figure and Figure 4-22 which are worth noting. First, there are more points here because smoke visualization allowed measurement of b_v more often than the probing did, since the latter required a crossing through both vortices. The longest vortex ages in this figure are less because the wakes frequently drifted out of the field of

---

*Longitudinal to the probe aircraft, not the generator.

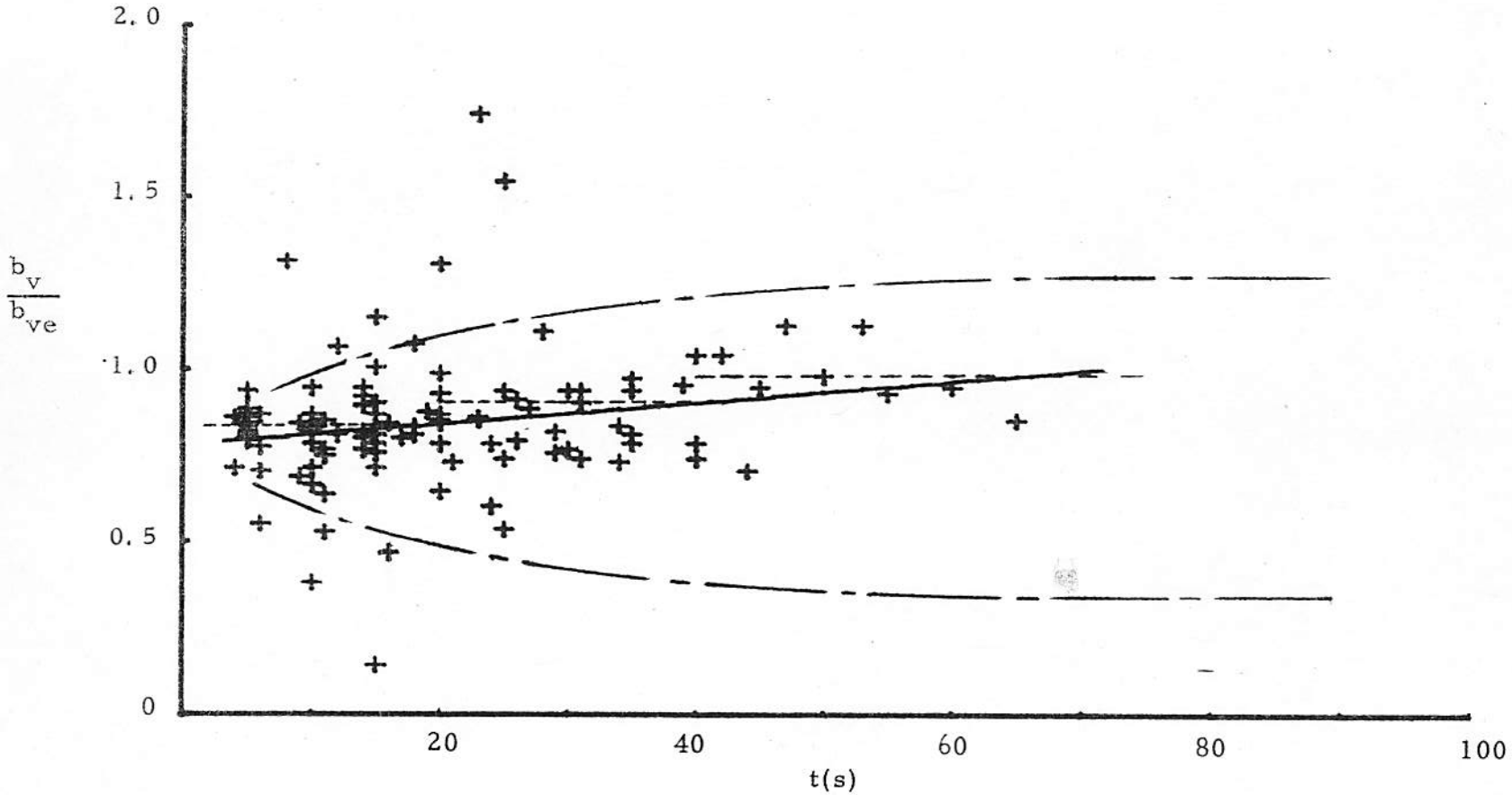

Figure 4-23. Vortex Spacings, b_v, Normalized by the Spacing for Elliptical Span Loading, b_{ve} (= 11.7 m), measured from Site 1 photographs of Wakes Generated at Least 60 m Above the Ground. Averages of b_v/b_{ve} for $t \leq 20$, $20 < t \leq 40$, and $t > 40$ s are shown by the broken lines. The solid line is the linear regression line. The envelope from Figure 4-22 bounds most of the observed points here also.

view of the fixed camera. Some very small spacings are indicated, since the photographic data acquisition technique is not limited by the orientation of the flow field in the same way the probes are.* With only two exceptions all of the points again lie below $b_v/b_{ve} = 1.3$. A final comparison concerns banked or tilted wakes. All of the probing measurements presented in Figure 4-22 were made on relatively level wakes, since penetration of both vortices of a banked wake would not have been possible by a level-flying probe aircraft. On the other hand, the only restriction on banking in Figure 4-23 was an arbitrary requirement that the vertical vortex spacing not exceed 4 m (corresponding to about 25° bank angle).

The averages of b_v/b_{ve} for $t \leq 20$, $20 < t \leq 40$, and $t > 40$ s are 0.82, 0.98, and 0.96 respectively in this case and the regression line is represented by the equation

$$\frac{b_v}{b_{ve}} = 0.79 + .0031\, t \quad .$$

Thus there is excellent agreement with the probe measured spacings at small times, but the photographic data indicates a 23% increase of vortex separation in one minute, which is considerably more rapid than the probing value. The sparseness of data for $t > 40$ s (only 9 points) does not give as much significance to this growth trend observation as could be assigned to the more numerous old points in Figure 4-22, however. The points at times exceeding 30 seconds all lie well within the same envelope curves as for the probed data.

*The point at $t = 15$ sec where b_v/b_{ve} is 0.15 is an incipient linking point of a rising wake in a turbulent, highly unstable atmosphere (Group I, Series 3, Run 2).

Another measure of wake size, the width of the buoyant portion of the oval wake volume, was also routinely measured. This dimension, denoted b^*, was obtained from the same high-frequency temperature traces from which ΔT was measured. Figure 4-24 shows four representative examples of temperature profiles and indicates how b^* was defined when the wake had a fairly uniform temperature and also when each cell had a different temperature. The lower two types of profiles in the figure were often seen, but a meaningful definition of b^* could not be derived from them.

In Figure 4-25 the temperature wake width (normalized by b_{ve}) is plotted against time, with atmospheric stability as a parameter. No systematic effect of atmospheric stability appears to be important here, except that all of the very wide wakes were generated in isothermal conditions, which tended most often to also be the least turbulent conditions. In the same way as for the vortex spacing, there is a growth in b^*/b_{ve} with time, but at a more rapid rate; the averages are 1.68 for $0 < t \leq 20$ seconds, 1.86 for $20 < t \leq 40$ seconds, and 1.97 for $t > 40$ seconds.* There is, however, too much scatter in the data for a meaningful linear fit similar to that done for the vortex spacing.

Since Figures 4-22 and 4-23 showed that $b_v < b_{ve}$ and that b_v increased slightly with wake age, a comparison of b^* with the simultaneously measured b_v would indicate whether the increase in b^* is

---

*The values of b^*/b_{ve} presented here are somewhat less than those in the report by Tombach and Bate (1973) because of a change in the definition of b^*. Here b^* is defined as shown in Figure 4-24. In the earlier report b^* was measured between the outer edges of the wake temperature profile, just above the horizontal external temperature line. The current definition is more consistent with the usual definitions of sizes of wakes and jets based on their velocity, temperature, or density profiles.

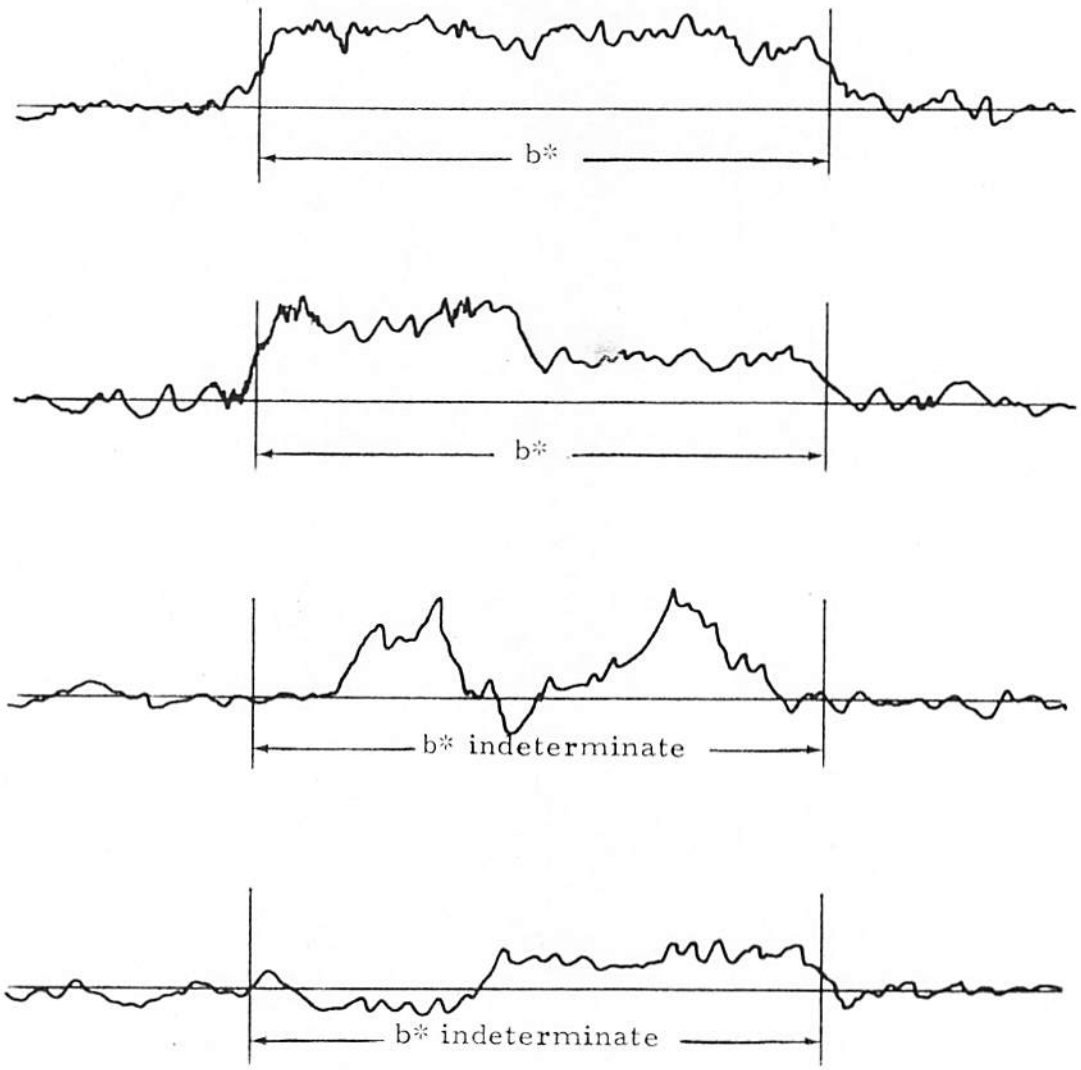

Figure 4-24. Representative Temperature Cross Sections of Wakes, Showing the Definition of the Temperature Wake Scale b* .

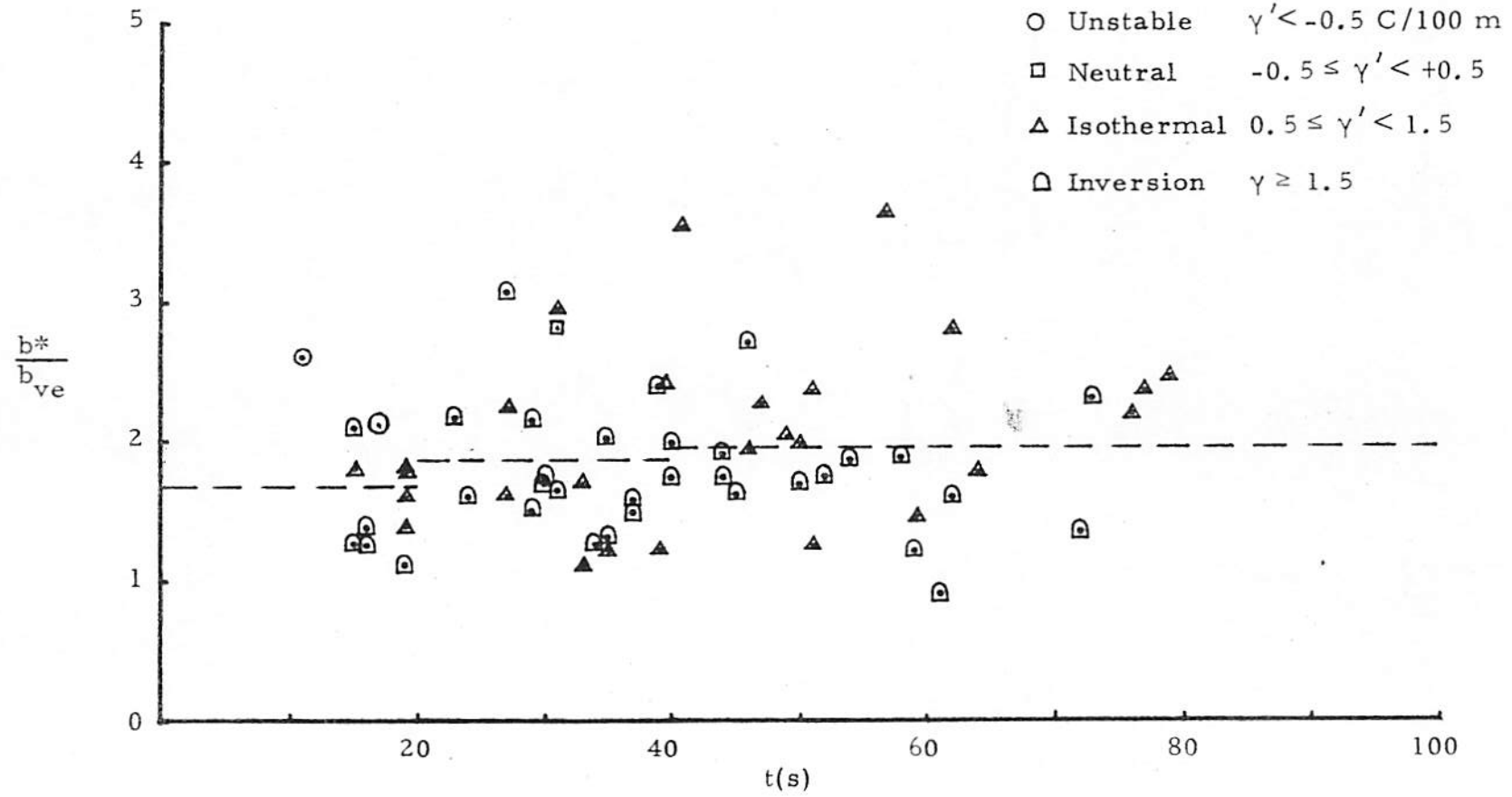

Figure 4-25. Measured Temperature Wake Widths Normalized by the Elliptic Span Loading Vortex Spacing b_{ve}. The broken lines indicate average values for $0 < t \leq 20$, $20 < t \leq 40$, and $t > 40$ seconds. All wakes were generated at least 60 m above the ground.

related to the increase in vortex spacing. This is done on Figure 4-26. The data scatter here is surprisingly large, and a significant variation in b^*/b_v with time is not discernible from the same three averages as before, which here have the values 2.21, 2.33, and 2.17. The line at $b^*/b_v = 2.09$, which would correspond to a well-mixed oval in a potential flow (Lamb, 1945), passes through the main concentration of data points. A very slight effect of atmospheric stability is apparent in the figure, with the inversion points generally showing higher b^*/b_v than the isothermal points. An analysis of the same data, but stratified by turbulence and stability, also supports this observation and shows no correlation at all with ambient turbulence.

The wide variation in b^*/b_v indicates that instantaneous wake oval sizes can be quite different from the 2.09 b_v value. Smaller values of b^* may indicate the presence of a sheath of cooler entrained air around the oval. Larger values may be a consequence of locally small vortex spacings, where b^* might not vary as rapidly as b_v does from one section of wake to another.

Overall, the conclusions which can be drawn from this discussion on wake size include:

1. The vortex spacing of a wake is constant or increases only very slightly with time, and seems not to be influenced by atmospheric stratification;

2. The measured vortex spacings for the Aero Commander are considerably less than those which would be computed for an elliptically loaded wing of the same span and lift;

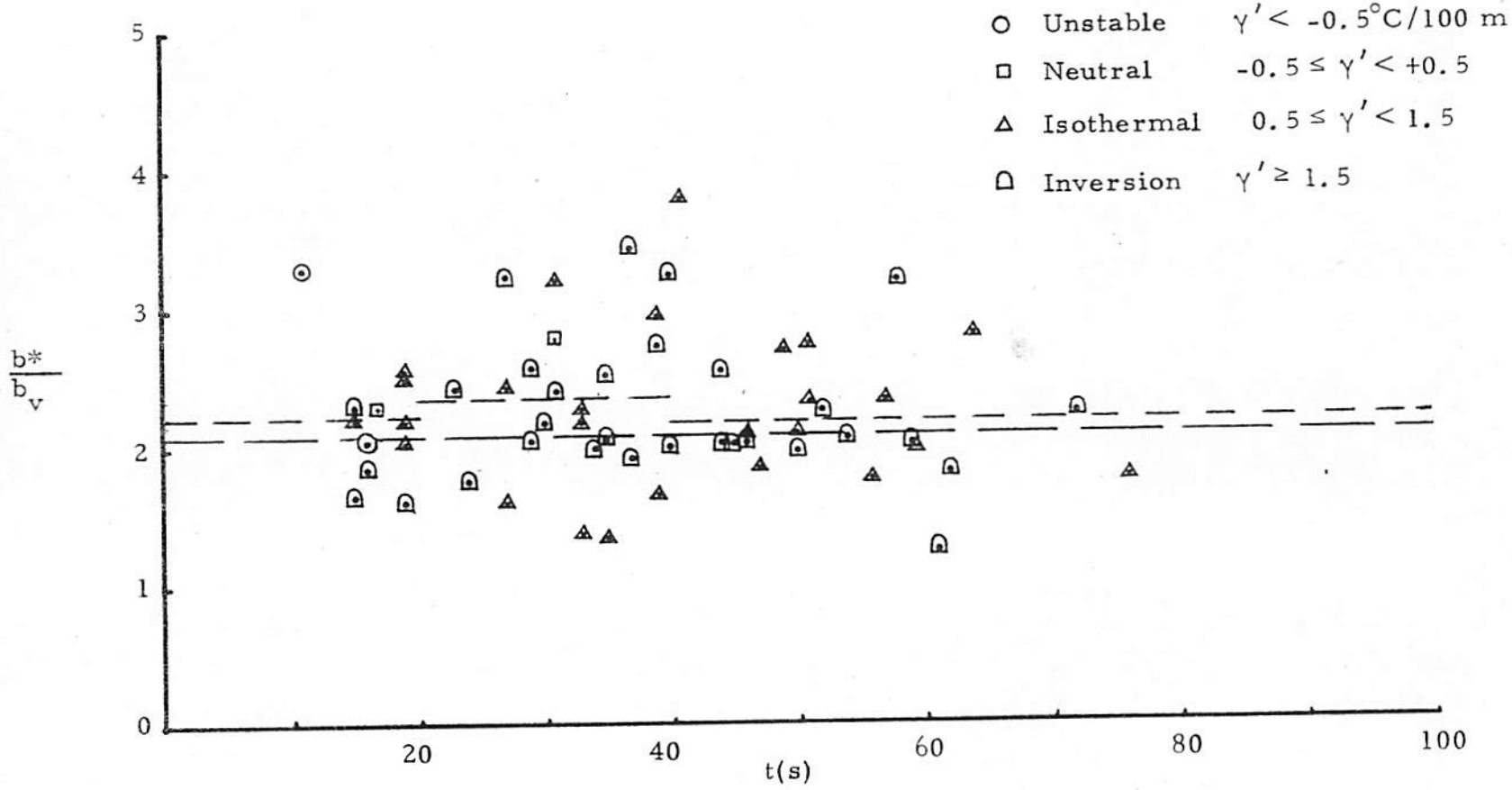

Figure 4-26. Ratio of Temperature Wake Size to Simultaneously Measured Vortex Spacing for Wakes Generated 60 m or More Above the Ground. The segment averages (----) and the potential flow oval size of $b^* = 2.09\ b_v$ (— — —) are shown.

3. The temperature oval width varies widely, but tends on the average to be essentially 2.09 b_v -- the size of the classical wake oval. Here again, atmospheric stratification does not appear to have a noticeable effect on the oval width.

4.6 Vortex Velocities

Considerable analysis was performed on the measurements of vortex velocities which were obtained by the fast response velocity sensors on the probe aircraft. Because of the complexity of the analysis procedures, a separate report (Bate, 1974) contains a detailed discussion of the procedures and their results. For completeness, however, a brief review of those results in the light of the other observations of the program seems appropriate.

Some 76 vortex crossings were analyzed and the velocity profiles were fitted with a functional representation of vortex velocities given by Lamb (1945) for viscous, laminar vortices. The fits achieved were not extremely good, and analysis showed that noisyness of the signal due to ambient turbulence was not the cause -- the actual flow fields just did not correspond very well to the formulation assumed, especially in the outer regions of the vortex. Use of the Betz (1933) form for the velocity distribution gave even poorer results, and the scope of the project did not allow development of flow models which could account for some of the properties which were observed. Core radii and vortex circulations were computed from the fitted data. Figures 4-27 and 4-28 present the results. The points on these figures have been identified with respect to broad ranges in the variance, σ, between the assumed and measured velocity profiles and the distance of closest approach between the probes and the vortex center, y_{min}. A great deal of scatter is exhibited by the data. No simple correlation between this scatter and either large or small values of σ and y_{min} is apparent from the figures.

A line representing the average of all the calculated core radii is shown on Figure 4-27. The value of this average is $r_o = 0.33$ m, which results in a dimensionless vortex diameter,

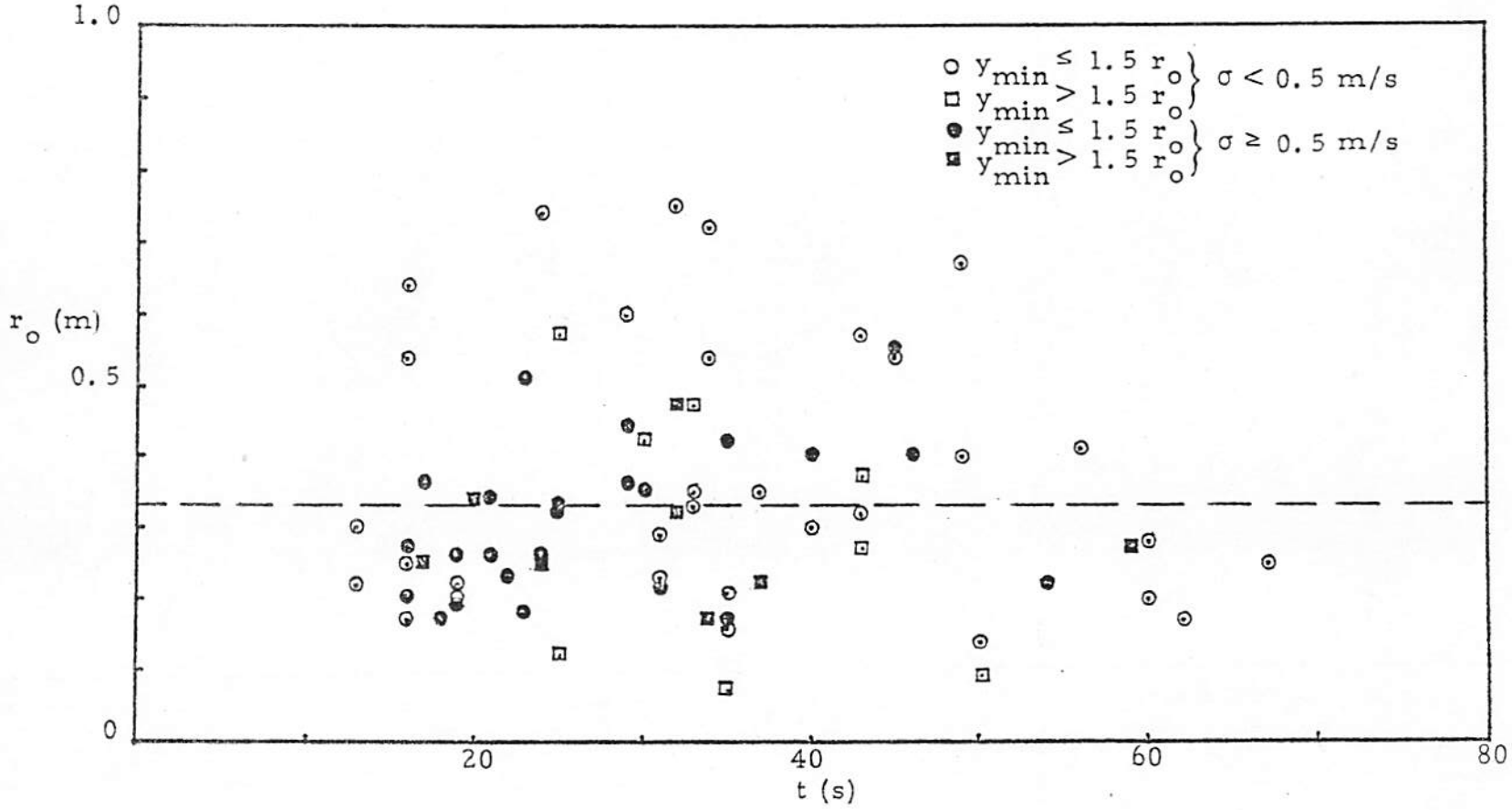

Figure 4-27. Vortex Core Radius as a Function of Wake Age. The dashed line represents the average for all points. y is the distance of closest approach of the probe to the core axis. σ is the rms error between the measured and assumed velocity profiles.

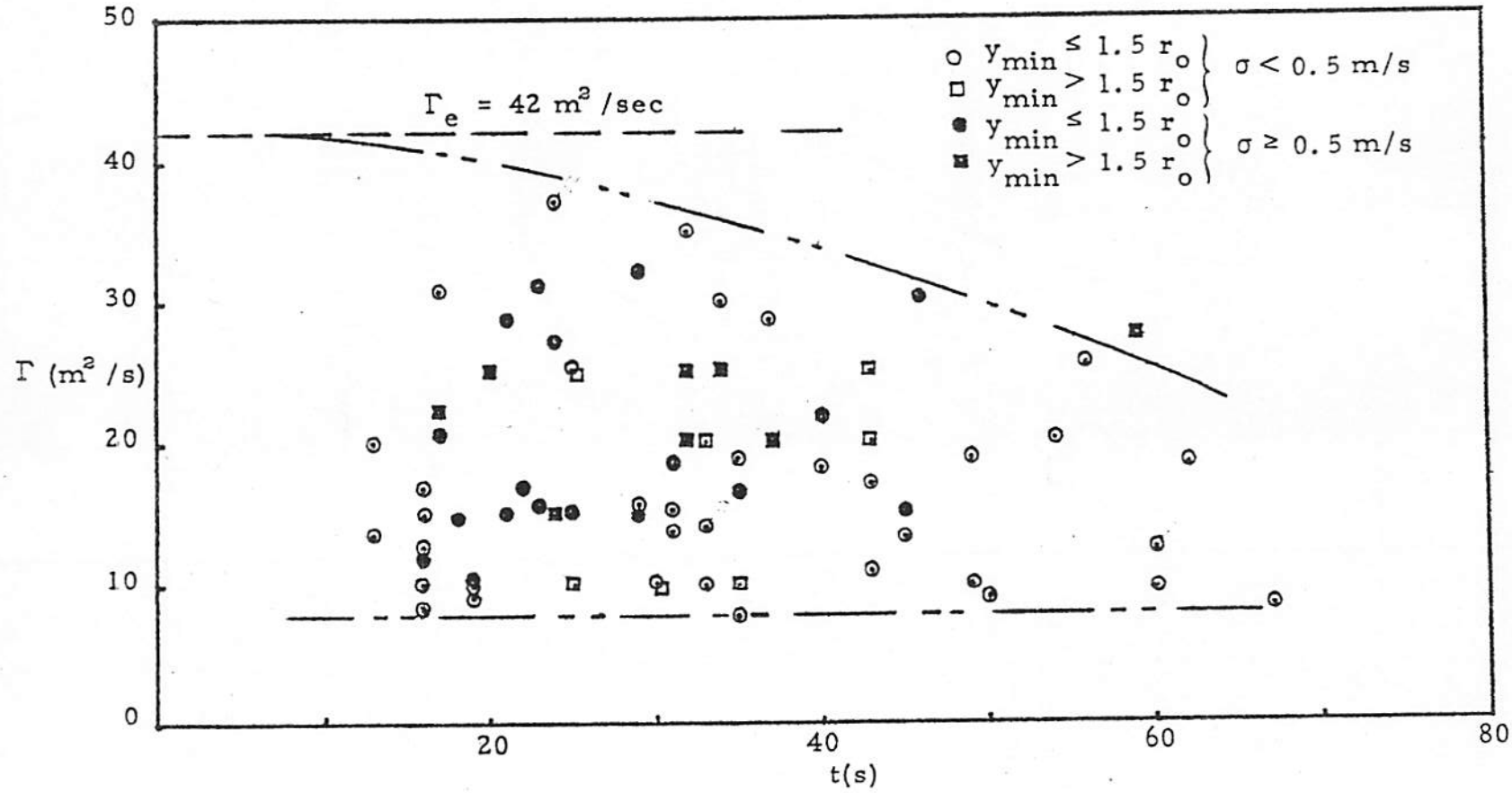

Figure 4-28. Vortex Circulation as a Function of Wake Age. The lines on the graph are discussed in the text. y and σ are defined on Figure 4-27

normalized by the Aero Commander wingspan, of $d/s = (2)(.33)/14.9 = .044$ ($\pm .021$, corresponding to one standard deviation). This value is consistent with the size of the vortex cores reported by Garodz (1970), and is well under the value of .155 postulated by Spreiter and Sacks (1951). Any trends in core growth with time are masked by the scatter in the data.

Figure 4-28 shows the calculated vortex circulation as a function of time. The dashed line represents the theoretical value of the total bound circulation for elliptic wing loading for the Aero Commander in its flight configuration during the test program. The two phantom lines indicate upper and lower limits of the data scatter. The upper limit defines a trend indicating a reduction in circulation with wake age. This upper limit also appears to approach, at small times, the theoretical value of the bound circulation for elliptic loading. The lower limit is constant for all times at approximately $\Gamma = 8\ m^2/sec$, probably because only those runs for which clearly defined velocity traces from both probes existed were analyzed. The maximum value of the computed circulations, at about $36\ m^2/s$, is well below the Γ of $54\ m^2/s$ which would be deduced from the previously presented data on vortex spacing and descent speed. Some possible reasons for this discrepancy, having to do with larger velocities outside of the core than predicted by the assumed formulation, are discussed by Bate in his 1974 report.

Some vortex velocity data could be obtained directly without the need to fit data to functional forms. The measured peak velocities encountered during all of the Group I vortex crossings are plotted in Figure 4-29. There is a large variation in velocity at any given time, resulting mainly from the fact that the probes on the Cardinal did not penetrate the vortex at the same point on each traverse. The true peak tangential velocity would be indicated directly by the hot wire probe trace only if it traversed through the upper or lower edge of the vortex core, where the longitudinal velocity change along the

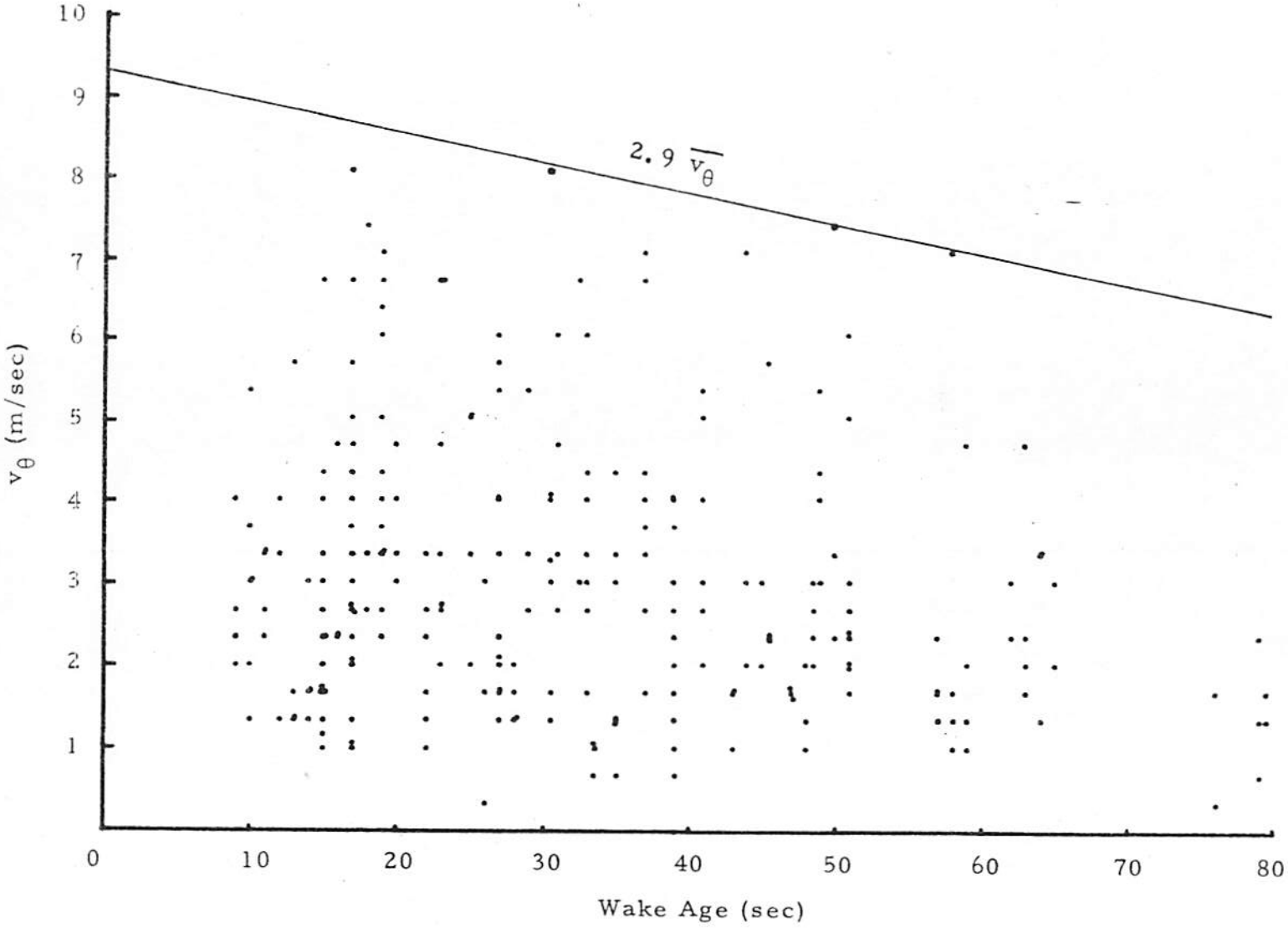

Figure 4-29. Peak Vortex Tangential Velocities Measured by the Probes During Wake Corssings. The envelope curve at the top is derived in the text.

probe would be greatest. Penetration at other points closer to the vortex center or outside the core gives lower readings. Thus only the relatively few data points at the top of Figure 4-29 define an envelope of vortex tangential velocities. It is of interest to determine whether these velocities decay as the wake ages. Since it is very difficult to determine this from the few points defining the envelope, an alternate procedure was used.

This procedure requires the assumption that the probability distribution of peak tangential velocities measured by probing the wake, normalized by the true peak tangential velocity, be invariant with wake age. In practice this means that the probability of hitting a given radius with the probing aircraft be the same for young wakes as for old ones. Although this probability involves undefinable factors related to cockpit visibility of the vortex, core size, turbulence, and wake distortion (assuming pilot technique to be an invariant) it can be argued that, to a good degree of approximation, this assumption of the invariance of the observed distribution of velocity measurements as the wake ages is a valid one.

Given this assumption, then all of the measurement statistics will be constant in time. Specifically, the ratio of the average of the measured velocities at a given time to the peak velocity at the same time will be a constant. Thus, given the average velocity at a number of instants of time and a few "envelope" points one can estimate the rest of the envelope curve.

Figure 4-30 shows the first step of this procedure. Average values of the v_θ measurements were computed for 5-second increments of time, that increment being chosen to give a large number of points in each interval. The points on the figure are the result. The linear regression line through the points, excluding the one at $t = 70$ s, is shown. The last point was excluded because it was

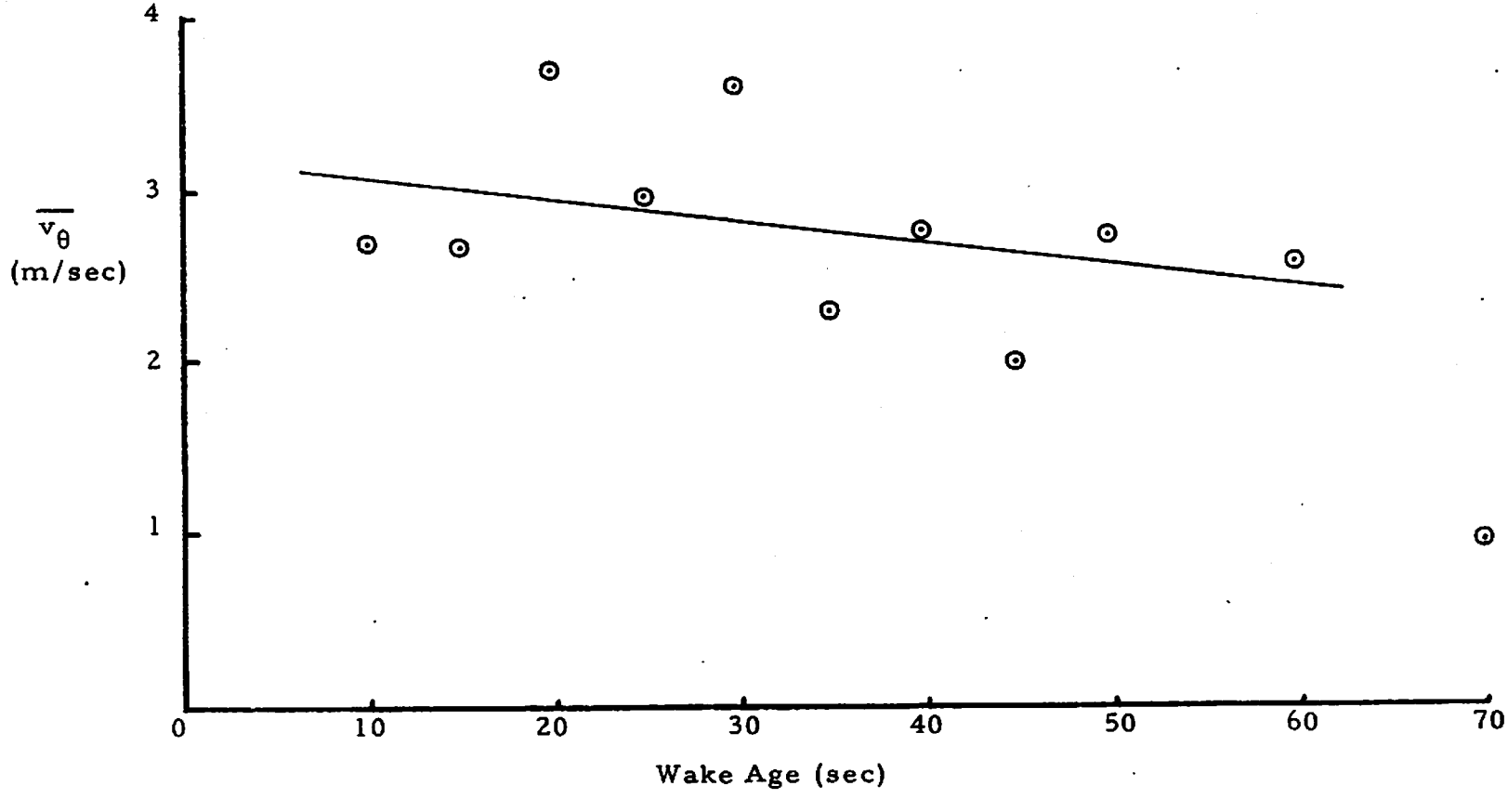

Figure 4-30. Mean of Measured Peak Velocities During All Wake Crossings. The linear regression line shown is based on all data for $t \leq 60$ s.

based on much fewer measurements than the others and because, even if it is valid, a linear fit to the data would no longer be appropriate, while higher degree fits are not warranted by the data scatter.

There is a clear decrease in the mean observed vortex velocity as the vortex ages, by about 20% in 60 seconds. The rate of decrease may become faster as the wake grows older. Applying this same mean curve to Figure 4-29, with an arbitrary multiplier chosen so that all of the data lies below it, one finds that $2.9\ \overline{v_\theta}$ gives a good envelope curve with only one point above it and three points lying on it. Here again, the linear curve may not be appropriate for $t > 60$ sec.

Thus it appears that, as expected, vortex velocities decay with time (although not be an extremely great amount during the first minute or so), most probably by viscous or turbulent core diffusion, though other processes such as vorticity detrainment could be imagined. This rate of velocity decay is greater than the rate of circulation decay presented previously. Since the total circulation is related to both the size of the vorticity-containing core and the peak tangential velocities, the expected diffusion of vorticity would require that velocity decay be greater than circulation decay, which is consistent with the observed behavior.

Overall, one can conclude with some certainty that, in these observations:

1. Vortex circulations decay with time at a rate which appears to accelerate as the wake decays.

2. Vortex diameters are about 4.4% of the aircraft wingspan.

3. Peak Aero Commander 560F vortex velocities are about 8 m/s and decay on the average by about 20% in one minute.

4.7 Special Observations

During the course of the experimental program, several special tests were performed in order to determine the effects of non-standard aircraft configurations and operations on wake behavior. Table 4-3 summarizes the conditions that prevailed during these tests.

Table 4-3. Summary of Special Test Conditions.

Group II		Description
Series	Run	
4	1	Flaps down at high altitude
4	2	"Porpoising" of aircraft at 2 sec intervals
4	3	Yawing of aircraft at 2 sec intervals
8	1	Power off descent
8	2	Climb
8	3	180° standard rate turn
12	1	Full flaps at low altitude
13	1	Two-second porpoising with probing
13	2	Touch and go landing
13	3	In-trail probe
18	1	In-trail probe
18	2	In-trail probe

Both flaps-down tests showed that the vortices moved much closer together than their normal, flaps-up spacing within about 10 spans behind the aircraft. Extreme fuzziness of the smoke-marked vortices was evident about 5-15 seconds after generation. Within 20 seconds, the vortices appeared to have diffused to a considerable extent. Although vortex velocity measurements were not made for these tests, the appearance of the smoke-marked cores suggests that diffusion of vorticity greatly reduced the magnitude of their original, rotational velocity fields. This accelerated diffusion of vorticity is probably the result of increased mechanical turbulence in the wake due to the increased profile drag of the flaps-down situation.

Both porpoising and cyclic yawing of the aircraft at 2 second intervals produced bursting of the vortex cores at the positions of the changes in direction (maximum acceleration) of each of these two similar maneuvers. Bursting commenced within about 10-15 seconds after passage of the generator aircraft. The vortex segments between the burst positions were devoured by the opposite moving bursts within 25-35 seconds after generation.

Incomplete photo sequences during the power off descent maneuver gave inconclusive results. The initiation of both Crow instability and core bursting were evident from the photos, but the proceeding of these phenomena to conclusion was not witnessed. During the climb both core bursting at 10 seconds and Crow linking at 20 seconds were observed. These times are comparable to those in Figure 4-15 for level wakes at the same level of turbulence ($\varepsilon^{1/3} = 2.0$).

The 180° standard rate turn resulted in Crow linking at 25 seconds, which again is consistent with the regular linking time for the existing level of ambient turbulence. The linking was followed by localized bursting of the smoke rings, so that only a series of broken, puffy smoke rings remained after 45 seconds.

The touch and go landing produced a wake which descended into ground effect and formed links with the underground image vortices about 30 seconds after wake formation. Extreme turbulent meander and subsequent localized bursting produced disintegration of the vortices after this time.

The results of the in-trail probing were not conclusive. It was nearly impossible to keep the probe aircraft in the selected vortex for a sufficient length of time to allow meaningful measurements to be made. Also, as a consequence of this intermittent penetration of one of the vortices, the resultant localized destruction of the wake's vortex pair precluded any normal interpretation of the photographic data taken simultaneously with the probing. Additionally, the test run of Series 13, Run 3 was performed during a period of extremely high ambient turbulence, so that the wake was torn apart almost immediately upon formation.

To summarize the significant results of these special observations:

1. Flaps down appear to accelerate the diffusion of vorticity from the vortices with resultant decrease in their rotational velocity fields likely.

2. Abrupt maneuvers of the aircraft, such as porpoising or cyclic yawing, appear to initiate core bursting at the positions of maximum acceleration of the aircraft during the particular maneuver.

3. Steady-state aircraft maneuvers such as descent, climb, and turns appear (at least to the limited extent examined here) to produce wake behavior similar to that encountered during level flight. Ground effects are of course important during landing maneuvers.

5. CONCLUDING DISCUSSION

A large number of observations of vortex wake behavior have been presented in this report. Some of the data has been comprehensive, and therefore interpretation has been straightforward. In some cases only fragments of the whole picture have been revealed. And, in other cases, the results of several different kinds of measurements were used to arrive at a single conclusion. Because of this, it might be well to review what the results of this program do tell about wakes, and also what they do not tell us.

Measurements of the rate of descent of the wake show that, in a stable atmosphere, the wake descends initially at the rate predicted by theory (using measured vortex spacings) but that the descent speed begins to slow significantly after 30-40 seconds and becomes some 50-75% of its initial value after about 1 minute. The maximum distance of descent was typically 65-75 meters, with wake bank angles of less than 30° having little discernible effect. Turbulent erosion of the wake strength is the probable cause of this slowing of descent. The boundary of the wake oval is not a shear layer, thus the presence of mixing means that there is turbulence in the wake oval interior. Consequently, mixing between the two halves of the oval, as well as with the outside atmosphere, will erode the circulation and result in a decreased descent rate, both of which are consistent with the experiments.

Atmospheric stability appears to have no direct effect on the rate of wake growth or on the maximum distance the wake descends. It has a strong effect on the descent speed of the wake, however. Initial descent rates correspond to the theoretical rates only in a stable atmosphere. Descents in neutral conditions were consistently 50% faster, while wakes rose upward in an unstable atmosphere.

Ambient turbulence, on the other hand, strongly affects several aspects of wake behavior through its effect on entrainment (as deduced from the buoyancy measurements) and the consequent weakening of the wake strength. Thus increasing turbulence accelerates wake decay and slows the descent of the vortices, but does not affect the initial descent rate.

Measured vortex spacings are about 80% of the elliptical loading spacing. This vortex separation increases, at least slightly, as the wake descends, which correlates with the expected behavior of an entraining wake. Measurements of the size of the temperature wake indicate that the region of temperature excess fills the classical wake oval, which increases in size proportionally with the increase in vortex separation. The temperature within the entire oval is usually uniform, although occasionally one cell has a different temperature than the other.

Wakes acquire buoyancy as they descend through a stratified atmosphere, and the rate at which this buoyancy is acquired decreases as the wake ages. Thus a wake increases in buoyancy initially, reaches a point of greatest buoyancy in, typically, about 40 seconds, and then begins to lose that buoyancy. The duration of this buoyancy growth/decay cycle is shortened as ambient turbulence increases, and the maximum buoyancy level is simultaneously decreased by increased turbulence.

The phenomenon of wake tilting correlates well with wind shear, with the sense of the banking being generally opposite to the sense of the shear when the wake is below 30 m above the ground. The expected banking at 20 seconds of wake age is always in this direction, to a degree which is proportional to the strength of the shear. Interpreted for boundary layer shear, the upwind vortex descends relative to the downwind one. The often-puzzling phenomenon of the long-lived

single vortex may also be a result of wind shear. The lower vortex of a banked wake near the ground consistently persisted much longer than the upper one, and resisted any interactions with its image beneath the surface. A definitive theoretical explanation for tilting and the asymmetric lifetimes is yet to be developed, however.

Aircraft wakes are destroyed in time by either core bursting, the sinuous instability, or by severe deformations in strong turbulence. In these experiments core bursting was the most common mode of decay. There was a general $1/\epsilon^{1/3}$ correlation of wake lifetime with turbulence for all of the cases examined, which included both links and bursts.

The theory of Crow and Bate which treats the vortices as coupled linear oscillators with the atmospheric turbulence as a forcing function and involves no fitted constants, appears to give approximately the geometric mean of the actual lifetimes of wakes undergoing the sinuous instability. Essentially all of the observed lifetimes are within a factor of 2 of the values predicted by the theory.

The characterization proposed by Lissaman, et al, (1973) to describe the life of a wake in three stages appears to be a useful description of vortex wake behavior which agrees in all aspects with the experimental observations. The three stages, which reflect the progressively increasing influence of atmospheric turbulence on the motion of the wake are:

1. Inviscid wake -- descends at constant speed, constant vortex spacing, no mixing with ambient fluid, acquires buoyancy in a stable atmosphere.

2. Entraining wake -- descent rate slows, vortex separation increases, entrainment occurs, wake oval enlarges, rate of increase of buoyancy slows down.

3. Decaying wake -- descent slows (or stops), buoyancy is dissipated, strong entrainment occurs, vortices decay. (This stage may never be reached because of decay by an instability.)

In this characterization, atmospheric stability, per se, appears to play no significant role, while ambient turbulence very much affects the rate at which wake behavior passes through these three stages.

There are areas of theoretical work which are needed for better understanding of the observed phenomena. Modeling of wake transport in a stratified medium needs to consider entrainment. Models which do not consider mixing, or do not allow it, predict wake behavior which is in conflict with the measurements of this study, although measurements in an extremely calm atmosphere may correspond more closely with these theoretical predictions.

Quantitative predictions of the decay of wake strength as a function of ambient and/or core turbulence still remain as an elusive goal, and no models exist yet to explain the many phenomena occuring in a sheared wind field.

The meteorological measurements made in conjunction with the flight tests showed that surface-based measurements of wind and turbulence can be used, for the types of conditions encountered here, to make useful inferences about turbulence aloft (up to 70 m, say). The normally assumed relationship between stability and turbulence, in which it is assumed that turbulence is the least in the most stable conditions, was totally invalid at the test site. In fact, drainage flows caused the strongest low-level turbulence to occur when the stability was the greatest.

6. REFERENCES

Barber, M. R., R. L. Kurkowski, L. J. Garodz, G. H. Robinson, H. J. Smith, R. A. Jacobsen, G. W. Stinnett, Jr., T. C. McMurty, J. J. Tymczyszyn, R. L. Devereaux, and A. J. Bolster (1975): Flight Test Investigation of the Wake Vortex Characteristics Behind a Boeing 727 during Two-Segment and Normal ILS Approaches. (A joint NASA/FAA report). NASA Technical Memorandum NASA TM-X-62, 398 and FAA Report FAA-NA-75-151.

Bate, E. R., Jr. (1974). A Study to Determine the Structure of Trailing Vortices from Full Scale Flight Test Data. AeroVironment Inc. Final Report FR 441 to Dept. of Transportation, Transportation Systems Center under Contract DOT-TSC-523.

Betz, A. (1933): Behavior of Vortex Systems. NASA Technical Memorandum No. 713.

Brashears, M. R., J. N. Hallock, and N. A. Logan (1974): Analysis of Predicted Aircraft Wake Vortex Transport and Comparison with Experiment. AIAA 7th Fluid and Plasma Dynamics Conference, Palo Alto, Calif., 17-19 June. AIAA Paper 74-506.

Burnham, D. C. (1972): Effect of Ground Wind Shear on Aircraft Trailing Vortices. AIAA Journal 10, pp. 1114-1115.

_____, J. Hallock, R. Kodis, and T. Sullivan (1972): Vortex Sensing Tests at NAFEC. FAA Report DOT-TSC-FAA-72-2.

Crow, S. C. (1970). Stability Theory for a Pair of Trailing Vortices. AIAA Journal 8, pp. 2172-2179.

Dee, F. W., and O. P. Nicholas (1969). Flight Measurements of Wingtip Vortex Motion Near the Ground. Aero. Res. Council Current Paper 1065.

Garodz, Leo J. (1971): Measurements of Boeing 747, Lockheed C5A and Other Aircraft Vortex Wake Characteristics by Tower Fly-by Technique. In Aircraft Wake Turbulence and Its Detection, Ed. J. H. Olsen, et al. Plenum Press, New York.

Lamb, H. (1945): Hydrodynamics. Sixth Ed., Dover, New York; p. 592.

Leahey, D. M., and J. Halitsky (1972): Low Wind Turbulence Statistics and Related Diffusion Estimates from a Site Located in the Hudson River Valley. Atmos. Envir., 7, pp. 49-61.

Lissaman, P. B. S., S. C. Crow, P. B. MacCready, Jr., I. H. Tombach, and E. R. Bate, Jr. (1973): Aircraft Vortex Wake Descent and Decay Under Real Atmospheric Effects. FAA Report FAA-RD-73-120.

MacCready, P. B., Jr. (1962): The Inertial Subrange of Atmospheric Turbulence. J. Geophysical Research, 67, pp. 1051-1059.

_____, (1971): An Assessment of Dominant Mechanisms in Vortex-Wake Decay. In Aircraft Wake Turbulence and Its Detection, Ed. J. H. Olsen, et al, Plenum Press, New York, pp. 289-304.

_____, L. B. Baboolal, and P. B. S. Lissaman (1974): Diffusion and Turbulence Aloft Over Complex Terrain. Preprint Volume, Symposium on Atmospheric Diffusion and Air Pollution, Santa Barbara, Calif., publ. by Am. Met. Soc., Boston, Mass., pp. 218-225.

Maxworthy, T. (1972): The Structure and Stability of Vortex Rings. J. Fluid Mech., 51, pp. 15-32.

Spreiter, J. R., and A. H. Sacks (1951): The Rolling Up of the Trailing Vortex Sheet and Its Effect on the Downwash Behind Wings. Journal of the Aeronautical Sciences, 18.

Tombach, I. H. (1971): Transport of a Vortex Wake in a Stably Stratified Atmosphere. In Aircraft Wake Turbulence and Its Detection, Ed. J. H. Olsen, et al, Plenum Press, New York.

_____ (1972): Transport and Stability of a Vortex Wake. AFOSR Technical Report AFOSR-TR-72-1159 (AD 742 305).

_____ (1973): Observations of Atmospheric Effects on Vortex Wake Behavior. J. Aircraft, 10, pp. 641-647.

_____ (1974): Influence of Meteorological Factors on the Vortex Wake of a Light Twin-Engine Aircraft. AFOSR Technical Report AFOSR-TR-74-1507.

Tombach, I. H., and E. R. Bate, Jr. (1973): Study of the Motion and Properties of the Vortex Wake of a Light Twin-Engine Aircraft. AeroVironment Inc. Final Report AV FR 351 to Dept. of Transportation, Transportation Systems Center under Contract DOT-TSC-523.

REPORT OF INVENTIONS AND SUBCONTRACTS

(Pursuant to "Patent Rights" Contract Clause)

Form Approved
Budget Bureau No. 22-R160

INSTRUCTIONS TO CONTRACTOR

This form *(in triplicate)* is for use in submitting INTERIM and FINAL reports to the Contracting Officer.

An INTERIM report shall be submitted at least every twelve months, commencing with the date of the contract, and should include only those inventions and subcontracts for which the information requested below has not previously been reported.

A FINAL report shall be submitted as soon as practicable after the work under the contract is complete and shall include (a) a summary of all inventions required by the contract to be reported, including all inventions previously reported and any inventions since the last INTERIM report; and (b) any required information for subcontracts which has not previously been reported.

1. NAME AND ADDRESS OF CONTRACTOR *(Include ZIP Code)*
AeroVironment Inc.
145 Vista Avenue
Pasadena, California 91107

2. CONTRACT NUMBER
DOT-TSC-523

3. TYPE OF REPORT *(check one)*
☐ a. INTERIM ☒ b. FINAL

SECTION I - INVENTIONS *("Subject Inventions" required to be reported by the "Patent Rights" clause)*

INVENTION DATA *(Listed below are all inventions required to be reported) (If NONE, so state).*

☒ a. THERE WERE NO INVENTIONS WHICH REASONABLY APPEAR TO BE PATENTABLE

☐ b. LISTED BELOW ARE INVENTIONS WHICH REASONABLY APPEAR TO BE PATENTABLE. ANY INVENTION DISCLOSURES WHICH HAVE NOT BEEN PREVIOUSLY SUBMITTED TO THE CONTRACTING OFFICER ARE ATTACHED TO THIS REPORT.

(i) NAME OF INVENTOR	(ii) TITLE OF INVENTION	(iii) PATENT APPLICATION SERIAL NUMBER, IF AVAILABLE, OR CONTRACTOR DISCLOSURE IDENTIFICATION NUMBER	(iv) CONTRACTOR HAS FILED OR WILL FILE U.S. PATENT APPLICATION		(v) CONFIRMATORY LICENSE OR ASSIGNMENT HAS BEEN FORWARDED TO CONTRACTING OFFICER	
			YES	NO	YES	NO
	None					

SECTION II - SUBCONTRACTS *(Containing a "Patent Rights" clause)*

LISTED BELOW IS INFORMATION REQUIRED BUT NOT PREVIOUSLY REPORTED FOR SUBCONTRACTS. *(If "None" so state.)*

NAME AND ADDRESS OF SUBCONTRACTOR *(Include ZIP Code)*	(ii) SUBCONTRACT NUMBER	(iii) DATE SUBCONTRACT WAS FURNISHED TO CONTRACTING OFFICER	(iv) DATE SUBCONTRACT COMPLETED
None			

SECTION III - CERTIFICATE

CONTRACTOR CERTIFIES THAT THIS REPORT OF INVENTIONS AND SUBCONTRACTS, INCLUDING ANY ATTACHMENTS, IS COMPLETE AND CORRECT TO THE BEST OF THE CONTRACTOR'S KNOWLEDGE AND BELIEF.

DATE	NAME AND TITLE OF AUTHORIZED OFFICIAL *(Print or Type)*	SIGNATURE
31 March '75	Paul B. MacCready, Jr., President	Paul B MacCready Jr.

DD FORM 1 MAY 68 882 PREVIOUS EDITION OF THIS FORM IS OBSOLETE

GPO 863 466